FACULTY OF TECHNOLOGY

IDENTIFICATION AND ENERGY OPTIMIZATION OF SUPERCRITICAL CARBON DIOXIDE BATCH EXTRACTION

Henri Hämäläinen

DEGREE PROGRAMME IN PROCESS ENGINEERING

Master's Thesis

October 2020

FACULTY OF TECHNOLOGY

IDENTIFICATION AND ENERGY OPTIMIZATION OF SUPERCRITICAL CARBON DIOXIDE BATCH EXTRACTION

Henri Hämäläinen

Supervisors: Prof. Mika Ruusunen, D.Sc. (Tech.) Petri Österberg

DEGREE PROGRAMME IN PROCESS ENGINEERING

Master's Thesis

October 2020

ABSTRACT
FOR THESIS

University of Oulu Faculty of Technology

Degree Programme (Bachelor's Thesis, Master's Thesis)			
Process Engineering			
Author		**Thesis Supervisor**	
Henri Hämäläinen		Prof. Mika Ruusunen	
Title of Thesis			
Identification and energy optimization of supercritical carbon dioxide batch extraction			
Major Subject	**Type of Thesis**	**Submission Date**	**Number of Pages**
Automation Engineering	Master's Thesis	October 2020	119

Abstract

The emergence of green chemistry, aiming to increase ecological and energy efficiency of processes, has gained supercritical fluid extraction increasing amounts of prominence. Traditional extraction methods utilize hazardous chemicals, have low extractive yield in relation to energy consumption, and produce large amounts of organic waste. Supercritical fluid extraction offers improvements to these challenges in the form of reduced processing energy inputs and an alternative solvent approach. Carbon dioxide (CO_2) is the most commonly employed solvent in supercritical fluid extraction due to the many advantages it brings over other solvents including price, smaller environmental and health risks, and simple separation.

The research on data-driven system identification and advanced process control of supercritical extraction has been very scarce. According to past research, the control of supercritical is mostly carried out using basic, non-model-based control schemes. Challenges such as coupling between control loops and nonlinearities of fluid and process dynamics create major challenges for the basic control schemes. With advanced control methods, it could be possible to address these challenges better.

Model-based control schemes, in theory, pose many advantages and benefits over basic control, such as improved production economics, optimized product quality and yields, and further possibilities in model-driven research and development. The goal of this thesis was to improve control performance and optimize energy consumption a pilot-scale batch supercritical carbon dioxide extraction process by utilizing model predictive control strategies.

The modeling of the unit processes of the target batch extraction was based on measurement data gathered by experimental design and careful examination of the system. The models were utilized in a simulator developed in this study. The arrangement of the implemented experimental design (central composite design, CCD) allowed the exploitation of linear regression analysis; the results of which indicated the existence of possible nonlinearities between steady-state electricity consumption and the operative variables of the process. Model predictive control schemes were developed in a simulator environment for CO_2 pressure control, CO_2 volumetric flow control, extractor temperature control and separator temperature control.

The developed control schemes showed major improvements in control performance of the simulated unit processes, resulting in significant decreases in total electricity and heating water consumptions (up to 25% and 21% respectively). Model predictive control also proved to be quite flexible over the base control system for some processes, providing the possibility of modifying control performance by simple tuning adjustments. The simulated control strategies demonstrate the benefits of model-based control in terms of process energy efficiency and economy. In addition to these results, the identified process and controller models have further potential in future research on control and process developments of supercritical fluid extraction.

TIIVISTELMÄ
OPINNÄYTETYÖSTÄ Oulun yliopisto Teknillinen tiedekunta

Koulutusohjelma (kandidaatintyö, diplomityö)			
Prosessitekniikka			
Tekijä Henri Hämäläinen		Työn ohjaaja yliopistolla Prof. Mika Ruusunen	
Työn nimi Ylikriittisen hiilidioksidipanosuuton identifiointi ja energiaoptimointi			
Opintosuunta Automaatiotekniikka	Työn laji Diplomityö	Aika Lokakuu 2020	Sivumäärä 119

Tiivistelmä

Prosessien ekologisuuden ja energiatehokkuuden lisäämiseen tähtäävä vihreä kemia edistää ylikriittisen uuton merkittävyyttä yhä enemmän. Perinteiset erotusmenetelmät käyttävät haitallisia kemikaaleja, niillä on alhainen uuteainesaanto suhteessa energian kulutukseen, ja ne tuottavat suuren määrän orgaanista jätettä. Ylikriittinen uutto tarjoaa parannuksia näihin haasteisiin prosessointienergian kulutuksen vähentymisen ja vaihtoehtoisen liuotinratkaisun muodossa. Hiilidioksidi (CO_2) on yleisimmin käytetty liuotin ylikriittisessä uutossa, koska sillä on monia etuja muihin liuottimiin verrattuna, mukaan lukien hinta, pienemmät ympäristö- ja terveysriskit sekä yksinkertainen erottaminen.

Ylikriittiseen uuttoprosessiin liittyvän datapohjaisen identifioinnin ja kehittyneen säädön tutkimus on ollut hyvin vähäistä. Aiempien tutkimusten perusteella ylikriittisen uuton säätö toteutetaan pääasiassa perustason ei-mallipohjaisilla säätörakenteilla. Ohjaussilmukoiden vuorovaikutukset sekä neste- ja prosessidynamiikan epälineaarisuudet luovat suuria haasteita perussäätörakenteille. Kehittyneillä säätömenetelmillä olisi mahdollista käsitellä näitä haasteita paremmin.

Mallipohjaiset säätöratkaisut tuovat teoriassa useita etuja ja hyötyjä perussäätöön verrattuna parantuvan tuotantoekonomian, optimoidun tuotelaadun ja -saannon sekä malliperusteisen tutkimuksen ja -kehityksen lisämahdollisuuksien muodossa. Tämän työn tavoitteena oli nostaa pilottikoon ylikriittisen hiilidioksidipanosuuttoprosessin säädön suorituskykyä ja optimoida energiankulutusta hyödyntämällä mallipredikriivisiä säätöstrategioita. Tutkimuksen kohteena olleen panosuuton yksikköprosessien mallinnus perustui koesuunnittelulla kerättyyn mittausaineistoon ja järjestelmän huolelliseen tarkkailuun. Malleja hyödynnettiin työssä kehitetyssä prosessisimulaattorissa. Toteutettu koessunnitelma (central composite design, CCD) mahdollisti lineaarisen regressioanalyysin hyödyntämisen, jonka tulokset osoittivat mahdollisten epälineaarisuuksien olemassaolon prosessin vakaan tilan sähkönkulutuksen ja operatiivisten muuttujien välillä. Mallipredikiiviset säätörakenteet kehitettiin simulaatioympäristössä CO_2-paineen, CO_2-tilavuusvirtauksen, uuttoreaktorin lämpötilan, ja erottajan lämpötilan säädöille.

Kehitetyt säätörakenteet toivat suuria säätöparannuksia simuloituihin yksikköprosesseihin, johtaen merkittäviin vähennyksiin käyttösähkön- ja lämmitysveden kulutuksissa (vastaavat vähennykset 25 % ja 21 % saakka). Mallipredikiivinen säätö osoitti myös joustavuutensa perusäätöjärjestelmään verrattuna joissakin prosesseissa, mahdollistaen säätösuorituskyvyn modifioinnin yksinkertaisilla viritysmuutoksilla. Simuloidut säätöstrategiat havainnollistavat mallipohjaisen säädön mahdollisia hyötyjä prosessin energiatehokkuuden ja taloudellisuuden kannalta. Näiden tulosten lisäksi identifioiduilla prosessi- ja säädinmalleilla on lisäpotentiaalia tulevaisuuden ylikriittisen uuton säädön tutkimuksissa ja prosessikehityksissä.

PREFACE

This thesis was mostly carried out at Kajaani University Consortium in the measurement technology research unit (MITY) between January 2020 and October 2020. It was a part of a project under the research of the Biorefinery Measurements professorship in the research group of Control Engineering at University of Oulu. The aim of the study was to improve the efficiency of a pilot supercritical carbon dioxide batch extraction plant.

I would like to express my gratitude to Professor Mika Ruusunen and D.Sc. (Tech.) Petri Österberg for their guidance regarding my work and giving the chance to work in this interesting project. Special thanks go to Pasi Karjalainen (B.Eng.) and Veijo Sutinen (Lic.Sc. (Tech.)) from MITY for their installation work, as well as to Petri Sundqvist (M.Sc. (Tech.)) from University of Oulu for providing expertise and operative knowledge of the process. All of you played a vital role in making this project happen.

TABLE OF CONTENTS

SYMBOLS AND ABBREVIATIONS

A	state (system) matrix
a	output variable weighing factor
B	input matrix
b	manipulated variable rate weighing factor
c	controller horizon
C	output matrix
CCD	central composite design
CO_2	carbon dioxide
D	feedthrough matrix
DS	difference between initial and final slopes of the process variables
DT	dead time (time of delay for the process to react to a step input change due to instrumentation/transportation lag)
E	electricity consumption
e	error value (difference between measured process value and setpoint)
ê	predicted error value
E_{ss}avg	average electricity consumption per minute in steady-state operation for experimental run
Ey	electricity consumption output
Ey	electricity consumption process output
F	CO_2 volumetric flow rate
F_{ref}	open-loop identified steady-state value for CO_2 volumetric flow settling at given valve position
F_{sp}	step time for CO_2 volumetric flow control valve step value
F_t	step time for CO_2 volumetric flow control valve step value
Fu	CO_2 volumetric flow process input
Fy	CO_2 volumetric flow process output (average from two full pump cycles),
H_2O	dihydrogen monoxide, heating water consumption
H_2Oy	heating water consumption process output
iPA	isopropyl alcohol
IR	infrared
J	cost function
K	number of design factors in a central composite design
k	sampling instant

K_C	proportional gain, or controller gain
K_D	derivative gain
K_I	integral gain
K_P	process gain (steady state change of the controlled variable divided by the change in the manipulated variable)
MPC	model predictive control
N4SID	numerical algorithm for subspace system identification
OPC	Object Linking and Embedding for Process Control Data Access
OS	overshoot (peak deviation of process from reference)
P	CO_2 pressure
p	prediction horizon
PB	proportional band
Pe	pressure error (difference between measured pressure value and setpoint)
PI	proportional-integral
PID	proportional-integral-derivative
PRBS	pseudo-random binary sequence
P_{sp}	CO_2 pressure setpoint value
P_t,	step time for CO_2 pressure setpoint
Pu	CO_2 pressure process input
Py	pressure process output (average from two full pump cycles)
r	the process reference or setpoint
RT	rise time (process value changing time from 10% to 90% of reference)
RTD	resistance temperature detector
S_1	initial slope of the process variable
S_2	final slope of the process variable
SF	supercritical fluid
SFE	supercritical fluid extraction
SSE	steady-state error (process value deviation from reference after settling)
ST	settling time (process value settling time within 5% of reference)
t	total simulation runtime
T_{CO2}	CO_2 preheater temperature
T_{CO2sp}	CO_2 preheater temperature setpoint value
T_{CO2t}	step time for CO_2 preheater temperature setpoint
$T_{CO2}u$	CO_2 preheater temperature process input
$T_{CO2}y$	separator temperature process output,

T_D	derivative time, or rate
T_E	extractor temperature
T_{Esp}	extractor temperature setpoint value
T_{Et}	step time for extractor temperature setpoint
T_Eu	extractor temperature process input
T_Ey	extractor temperature process output
T_I	integral time, or reset time
t_s	sampling time
T_S	separator temperature
T_{Ssp}	separator temperature setpoint value
T_{St}	step time for separator temperature setpoint
T_Su	separator temperature process input
T_Sy	separator temperature process output
U	design factor in a central composite design
u	process input variable, manipulated variable, or input vector
u_{max}	upper limit for manipulated variable u
u_{min}	lower limit for manipulated variable u
x	state vector
y	measured process output variable, controlled variable, or output vector
$\hat{y}$	predicted process output variable
Y	modelled response
y_{max}	upper limit for controlled variable y
y_{min}	lower limit for controlled variable y
α	distance between center point and star point in a circular central composite design
β	coefficient of a term in a linear quadratic regression model
ΔCO	difference between initial and final controller outputs
ΔPV	difference between initial and final process values
Δu	manipulated variable rate (u(k)-u(k-1))
Δu_{max}	upper limit for manipulated variable rate Δu
Δu_{min}	lower limit for manipulated variable rate Δu
λ	desired closed-loop time constant after setpoint step
τ	dominant time constant (the time for the system's step response to reach 63% of steady-state process value)

1 INTRODUCTION

Supercritical fluid extraction (SFE) employs solvent compounds that are at or near their critical region at the condition of operation. The most commonly employed solvent in SFE is carbon dioxide (CO_2). A typical feature of SFE solvents is that their critical pressure is high, and their critical temperature is relatively low. Therefore, SFE processes operate at elevated pressures and moderate temperatures. SFE processes have been established as a promising alternative to conventional separation techniques, such as distillation, absorption, and (non-critical) extraction. (Gani et al., 1997)

The continued impact of energy conservation has resulted in a trend towards increased attention to economics, safe operation, and environmental consciousness. Consideration of these factors would improve the overall competitiveness of the processing industries to remain viable in rapidly changing conditions. However, the economic need to operate industrial processes as close as possible to optimum specifications with minimum energy consumption, while safety and environmental constraints are not violated, has produced multi-unit processing plants which are tightly coupled. (Samyudia et al., 1995)

Past research on optimal and advanced process control of supercritical fluid extraction processes has been extremely scarce. Due to this, like for many other industrial processes, the control of supercritical extraction is mostly carried out using basic level control, proportional-integral-derivative (PID) control in particular. This severely limits control performance, especially in the case of nonlinear, multivariable processes such as SFE. Therefore, more advanced control schemes should be favored if scaling-up to an industrial level is desired.

The goal of this study is to develop model predictive control (MPC) strategies for the unit processes of a batch SFE pilot process system in order to improve control performance. The hypothesis is that improving control performance of the SFE leads into reduced energy consumption, and ultimately may improve the production economics of existing and future extraction plants. To achieve this goal, a simulator of the target process is identified through data-driven system identification, and MPC strategies are developed and evaluated in this simulator environment.

2 SUPERCRITICAL FLUID EXTRACTION PROCESS

Solvent extraction is one of the oldest methods of separation known, dating back to the Paleolithic age (Herrero et al., 2010). The science of extraction has evolved over centuries of development, and much progress has been made in the understanding of solvation and the liquids used in extraction processes. Early observations by Hannay and Hogarth on the dissolutions of solutes in supercritical fluid (SF) introduced a possibility of a new solvent medium: In 1879, they proposed a model where the simultaneous increase in pressure and temperature of certain chemical substances increased its solubility. In the early 1900's, this was confirmed through experiments by Buschner, better systemizing the process. (Khaw et al., 2017; Pourmortazavi et al., 2018)

It was only throughout the second half of the twentieth century when these fluids were started to be applied on an industrial scale. One of the aspects responsible for the delay was the difficulty in devising safe equipment to operate depending on the type of fluid used; a problem that has been overcome in the past years (Maxhado et. al). Since the end of the 1970's, SF's have been used to isolate natural products. However, the applications relied on only a few products for a long time. Now, the development of processes and equipment is beginning to pay off and industries are getting more interested in supercritical techniques, which is reflected by the number of publications and patents on the topic (Herrero et al., 2010; Khaw et al., 2017). SFE is nowadays utilized in a range of industrial areas, which include food, pharmaceutical, and biofuel industries (Machado et al., 2013; Herrero et al., f2010; Khaw et al., 2017).

The emergence of green chemistry for extraction purposes occurred in the 1990's with the aim of reducing energy consumption and replacing the conventional solvents with less environmentally harmful alternatives (Khaw et al., 2017). Traditional methods, such as methanol or Soxhlet extraction and steam distillation methods, are relatively simple but they have numerous drawbacks concerning energy usage and environmental factors. These methods utilize hazardous processing solvents requiring additional steps to remove, have typically low extractive yield in relation to energy input and require disposals of large amounts of organic waste (Khaw et al., 2017). Supercritical fluid extraction offers both reduced processing energy inputs and an alternative solvent approach.

2.1 Principle

The critical temperature is the highest temperature at which gas can be converted to a liquid by increasing the pressure. The critical pressure is, accordingly, the highest pressure at which a liquid can be converted to a traditional gas by an increase of liquid temperature (Hedrick et al., 1992). Above the critical pressure, a gas or liquid becomes a supercritical fluid. In this supercritical region, the surface of demarcation between gas and liquid disappears, forming a homogenous fluid with both liquid-like and gas-like properties. SF has liquid-like density, and exhibits gas-like diffusivity, surface tension and viscosity. Typically, supercritical extraction solvents have a (relatively) high critical pressure and low critical temperature (Gani et al., 1997). The phase diagram of carbon dioxide is presented in Figure 1.

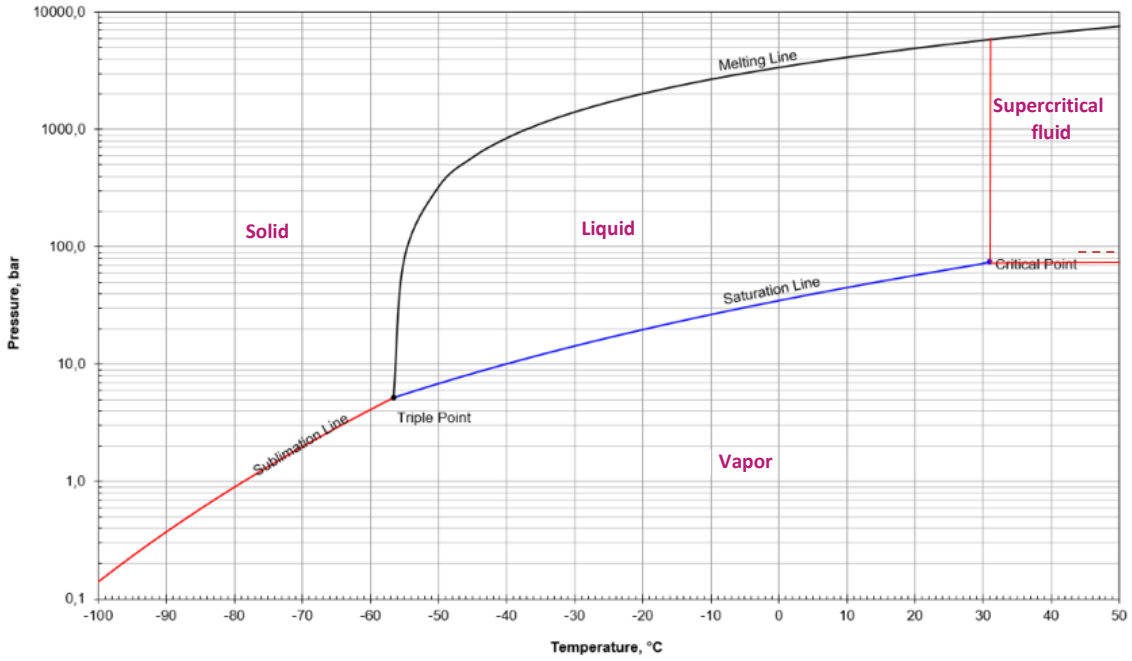

Figure 1. Phase diagram of carbon dioxide (modified from Cavalcanti et al., 2012).

Due to the gas-like low viscosity and high diffusivity, when SF's are used as solvents, they easily penetrate material with a rapid transfer rate (Khaw et al., 2017). Changing the pressure or temperature affects the solubilizing potency of the fluid, making it possible to extract complex compounds (Pourmortazavi et al., 2018). The properties of SF's lead to high mass transfer rates, greater penetration into porous solids and liquid-like solvent strength. The critical temperatures and pressures of various solvents are presented in Table 1.

Table 1. Critical conditions of different solvents (modified from Lozowski, 2010).

Solvent	Critical temperature (°C)	Critical pressure (bar)
Ammonia	132.5	112.8
Benzene	289.0	48.9
Carbon Dioxide	32.1	73.8
Cyclohexane	280.3	40.7
Ethane	32.2	48.8
Ethylene	9.3	50.4
Isopropanol	235.2	47.6
Propane	96.7	42.5
Propylene	91.9	46.2
Toluene	318.6	41.1
Water	374.2	220.5

The density of these fluids, in opposite of liquids, varies by a change in temperature and pressure values. Therefore, solvent strength can be tuned by varying these parameters. In contrast, liquid solvents require relatively large pressure changes to affect the density. (Lozowski, 2010)

SFE has various distinctive properties compared to conventional extraction methods. The main advantage is the possibility of easy manipulation of fluid density by small changes in pressure and temperature. In other words, SFE has high selectivity. Another advantage is that SF's such as nitrous oxide or CO_2 are in gaseous forms at room temperature and pressure, making the recovery of components simple. Sample preparation in classic extraction techniques is tedious and takes lots of time, but SFE requires short time for sample handling and preparation. In addition, SFE enables direct coupling with assessment instruments such as gas chromatograms, making it possible to detect substances qualitatively and quantitatively. (Pourmortazavi et al., 2018)

2.2 Supercritical carbon dioxide

Selecting an appropriate supercritical fluid for solvent is crucial for the development of SFE processes, since a wide range of compounds can be utilized as supercritical solvents. Even considering the wide number of compounds, most systems use carbon dioxide (critical temperature of 32.1 °C, critical pressure of 73.8 bar). Carbon dioxide is cheap, environmentally friendly and nontoxic, non-flammable, non-corrosive; generally recognized as safe by the U.S. Food and Drug Administration and the European Food Safety Authority (Herrero et al., 2017; Ahmad et al., 2019). CO_2 is readily available in bulk quantities with a high degree of purity. Also, it can be easily removed from the extractive mixture since the solvent is in gaseous at room temperature, providing simple separation and solvent-free extracts (Ahmad et al., 2019).

Besides low viscosities and high diffusivities, CO_2 also provides potential for faster reactions, particularly for diffusion-controlled reactions or processes involving gaseous reagents such as hydrogen, oxygen, or carbon monoxide (Norhuda et al., 2008). Despite the many advantages of supercritical carbon dioxide (SC-CO_2) extraction, some flaws remain. Since CO_2 is a non-polar solvent, it has a low tendency to dissolve highly polar components. Organic modifiers must be added in order to extract polar components. These modifiers cause problems in the collection step, since it may be required to separate them from the extractives (Pourmortazavi et al., 2018).

2.3 Parameters

Understanding the effects of different parameters on the extraction rate and yield of supercritical fluid extraction is essential for the optimization and economic evaluation of the process, as well as for scale-up and for the design and optimization of an industrial plant (Jokić et al., 2012). Several factors affect the yield of supercritical fluid extraction: These include the physical form of the materials (i.e. particle size, surface area, shape porosity), variation of operating temperature and pressure, existence of organic modifiers, fluid flow rate and time of extraction (Pourmortazavi et al., 2018). The effectiveness of the extraction is determined in terms of the yield and recovery of the target components.

The physiochemical properties of supercritical fluids are directly related to their applications. The high-density values combined with the pressure dependent solvent

power provides high solubility and selectivity to the supercritical fluid. In addition, low viscosity values and intermediate values of diffusivity combined with the absence of surface tension of these fluids allow its rapid penetration into the cells and particles of the sample matrix extracting their interior material. (Ahmad et al., 2019)

2.3.1 Temperature and pressure

Operating variables, including pressure and temperature, are the most discussed among the parameters of SFE (Pourmortazavi et al., 2018). Solubility of a solute in SC-CO_2 is highly dependent on temperature and pressure, which influences the physiochemical properties of the solute, such a density, viscosity, and diffusivity (Ahmad et al., 2019). Thus, the solvating power of CO_2 is directly affected by these operating variables. The effects of CO_2 pressure and temperature on density is shown in Figure 2.

An initial increase in pressure (in constant temperatures) results in an increase in fluid density and enhances solubility of the solute. Nevertheless, increasing pressure to a certain point may reduce the diffusivity of the SF solvent, and result in a reduced contact with pores in the raw material, thereby potentially decreasing solute dissolution. A research on rosehip seed oil extraction indicated that yield increased with increasing pressure at short extraction time but decreased as extraction time progressed (Machmudah et al., 2007). In some cases, an increase in pressure caused the solid matrix to compact and the void fraction leads to unfavorable extraction outcomes (Khaw et al., 2017).

The effects of temperature in constant pressure have been researched in a number of experiments. Generally, these experiments have proven that increasing the temperature to a certain point, which is dependent on the targeted extractive, increases extractive yield. This is because the increase in process temperature increases the solubility due to solute vapor pressure enhancement and reduces the solubility due to the decrease in solvent density (Jokić et al., 2012; Rai et al., 2018). It has been stated that at constant pressures, the solubility of supercritical CO_2 decreases at high temperatures (Guerra et al., 2002). In a study researching the effect of temperature changes in extractor for the dehydration of ethanol, it was noted that decreasing the temperature has both a positive effect (smaller loss of solvent and smaller amount of water in extract) and a negative effect (bigger loss of product in raffinate) (Gani et al., 1997). An obvious optimization problem therefore is to relate the condition of operation to the costs related to lost product and wasted energy.

Temperature can exert an inconsistent "solvent" effect, where a higher temperature confers more "energy" to a fixed wall system, increasing diffusivity, and increasing the apparent volume, and density reduces, along with the "solvent" power of the SF. On the other hand, decreasing the temperature decreases the vapor pressure of the solutes, and the density rises, along with the solvation of the solutes (Khaw et al., 2017). The net effect of these two opposing factors dictates the change in solubility, and their significance varies if solute pressure is high or close to the critical point. This phenomenon is called the "crossover effect" (Ahmad et al., 2019). This relationship between pressure and temperature is essential to understand if high yields are desired. The choice of best experimental conditions starts with the knowledge of temperature and pressure where the analytes present the highest solubility. It is especially important when the objective is to remove substances from the sample at high levels of concentration (Guerra et al., 2002).

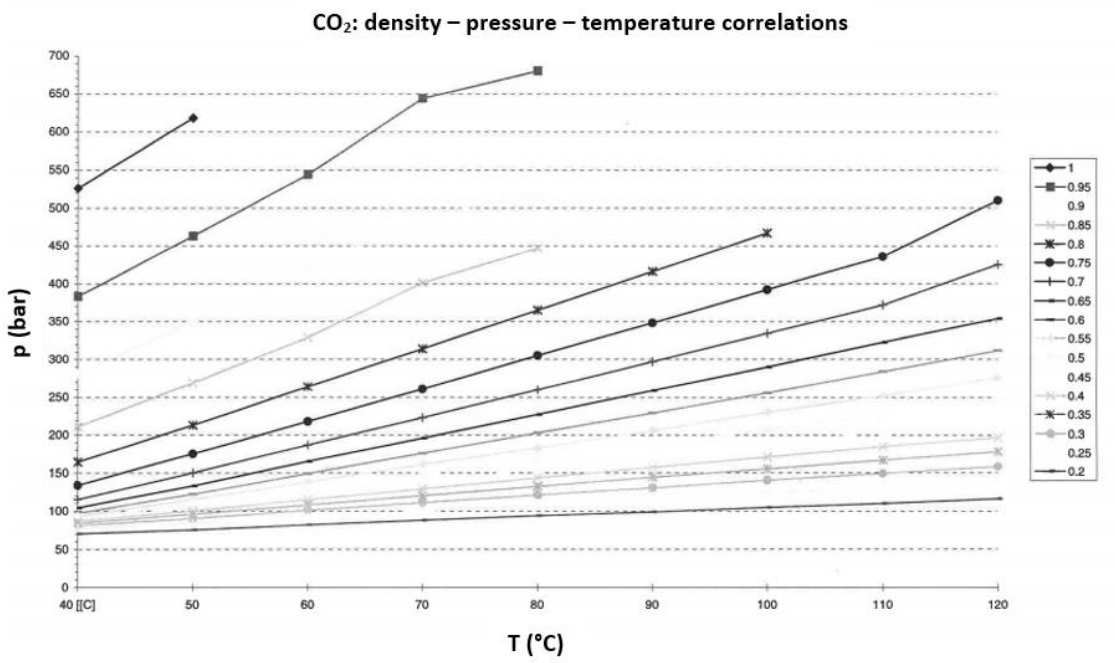

Figure 2. Correlations between CO_2 density, temperature, and pressure (modified from Chematur Ecoplanning Ltd, 1998).

2.3.2 Solvent flow rate

The flow rate of CO_2 should be measured in terms of mass flow rather than volume, because the density of CO_2 changes according to the temperature both before entering the pump heads and during the compression (Cavalvanti et al., 2012). In a study made for the extraction of watermelon seed oil, the extraction was almost complete at a higher flow rate (Rai et al., 1997). As flow rate increases, the resistance to mass transfer decreases;

Therefore, extraction yield increases. However, as with temperature and pressure, the increase of flow rate is only effective to an extent, and dependent on the target compound. This was demonstrated in a study for the extraction of a bioactive component (andrographolide) using CO_2 (Kumoro et al., 2007); The extraction yield increased with the increase of solvent flow rate from 7.95×10^{-6} to 3.18×10^{-5} kg/s, but further increases of solvent flow rate reduced the extraction yield.

The general effect of increasing the solvent flow rate at constant temperature and pressure is an increase in extraction yields. However, using higher solvent flow rates is wasteful of solvent. To minimize the amount of solvent used, the extraction should be completely solubility limited, which will take a long time. The flow rate must be determined depending on the factors of time and solvent costs. The optimum is typically found in the region where both solubility and diffusion are significant factors. (Cavalvanti et al., 2012).

2.3.3 Particle size

Decreasing particle size of extraction raw material leads into an increase in extraction yield. This is because as the particle size decreases its surface area per unit mass increases, and therefore extraction is favorably increased (Rai et al., 2018; Pourmortazavi et al., 2018). At fixed conditions of extraction time, solvent flow rate and solvent density, it has been observed that the extraction yield of soybean oil was higher for smaller particles. However, it has also been noted that if particles are too small, they can pose challenges with channeling inside the extraction bed, causing a loss of efficiency and yield decrease (Jokić et al., 2012).

2.3.4 Co-solvent

CO_2 is intrinsically non-polar, and thus a great solvent for extracting non-polar compounds. However, it is less effective in the extraction of polar components. The addition of small amounts of organic co-solvent or solvent modifier in the SFE process can enhance the solvation power of SC-CO_2 (Khaw et al., 2017). The most commonly used organic solvents in this regard are ethanol and methanol. Co-solvents can be introduced as mixed fluids in the pumping system with a pump and a mixing chamber, or by injecting the modifier as a liquid into the sample before extraction. (Pourmortazavi et al., 2007; McNally et al., 1988)

One study indicated that as the concentration of co-solvent in the supercritical CO_2 increased, the initial slope of the extraction curves also increased, indicating that the solubility of watermelon oil in supercritical CO_2 increased due to increase in the polarity of supercritical CO_2 (Rai et al., 2018). A proportion of co-solvent has proved essential in recovering certain highly polar compounds with high selectivity. Other example of similar behavior was proven in a study made for extraction of proanthocyanidins from grape marc (Da Porto et al., 2014). The addition 15% volume concentration ethanol in the extraction step gave a higher recovery of up to 7.3%, compared to that of the method without the additional ethanol steps.

The effects of temperature and pressure on the dissolution of solutes in any given plant extraction system are not necessarily readily predicted, and the addition of co-solvents further complicates issues (Khaw et al., 2017). Since interactions may occur not only between the solvent and solutes, but also between CO_2 and co-solvents, the use of a co-solvent may reduce the targeted extraction as these interactions reduce the availability of CO_2 as a solvent for certain molecules. Further issues may arise in the separation: The co-solvent is mixed in the extractive-CO_2 mixture, and requires its own separation stage. However, this separation is not necessary if the extractive can be used without further treatment: One approach used vegetable oils for the recovery of fat-soluble carotenoids, improving the total yield (Temelli, 2009). The carotenoid-rich oil can be further utilized without separating the co-solvent.

2.3.5 Moisture

Moisture, or water content in the raw material is a key factor in SFE. Water can aid the extraction process or be detrimental; what is necessary for effective extractions depends on the type of compounds targeted (Khaw et. Al, 2017). Even though water is only 0.3% soluble in supercritical CO_2, it serves to increase polarity of the fluid and enable higher recoveries of relatively polar materials. In excess water, highly water-soluble analytes will dissolve in the aqueous phase, but readily partition in supercritical CO_2, resulting in high yields. On the contrary, for analytes that are insoluble in water, the water acts as a barrier in transfer of the analyte to the fluid (Pourmortazavi et al., 2007). Each raw material has an ideal moisture content for obtaining the highest possible extractive yield. Thus, it is important to determine the ideal percentage of moisture. The effect of pretreatment is critical for achieving this goal (Cavalcanti et al., 2012).

The maximum limit in SFE of herbal medicines has been reached at nearly 10% of moisture content (Ling et al., 1999; Pourmortazavi et al., 2018). On the other hand, the moisture content of paprika is as high as 85%, and SFE without drying results in extremely low yields (Khaw et al., 2017). In another study, it was observed that pre-soaking of the samples in water to a moisture of 28.4% resulted in an increase in the extraction yield of essential oils from flowers of Helichrysum italicum and reduced CO_2 consumption (Ivanovic et al., 2012; Khaw et al., 2017). The varying results of the studies point out that suitable water content varies significantly between raw materials and targeted extractives. Removal of water can be done by conventional air-drying or by freeze-drying, as oven drying may result in solute volatilization. However, it is obvious that drying may have an influence on the content of compounds. Selection of appropriate drying methods may minimize the loss of aroma (Pourmortazavi et al, 2007).

2.3.6 Extraction time

In supercritical extraction, two types of process times can be adjusted: time of static extraction and time of dynamic extraction. Static extraction time occurs when the matrix is first submitted to the temperature and pressure parameters, resulting in the breakdown of cellular structures caused by the cell swelling that occurs during the initial contact between the solute and the solvent. Dynamic extraction time occurs as the solute and/or solvent flow in the output of the processing line. Increasing the dynamic extraction time result in higher extract recovery and costs. Residence time, which includes static and dynamic extraction time, has a direct effect on the yield and economic viability of the process, and the optimum must be picked between these two deciding factors (Cavalvanti et al., 2012).

A study reported that in SFE of aflatoxins, a 10 to 20-minute static extraction time prior to dynamic extraction improved the extract recoveries (Stahl et al, 1988; Pourmortazavi et al, 2007). In another study, it was observed that a static extraction longer than 10 min did not increase extraction efficiency (Cui et al., 2002.). Pourmortazavi et al. researched the influence of the dynamic extraction time on the composition of the essential oil of Juniperus communis L. leaves and isolation of fennel oil (Pourmortazavi et al., 2007). It was found that increased dynamic extraction time enhanced the extraction for most of the compounds.

2.4 Industrial uses

Due to the increasingly stricter environmental regulations, SFE has gained a large acceptance as an alternative to conventional solvent extraction for separation of organic compounds (Lang et al, 2000). Many industrial sectors are concerned including food, pharmaceutics, materials, chemistry, energy, and waste treatment. Nowadays, supercritical fluid-based technologies, including SFE, are involved in a wide variety of industrial applications which have shown significant progress in recent years. The method is an important alternative to conventional extraction methods using organic solvents. Even though these processes usually offer clear advantages over traditional ones, the main drawback for industrial scale use is the lack of realistic economic studies One of the main aspects that should be considered in SFE is the extraction optimization. The use of the optimum values for the different variables influencing the SFE extractions could significantly enhance the recovery or extraction yield of a target compound. (Herrero et al., 2010). Since many industries generate a large number of by-products and waste streams, a lot of research is focused on the development of new technologies and uses for these materials to recover components. By-products extraction allows the removal of valuable/interesting compounds that otherwise cannot be utilized. Existing applications of SFE are present in the areas of food and agricultural processing waste and byproduct utilization (Perretti, 2006).

2.4.1 Food industry

The utilization of supercritical CO_2 in natural product extraction is the most developed process on an industrial scale, with most of the applications in the food industry. Supercritical carbon dioxide is industrially widely used to extract caffeine from green moist coffee beans. Compared with conventional solvents such as hexane, carbon dioxide does not leave any harmful solvent residue after extraction. The largest plants use batch extraction vessels with volumes up to tens of cubic meters (Laitinen, 2000).

For many applications, crude vegetable oils are commonly used in the food industry. They typically need to be refined to remove undesirable compounds. SFE has been suggested as an alternative to obtain extracts enriched with the particular compounds of interest (De Azevedo et al., 2008; Eisenmenger et al., 2008). Essential oils, fatty acids and bioactive compounds have also been extracted using SFE (Herrero et al., 2010). Supercritical CO_2

is the most widely used near-critical fluid for the extraction of lipids (Catchpole et al., 2008). SFE has been also widely employed as a sample treatment technique prior to volatiles analysis in different beverages, such as aroma compounds from sugar cane (Gracia et al., 2007) and removal of ethanol from alcoholic beverages (Fornari et al., 2009).

SFE has been used to extract bioactive compounds from plant materials for a long time. Antioxidant compounds have been the most frequently studied. Most researched applications include the characterization of bioactives from medicinal herbs, or on the extraction of these compounds to be used as ingredients intentionally added to other products, mainly food products (Herrero et al., 2010).

2.4.2 Pharmaceutical industry

Pharmaceutical companies are more and more urged to develop production processes with very low environmental impact, in particular to reduce the use of volatile organic compounds in medicine manufacturing as well as to avoid residues in the finished product. In general, the main use of supercritical fluids in the pharmaceutical industry deals with the extraction of bioactive compounds from a mixture or with the extraction of the matrix. (Cavalcanti et al., 2012)

The main uses of supercritical fluids in pharmaceutical industry include processes such as particle and crystal engineering, formation of complexes with cyclodextrins, coating, foaming and tissue engineering, enzymatic reactions in supercritical media, extrusion, production of liposomes and biotechnological compounds, purification of pharmaceutical excipients, sterilization, solvent removal, enantioselective separations and extraction and purification of active principles from raw materials and from synthetic reaction media (Herrero et al., 2010).

2.4.3 Environmental industry

Industrial emissions and practices that frequently have generated harmful materials in the last century threatens both public health and the environment. The use of supercritical carbon dioxide can significantly help to reduce further CO_2 emissions by the means of replacing conventional hazardous organic solvents, such as hexane. In fact, several recently developed applications of supercritical fluids not only tend to eliminate organic

solvents, but also to reduce the environmental impact of human activities. In this sense, applications like removal of heavy metals from soils, sludges and wastes, reduction of secondary wastes generation, regeneration of inactive catalysts or methods for treating soils contaminated with non-polar compounds (Polycyclic aromatic hydrocarbon, polychlorinated biphenyl etc.) are being studied (Sunarso et al., 2009; Herrero et al, 2010).

2.4.4 Biofuel industry

SFE has notable potential in biofuel production applications. Supercritical CO_2 is utilized in ethanol production for biodiesel manufacturing. The use of SC-CO_2 is favorable to produce bioethanol. A study observed that the fermentation under supercritical CO_2 pressure has real potential in the recuperation of highly pure bioethanol, avoiding the expensive and highly energy-consuming distillation process (Melo et al., 2011; Yépez et al., 2002). Another study researched the usage of SC-CO_2 in extraction of seeds oil, and converting the oil into biodiesel (Breet et al., 2011). This study identified SFE as a clean technology that could rapidly substitute the decrease in the use of fossil fuel resources.

2.5 Process apparatus

SFE technology has developed significantly in recent years, and it has been applied successfully to several applications. Commercial SFE instrumentation has largely been developed in the USA and marketed throughout the world (King, 2002). The concept of SFE could be further developed within well-established processes, for integration of biorefinery approach in obtaining high-value-added products while keeping the standards required for environmental sustainability (Molino et al., 2020).

2.5.1 General process description

The functionality of supercritical fluid apparatus is based on the ability of circulating the solvent, passing it through the raw material and extracting the desired components by depressurizing the solvent-extractive mixture (Horvat et al., 2017). The basic components of a supercritical CO_2 extraction system include a CO_2 pump (or compressor), extractor and separator/fractionator/collection vessel. Additionally, a modifier pump where an organic solvent or water is added, can be implemented in the system (Khaw et al., 2017).

If desired, more than one extractor can be connected to the same system (Cavalcanti et al., 2012). A schematic of a basic SFE process is described in Figure 3.

The solvent is pumped into the system as liquid or gas. If the solvent is in liquid form, it will be either cooled in a reservoir or kept in a liquid phase by cooling the pump head. The fluid is then pressurized and heated to a desired temperature. Temperature fluctuations can be avoided by adding a solvent preheater into the system (Cavalcanti et al., 2012).

The solute is contacted with a supercritical fluid solvent in the extractor, where supercritical CO_2 extracts the solute. Following extraction, the pressure is reduced, or flashed, causing the precipitation of the extract through a control valve. The pressure of the system is controlled by the rate of pumping and a backpressure valve setting. The solvent is recovered in the separator by the means of distillation. The heat required for the distillation can be provided by the recompressed solvent (Ramchandran et al, 1992). Next, the CO_2 can be cooled, recompressed, and recycled or discharged into the atmosphere. (Cavalcanti et al., 2012, Ramchandran et al, 1992)

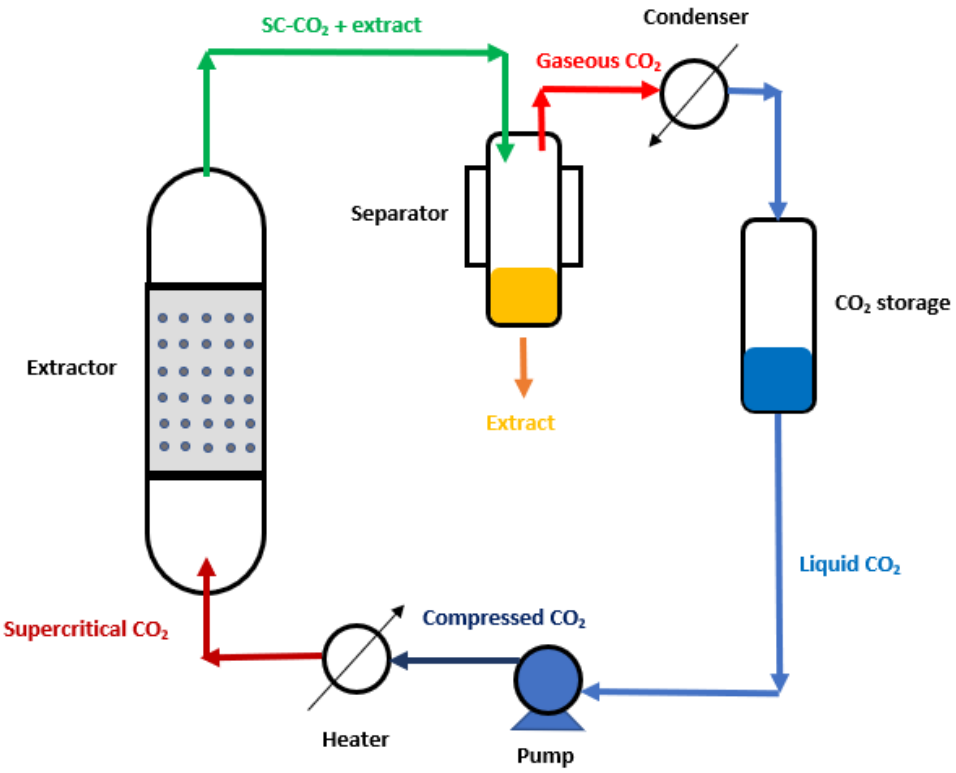

Figure 3. Basic schematic of a SFE process (valves not included).

The extraction system can be operated in batch, semi-batch, and continuous configurations. The utilization possibilities of these techniques depend heavily on the phase of the raw materials. For solid raw materials, the processing is performed in batch or semi-batch configurations, whereas for liquid feeds, the process is typically semi-batch or continuous. Solid raw materials are packed into the extractor for example in a mesh basket to prevent it from escaping the cell during extraction (Cavalcanti et al., 2012). In batch processing, the raw material is placed in the extractor as a batch, and the supercritical solvent is fed in until the desired conditions for extraction are reached. Semi-batch processing is a widely employed technique: The raw materials are charged into the extractor, and the solvent is fed continuously at a fixed flow rate. In continuous processing, the raw material is fed continuously along the column, and the solvent is fed at the bottom of the column (Reverchon, 1996).

Choosing a continuous process rather than a batch or semi-batch process may significantly improve the economics of an industrial-scale system. Continuous transport of a large volume of solid feed, such as oilseeds, in and out of a high-pressure extractor is costly and difficult. However, advances in high-pressure technology, such as lock hopper valves, may allow the continuous feed of solid materials. Such an extractor design

has important advantages, including minimizing raw material feeding, vessel unloading times and compression costs, since feed loading and unloading are carried out simultaneously while pressure is maintained. (Reverchon, 1996)

2.5.2 Pumps

Most SFE systems are based on pumps with reciprocating piston design. Syringes, high pressure diaphragm compressors and gas booster pumps have also been used (Cavalcanti et al., 2012). Carbon dioxide is usually pumped as a liquid, typically below 5 °C and at 50 bar. The pump heads will usually require cooling, and CO_2 will also be cooled before entering the pump to ensure liquefaction of the CO_2 (Sapkale et al., 2010).

2.5.3 Extraction vessels

Extraction vessels, or pressure vessels, can range from simple capillary tubing to more sophisticated containers with quick release fittings (Sapkale et al., 2010; Cavalcanti et al, 2012), depending on the system size and pressure requirement. The vessel must be equipped with a means of heating. In case of small vessels, the vessel can be placed in an oven. Oil or electrical heating jackets must be used for larger systems (Cavalcanti et al, 2012).

2.5.4 Pressure maintenance

The pressure must be maintained from the pump right through the pressure vessel. Simple restrictors, such as capillary tubes or needle valves, can be used for smaller systems (up to 10 ml/min). In larger systems a backpressure regulator, such spring-based, compressed air-based or electronically driven valve must be used (Sapkale et al., 2010; Cavalcanti et al, 2012). Heating must be supplied, as the adiabatic expansion of the CO_2 leads into cooling down. This cooling can be problematic as the sample may freeze and cause blockages.

2.5.5 Collection

The supercritical solvent is passed into a collection vessel at a pressure lower than in the extraction vessel. The density and related dissolving power of supercritical fluids vary sharply with pressure, making the material precipitative for collection. The dissolved material is thereby possible to fractionate using a single vessel or a series of vessels at

reducing pressures. The CO_2 can be recycled or depressurized to atmospheric pressure and vented. (Sapkale et al., 2010; Cavalcanti et al, 2012)

2.5.6 Heating and cooling

The supercritical fluid is cooled before pumping to maintain liquid form, and then heated after pressurization. As the fluid is expanded into the separator, heat must be implemented in order to prevent excessive cooling. For smaller-scale systems, it is usually sufficient enough to preheat the fluid using, for example, electrical heating. For larger systems, the energy required for each stage can be calculated using the thermodynamic properties of the fluid. (Sapkale et al., 2010; Cavalcanti et al, 2012)

3 PROCESS CONTROL

Specific solvent densities, and hence solvent effectiveness of SF's, can be controlled by pressure and temperature. Liquid-like densities and gas-like viscosity, coupled with diffusion coefficients that are at least an order of magnitude higher than those of liquids, contribute to enhancement of mass transfer. The solvency property of SF's can also be modified by adjusting pressure, temperature, as well as other parameters such as moisture contents. (Li et al., 2001). The highly pressurized environment of SFE creates certain robustness requirements for the process measurement instrumentation.

The automation and control of supercritical fluid extraction plants shows a high complexity due to; negative effects of re-circulation, coupling between control loops, and the strong nonlinearity of the change in the state of the fluids (Corostiaga et al., 2002). A lack of demonstrated control for maintaining product quality is one of the factors that hamper the application of the SFE technology in industry (Samyudia et al., 1995). The SFE process is characterized by a high degree of multivariable coupling and exhibits varying response times in different units of the process; hence, the control system design is complicated (Samyudia et al., 1995). Unfortunately, not many studies have been reported in literature regarding control of SFE processes. In the few studies that have been reported, both basic and advanced control methods have been considered.

3.1 Measurements and instrumentation

Primary measurement sensors for SFE processes require special considerations due to the high operating pressures in operation: Adequate and robust measurement instrumentation is required. A sensor failure could ultimately lead to a control system failure, causing a possible hazard for the operating personnel and plant integrity (Martinez, 2008, p. 41). The control response to process variations must be rapid and effective, and the selection of sensors must be made in terms of sensor failure, leakage, and error possibilities.

3.1.1 Pressure

Bourdon type pressure gauges are the most commonly utilized pressure measurement devices, with pressure ranges up to 7000 bar and a tolerance of only 0.01% of span. Another typical pressure gauge is built on a metallic membrane cell, which are based on

the inclination of a membrane, causing the pressure-proportional variation of the electrical resistance of the system. The pressure range of those systems reaches up to 400 bar, with allowable temperatures up to 100 °C. The so-called dead-end instruments use strain-gauge transducers mounted on a pipe with internal flow. These sensors are based on the elastic deformation of metallic cylinder, which is measured by strain gauges. Measurement ranges up to 15 kilobar can be measured with these devices (Bertucco et al., 2001, pp. 235–237). Thermowells or liquid seals may be required for pressure gauges/transducers. For safety measures, the gauges must include rupture discs (Martinez, 2008, p. 41).

3.1.2 Temperature

In chemical plants, thermocouples and resistance temperature detector (RTD) sensors are applied because they are easy to fit and maintain. Thermocouples are suitable for pressures up to 6 kbar and temperatures up to 800 °C. Above these ranges the exact measurement is negatively influenced by several parameters, and the deviations must be considered. Both methods have a wide temperature range, and their response time is short, making them favorable for high-pressure systems. The small dimensions of these devices further increase their applicability in high pressures. The temperature measurement devices, which do not contact the hot surfaces, for example optical, radiation pyrometers, and infrared (IR) techniques, are not typical for high-pressure applications (Bertucco et al., 2001, pp. 237–238). The response of temperature sensors must be weighed against thermowell isolation (Martinez, 2008, p. 41).

3.1.3 Flow

The use of flow measurement devices in the high-pressure loop of a process step in small-scale plants is necessary to check the mass balance, especially for SFE. Concentric-orifice devices can be easily installed in high-pressure lenses. All the mentioned orifice devices are technically proved and are applied in the high-pressure area. Magnetic flow meters are seldom used in high pressure processing (Bertucco et al., 2001, pp. 238-240). The turbine flow meters are suitable for use at high pressure up to 4000 bar. The measuring device could be easily mounted into high-pressure tubes. For this purpose, small instruments have been developed. Devices using the Coriolis effect are available for moderate pressures, up to 400 bar. For high flow rates the maximum pressure is approximately 250 bar. The advantage of these instruments is their wide range of flow.

Pump and compressor flow rates of SFE processes are commonly measured by Coriolis meters, and flow is controlled by distributed control with computer capability (Martinez, 2008, p. 41).

3.1.4 Fluid level

The knowledge of the level of fluids in different apparatus is important for safe and continuous operation of chemical plants, and level, making the importance of accurate and reliable level sensors significant, for example in supercritical fluid extractors or separators (Martinez, 2008, p. 41). Sight-glasses are available for pressures up to 700 bar. The differential-pressure transmitters are only available for moderate pressures, up to 400 bar. Membrane systems give the possibility of choosing corrosion-resistant materials for the parts of a device, or to protect the inside of the device by using an additional membrane which divides the instrument side from corrosive media. An expensive method is the use of nuclear radiation to obtain information on the level in an apparatus. A continuous level indicator using nuclear radiation is very complicated and thereby seldomly applied. Special constructions use ultrasonic signal devices to measure values for the height of fluids or solids in high-pressure apparatus (Bertucco et al., 2001, pp. 240–241).

3.1.5 Analytes

The growing interest for automation of analytical processes in the end of the twentieth century has led to the development of on-line coupling of the supercritical fluid extractor to optical detectors for measuring properties of analytes. Most of the studies regarding the topic come from this time period.

Thermal lens spectrometry has been shown to be a highly sensitive technique in the ultra-violet and visible region. One study demonstrated the viability of on-line detection for supercritical fluid extraction with a pulse thermal lens spectrometer (Amador-Herández et al., 1999b). Another study discussed the advantages and limitations of monitoring supercritical fluid extraction by thermal lens spectrometry with pulsed laser excitation (Amador-Herández et al., 1999a) The results from both studies implied that a satisfactory estimation of the concentration of the analyte from the analytical signal at optimized process conditions could be reached.

Several applications have succeeded in coupling SFE with Fourier-transform IR detection (Kazarian, 1997). One of these is an application of fiber optic transmission cell obtaining IR spectra of analytes in the extraction of limonene from orange peel (Tilotta, 1996). Another interesting study applied the use of Fourier-transform IR detection to study IR spectra of caffeine as a function of SC-CO_2 density (Morin, 1988). Near-IR fiber optic spectroscopy has been applied to measure mass transfer coefficients and equilibrium solubilities in SFs (Zehnder et al., 1993).

An interface for spectrofluorometric measurements in the supercritical CO_2 emerging from the extraction cell of a supercritical fluid extractor prior to depressurization was developed in a study (Tena et al., 1996). Qualitative and quantitative information from supercritical extracts was obtained by using the coupled devices prior to depressurization and analyte collection.

3.2 General control hierarchy

Industrial process control hierarchy is illustrated in Figure 4. Actuators, such as pumps and valves, as well as sensors are included in the instrumentation layer. The basic control layer is devoted to obtain direct process information and maintaining selected process variables in their targets by means of local controllers, typically proportional-integral-derivative (PID) controllers or its variations, in a feedback loop, the design of which may be model-based or model-free. The advanced control layer handles all interactions, disturbances and process constraints using a process model in order to compute the control actions that optimize a control performance, typically by the means of model predictive control (MPC). Linked to the MPC controller and taking advantage of its model, an optimizer may look for the best operating point of the unit by computing the controller set points that optimize an economic cost function of the process unit considering the operational constraints of the unit. This task is usually formulated and solved as a linear programming problem, i.e. based on linear or linearized economic models and cost function (De Prada, 2014).

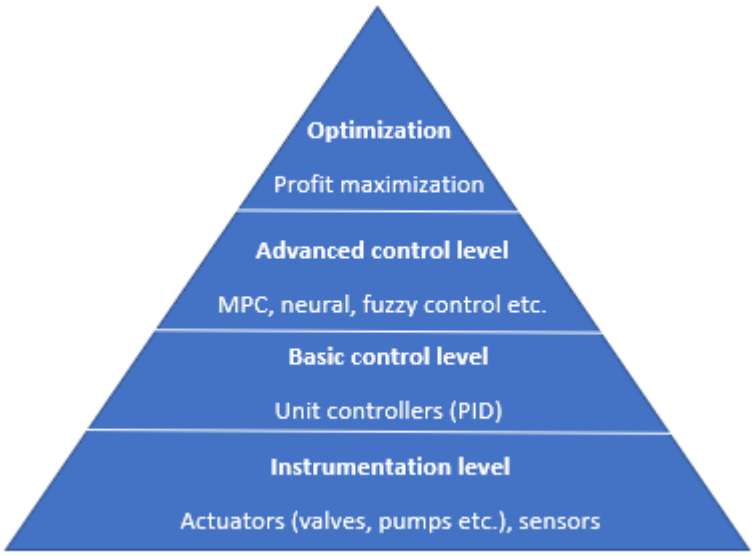

Figure 4. Industrial control hierarchy (modified from De Prada, 2014).

3.2.1 Basic control studies

Previous studies have shown that only using traditional, basic control schemes such as PID controllers generally lead to poor control performance. A simulated control study on the supercritical extraction of beta-carotene from water with CO_2 indicated that the setpoint response of the PI (proportional-integral) controller was acceptable, but its response to disturbance rejection was poor (Cygnarowicz et al., 1990). In another study, Skogestad's Internal Model Control was used to design PI controllers and a hydrodynamic model for an SFE pilot process (Roodpeyma et al., 2018). The resulting controller parameters were largely consistent between these two sources to design data and performance data. The best controllers provided low overshoot, rapid response time, little oscillatory behavior, low integral of the absolute error of the controlled pressure and low total variation of the input carbon dioxide flow. In addition, the hydrodynamic model was used to explore the impact of alternative operating pressure conditions. The nonlinearity led to distinctly different controller parameters and performances at different pressures, thus reinforcing the importance of designing PI controllers to specific operating conditions.

PI controllers have also been tested in separating isopropyl alcohol (iPA) by SC-CO_2 (Ramchandran et al., 1992); it was suggested that the controllers were unable to maintain any of the controlled variables at their desired set-points. PID controllers may be developed and implemented with and without a model, but manual tuning complicates

the targets of optimal control, and the controllers have limitations when applied to more complex systems. However, the commercial industrial SFE systems are mainly controlled using these conventional PID controllers. This could be a result of the lack of demonstrated control and/or the extensive maintenance needs that advanced control systems are deemed to have.

3.2.2 Advanced control studies

Conventional control is based on the assumption of linear behavior of the process. This severely limits control performance, especially when control challenges associated with multivariable control are present (Ramchandran et al., 1992). The utilization of advanced control, such as model-based control, has been researched for SFE processes. Most of the utilized models perform linear approximations of the process or experimental data for predicting the behavior of the process. It has been suggested that model predictive control strategies may lead to improved control (Cygnarowicz et al., 1990). Nonlinear process model-based control has been researched in the separation of iPA from water by SC-CO_2 based on a dynamic simulation model, where the main controlled variable in the process was the composition of iPA in the raffinate and manipulated variable was the solvent flow rate (Ramchandran et al., 1992). The nonlinear process model-based control strategy successfully controlled the process in both stand-alone and integrated mode. For this same process, the use of a decentralized controller for different plant decompositions was also tested. It was concluded that centralized control of a multi-unit process does not always lead to superior control performance in comparison with a strategic decomposition of the multi-unit process (Samyudia et al., 1995). Generic model control was used to bring a mathematical model for a process for decaffeination of coffee using SC-CO_2 into the control logic, and the performance was compared to the one of decoupled PID controllers (Riverol et al., 2005). The generic model control approach led to increases of 0.5–0.8% in the caffeine recovery relative to the PID controlled process.

One study created an MPC framework for improving feasibility, stability, and optimality properties for decentralized control of large, networked systems (Venkat et al., 2007). Communication-Based MPC and Feasible Cooperation-Based MPC strategies were developed in this study. In the Communication-Based MPC formulation, each subsystem's MPC exchanged predicted state and input trajectory information with MPCs of interconnected subsystems until all trajectories converged. In the Feasible

Cooperation-Based MPC formulation, each local objective was replaced by a systemwide objective function. SFE process was used as an example for illustrating the challenges presented by complex coupling between different process units. These strategies and decentralized MPC's were implemented in an SFE process consisting of four process units (extractor, stripper, reboiler and trim cooler) and compared to the centralized MPC approach. The setpoints for raffinate composition and solvent flow rate were unreachable under decentralized MPC. After 1 iterate, the FC-MPC closed-loop performance was found to be 0.35% of centralized MPC performance. After 10 iterates, the closed-loop performance of FC-MPC was indistinguishable from centralized MPC.

Multi-artificial neural network predictive control has been proposed for predicting output variable under disturbance of system flow and pressure (Zhou et al., 2011). The back-propagation artificial neural network controller estimated the optimal control signal by feedback correction and rolling optimization to overcome the time-variation and inertia. Results indicated that the strategy has excellent dynamic response performance, small steady-state error, and strong robustness.

A fuzzy logic control system was developed for pilot-scale SFE process for extracting edible oils from seeds (King et al., 1996, pp. 137-141). The controller was tuned based on the experience of manual operation of the process. The SFE process was represented by a highly interacting 3x3 multiple-input-multiple-output system having the CO_2 recycling rate and the extractor and separator pressures as output variables and the air pressure to the gas booster, and to the extractor and separator control valves as manipulated variables. Three control pairs between manipulated and controlled variables were selected, and a set of 49 fuzzy control rules were defined. The proposed fuzzy control scheme was found to be successful in experiment and simulation.

4 EXPERIMENTAL METHODS

This study aims to identify the target SFE system by data-driven system identification, forming a complete simulator of unit process and energy consumption responses. Utilizing this simulator, MPC strategies for unit processes are developed for find the optimal sequence of inputs for reaching desired conditions and optimizing energy consumption. Identifying the model of a previously unknown process unit requires systematical designing of experiments, and throughout analysis of output data. A good design can lead to maximally informative experiments which reduce operational costs associated with identification tests. The design of the experiments is heavily dependent on process behavior, which needs to be thoroughly screened and analyzed in preliminary experimental runs. As the basic level PID control loops act as base for the identified model, the control loops should be tuned as sufficiently as possible. In this chapter, the experimental methods used in this study for PID controller tuning, system identification and model predictive control are covered in detail.

4.1 PID controller tuning

PID control is a control algorithm that utilizes process feedback. PID controller calculates an error value (difference between setpoint and measured process variable) and applies a correction based on the P (proportional), I (integral) and D (derivative) terms. PID controllers are the most widely used industrial controllers. Even complex industrial control systems may comprise a control network whose main control building block is a PID control module (Johnson et al., 2005, p. 1).

With advances in digital technology, the science of automatic control now offers a wide spectrum of choices for control schemes. However, more than 90% of industrial controllers are still implemented based around PID algorithms, particularly at lowest levels as no other controllers match the simplicity, clear functionality, applicability, and ease of use offered by the PID controller (Ang et al., 2005). PID control does however have significant disadvantages. Maybe the most important one is that PID control assumes linear behavior of the system since it uses linear feedback functions, making it difficult, and in some cases impossible to stabilize a nonlinear system with PID-control alone. Also, multiple-input-multiple-output PID control is much less understood and developed,

compared with the single variable case and actual need for industrial applications (Wang et al., 2008). A standard-form PID controller in a process feedback loop is presented in Figure 5.

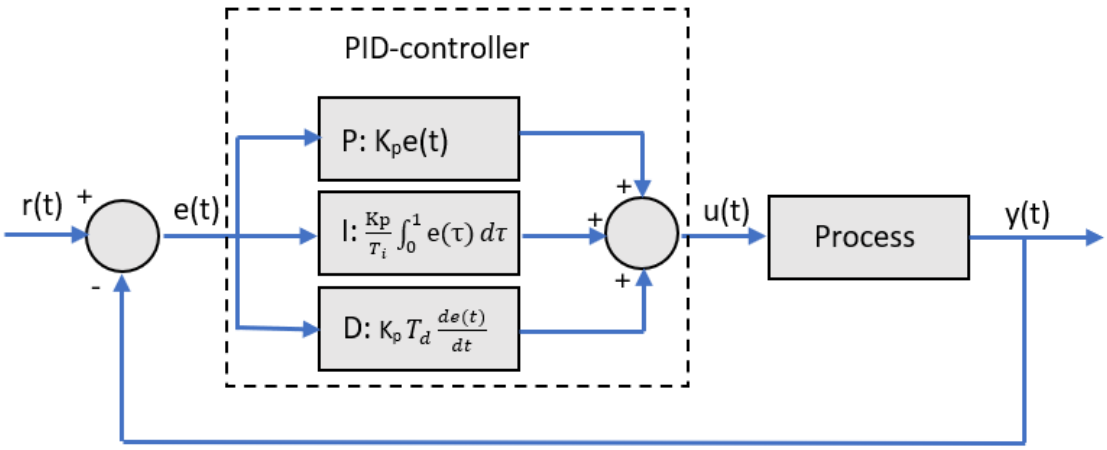

Figure 5. Schematic of a standard-type PID controller in a feedback loop, where r is the process reference (setpoint), u is the process input variable, and y is the measured process output variable.

Since the operating conditions determine the SFE process critically, the base level control performance should be improved to a level where setpoints are reached with minimal oscillation. Although a PID controller has only a few adjustable parameters, the optimization of these parameters in the absence of a systematic procedure is not a trivial task; thus, many industrial controllers are poorly tuned (Shamsuzzoha, 2018, p. 1). The structure of these terms and the change in the proportionality constants change the type of response of the system, which is why PID tuning is very important. In addition, special considerations must be made for varying process dynamics.

4.1.1 PID algorithm

In practice, manufacturers of controllers do not adhere to industry wide standards for PID algorithms, and different manufacturers use different PID algorithms and sometimes have several algorithms available within their own products. However, three major groups of algorithms used by manufacturers exist: Standard or ideal (Equation 1), parallel (Equation 2), and series or interacting (Equation 3). Out of these three, the standard form algorithm is the most commonly encountered in history and the most relevant to tuning techniques

(Åström, 2002; Metso, 1987). The common PID algorithm structures are presented in the following equations:

$$u(t) = K_C e(t) + \frac{1}{T_I}\int_0^1 e(t)\,dt + T_D\frac{de(t)}{dt}; \quad (1)$$

$$u(t) = K_C\left(e(t) + \frac{1}{T_I}\int_0^1 e(t)\,dt + T_D\frac{de(t)}{dt}\right); \quad (2)$$

$$u(t) = K_C\left[\left(\frac{T_D}{T_I}+1\right)e(t) + \frac{1}{T_I}\int_0^1 e(t)\,dt + T_D\frac{de(t)}{dt}\right]; \quad (3)$$

where K_C is the proportional (or controller) gain,
e is the error (difference between measured output and setpoint),
T_I is the integral time (or reset time), and
T_D is the derivative time (or rate).

The functionalities of a standard PID controller can be presented in terms of different gains: The proportional gain, integral gain $K_I = K_C/T_I$, and derivative gain $K_D = K_C \cdot T_D$. Sometimes, the proportional gain is expressed in terms of proportional band, which is typically determined according to the following equation (Metso, 1987):

$$PB = \frac{100}{K_c}, \quad (4)$$

where PB is the proportional band.

PID controllers used in this study are treated as standard-form controllers. The modifiable parameters of these controllers are proportional band, reset time, and rate.

4.1.2 Manual and Lambda tuning

PID tuning refers to the adjustment of PID algorithm parameters for reaching optimal control performance. Understanding the general effect of the PID controller parameters is essential in tuning. Increasing K_C has the effect of proportionally increasing the control signal. This results in closed-loop system reacting more quickly, but also to overshoot more. Also, the proportional term minimizes but does not eliminate the steady state error. Increasing K_I eliminates steady-state error at the cost of sustained oscillations. On the contrary, increasing the K_D results in decreased amounts of oscillations, but does not affect the steady-state error (Bansal et al., 2012). The individual effects of these three

terms on closed-loop performance, which are commonly utilized in manual controller tuning, are summarized in Table 2.

Table 2. Commonly utilized guidelines for manual PID controller tuning (modified from Metso, 1987; Goodwin et al., 2000).

Closed-loop response	Rise time (process value changing from 10% to 90% of reference)	Overshoot (peak deviation from reference)	Settling time (process value settling within 5% of reference)	Steady-state error (deviation from reference after settling)	Stability
Increasing proportional gain	Decrease	Increase	Minor decrease	Decrease	Decrease
Increasing integral gain	Minor decrease	Increase	Increase	Major decrease	Decrease
Increasing derivative gain	Minor decrease	Decrease	Decrease	Minor decrease	Increase

Every tuning involves two steps: 1) experiments undertaken over the process to measure some characteristics of this process; 2) controller tuning is then done based on the measurements obtained during the tests (Shahrokhi et al., 2012). PID controller tuning methods can be classified into two main categories: Open-loop and closed-loop tuning. Open-loop techniques refer to tuning a controller in open-loop (manual) mode; whereas in closed-loop techniques, the controller is tuned when the plant is operating in closed-loop (automatic) state by making changes to the setpoint, causing the output to react indirectly. These methods are generally not desired for determining PID controller parameters, since most models are formed between the control and measurement signals; thus, not all information between the setpoint change and controller output can be utilized (Harju et al., 2000). Also, closed-loop methods are typically based on trial-and-error and lead to time consuming operations (Roodpeyma et al., 2018). Closed-loop methods do however have some advantages over open-loop methods, such as safer and easier executes during normal operation, since the process value is guaranteed to settle at the new setpoint, unless the loop is tuned to be unstable. Some known closed-loop methods include the Ziegler-Nichols method, Tyreys-Luyben method and damped oscillation method (Shahrokhi et al., 2012). Purely manual tuning is also classified as a closed-loop method.

Well known open-loop methods are the open-loop Ziegler-Nichols method, the Cohen-Coon method, the Fertik method and the Internal Model Control method (Shahrokhi et al., 2012). In these methods, a step input is applied to the plant and the process reaction curve is obtained, and process dynamics are approximated by a simple model such as a First Order Plus Dead Time estimation model:

$$G(s) = \frac{K_P}{\tau s+1} e^{-DTs}, \tag{5}$$

where K_P is the process gain (steady state change of the controlled variable divided by the change in the manipulated variable),
τ is the dominant time constant (the time for the system's step response to reach 63% of steady-state process value), and
DT is dead time (time of delay for the process to react to a step input change due to instrumentation/transportation lag).

Open-loop tests disturb the process and require the attention of operators, a typical disadvantage of open-loop tuning. Due to this, and the lack of required skills, many operators of industrial processes resort to closed-loop, and specifically manual trial-and-error tuning in practice (Ruel, 2010).

Lambda tuning is a model-based tuning method related to Internal Model Control and has proven successful in multiple control loops of different industries. The process dynamics are typically identified from step testing in manual mode, which identify the nonlinearities in the process (Coughran, 2013). The purpose of the method is to generate smooth, non-oscillatory control efforts when responding to changes in the setpoint by utilizing a user-specified parameter lambda (λ) that determines how long the controller is allowed to spend on the task of changing the process variable to a desired value. This parameter can be chosen according to wanted control strategy. The tuning methodology aims at producing a “critically damped,” non-oscillatory response, making it also suitable for integrating processes (Beall, 2016a)

The Lambda tuning procedure involves the following steps (Beall, 2016a):

1) Identify the process dynamics
2) Choose the desired closed-loop speed of response (λ)
3) Calculate the required PID tuning constants

For stable (self-regulating) processes, the process gain (K_P) is calculated according to the following equation:

$$K_P = \frac{\Delta PV}{\Delta CO}, \tag{6}$$

where ΔPV is the difference between initial and final process values, and
ΔCO is the difference between initial and final controller outputs.

If controller output is denoted in percent (%), the process values must be scaled in a similar manner as well. The PID tuning parameters can be calculated according to the following equations:

$$K_C = \frac{\tau}{K_p(\lambda+\mathrm{DT})}; \tag{7}$$

$$T_I = \tau; \tag{8}$$

$$T_D = 0; \tag{9}$$

where K_c is the proportional gain,
T_I is the integral time, and
T_D us the derivative time.

For integrating processes, the dynamics differ significantly from self-regulating processes, as the process value does not settle when constant controller output is provided. Due to this, the time constant of the process is unfeasible to determine. Instead, the process gain can be calculated using the differing slopes of process variable after a step change (Figure 6).

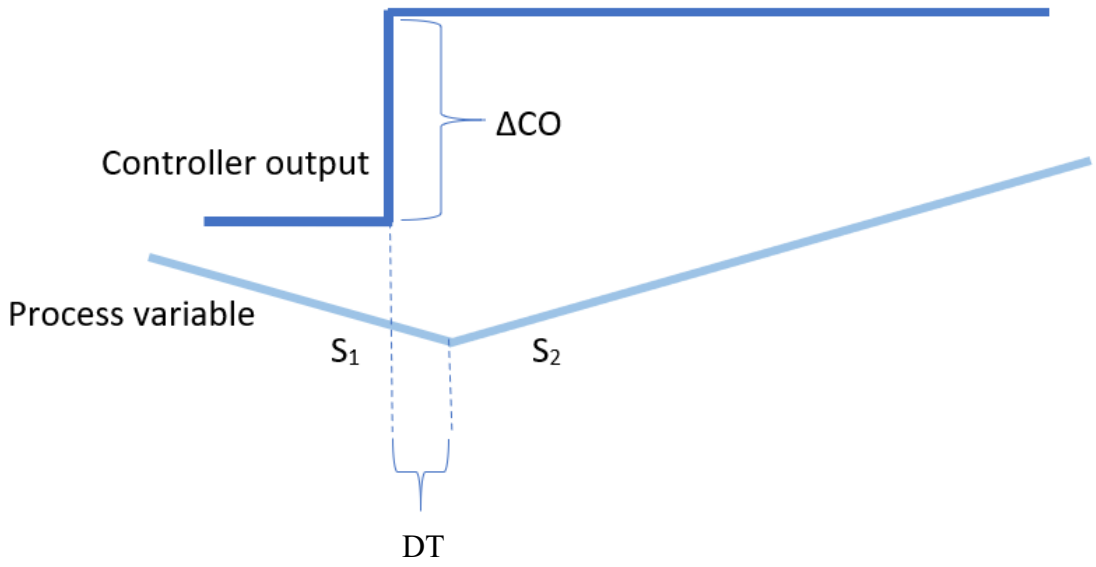

Figure 6. Identification of integrating process dynamics for Lambda tuning, where S1 is the initial slope of the process variable, S2 is the final slope of the process variable, DT is dead time, and ΔCO is the difference between initial and final controller outputs (modified from Coughran, 2013).

The process gain is calculated according to:

$$K_p = \frac{S_2 - S_1}{\Delta CO} = \frac{\mathrm{DS}}{\Delta CO}, \tag{10}$$

where S_1 is the initial slope of the process variable,

S_2 is the final slope of the process variable, and

DS is the difference between initial and final slopes of the process variables.

The PID controller parameters can be determined according to:

$$K_c = \frac{2\lambda + \mathrm{DT}}{K_p(\lambda + \mathrm{DT})^2} \tag{11}$$

$$T_i = 2\lambda + T_d \tag{12}$$

$$T_d = 0 \tag{13}$$

These equations are valid for standard and series PID algorithms implementation. Controller gain and integral time depend on the desired value for λ: a small value is typically picked for good load regulation, whereas a large value suits minimizing changes

in the controller output and manipulated variable by allowing the process variable to deviate from the set point. (Beall., 2016a)

4.2 System identification

Modeling of processes is an important topic in many disciplines of engineering and science. Standard modeling approaches can be classified in two main ways: In first principles modeling (also known as theoretical modeling or white-box modeling), the mechanisms of the processes are represented by analytic equations which must be simplified. This approach is based on a thorough understanding of the system's physical and chemical phenomena, represented by mathematical equations such as a simplified transfer function. However, real systems are usually too complex and poorly understood for a complete theoretical construction to be made on an acceptable level of complexity and accuracy. This is specifically true in the case of SFE processes, where the complex interaction of affecting factors and lack of knowledge on the in-depth fluid dynamics of supercritical fluid in extraction are vividly present (Sharif et al., 2014). In addition, first principles modeling is relatively time consuming, and completed model may end up unnecessarily complex (Ikonen et al., 2002, p. 5).

In complex processes, variables characterizing the behavior of the considered system can be measured and used to construct a model. This procedure of experimental modeling is usually called identification (Ikonen et al., 2002, p. 6). The models identified through this procedure are referred to as black-box models or data-driven models. The identification procedure is quite straightforward and easy if appropriate process data is available. This route seems more suitable over first principles modeling in SFE identification due to the saved design time, although collecting of valid input-output observations can be time consuming. The model identification procedure is illustrated in Figure 7.

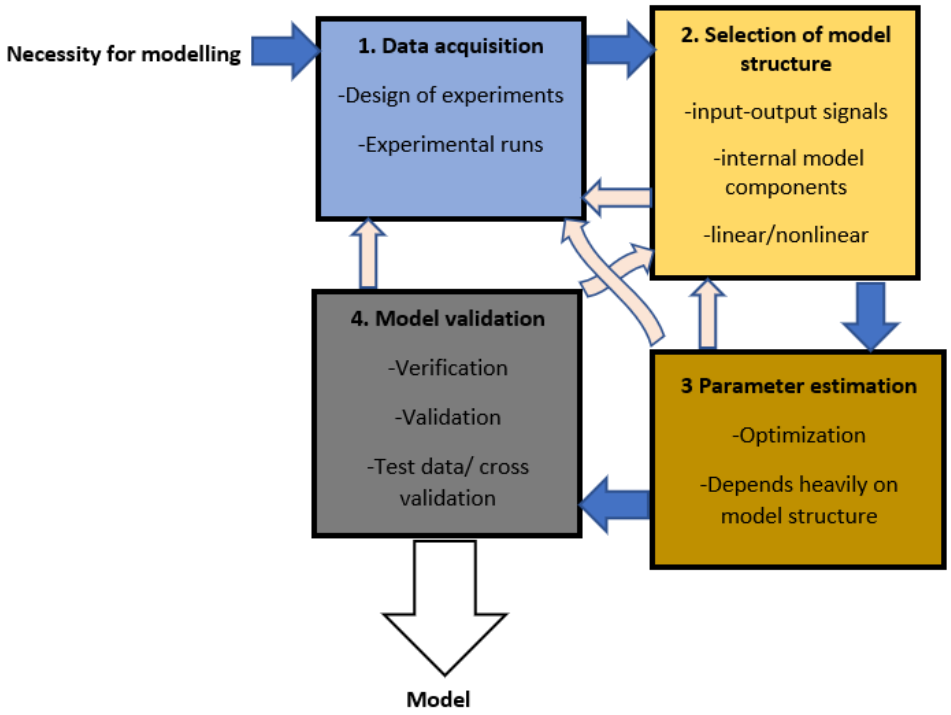

Figure 7. Model identification procedure (modified from Ikonen et al., 2002).

Despite the straightforward nature of system identification, the procedure is iterative, and may require returning to previous steps multiple times before a desired model is formed. The causes for model deficiency may include lack of informative data due to poor experimental design, model set not containing a good description of the system, badly chosen criteria or failing to find a good fit according to criterion (Zhu, 2001, p. 3).

4.2.1 Central composite design

The objective of experimental design is to understand which set of variables in a process affects the performance most and then determine the best levels for these variables to obtain satisfactory output performance (Antony, 2014, p. 2). Depending on the raw material and target extractives, supercritical fluid extraction can be run in a variable number of conditions. Therefore, the base experimental design for the identification experiments should cover a wide range of operating parameter values (temperature, pressure, flow). All combinations of these variables in sufficient amount of levels would require an extensive number of experiments. However, with proper experimental design, the same or better information can be obtained with as few as 20 trials. Central composite design (CCD) is a response surface based on a two-level factorial experimental design with center points augmented with a group of 2K (K is the number of design factors) “star points” between the axes (Wagner et al., 2014; Filliben et al., 2003). CCD as an experimental design is suited for determining linear and nonlinear interactions of factors,

and it can be also used for process optimization. The distance from the center of the design space to a star point is $|\alpha| > 1$, where the value of α and the number of center point runs are dependent on certain properties of the design and the number of factors. The star points represent new extreme values for each design factor (Filliben et al., 2003). In any design, all experimental points must be physically for the process to reach. Figure 8 illustrates the experimental space for a three-factor circumscribed CCD, where the start points are located at a symmetric circular distance α from the center.

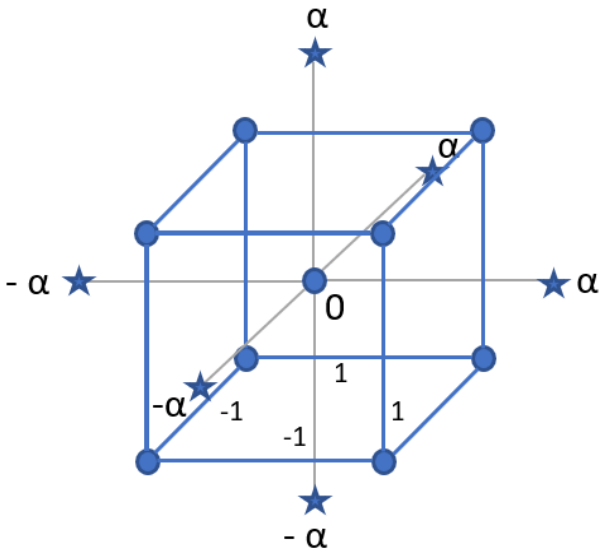

Figure 8. Circular CCD design for three factors, where α is the distance from a center point to a star point (modified from Diamond, 2001; Filliben et al., 2003).

Circumscribed CCD is "rotatable" since the variance of the predicted response at any point depends only on the distance from the center point. To maintain this rotatability, the value of α depends on the number of experimental runs in the factorial portion of the central composite design. In the case of a full-factorial design with three factors, the value for α is calculated using the following equation:

$$\alpha = (2^K)^{\frac{1}{4}} = (2^3)^{\frac{1}{4}} \approx 1.682 \quad (14)$$

The coded CCD design for factors U_1, U_2 and U_3 is illustrated in Table 3. The terms –1 and +1 have the same meaning here as in a Hadamard matrix (the limits of the spaces of factors), and 0 level is the center value. It is significant to note that all the points in the design must be within safe/feasible process values. Therefore, the operating space of factors should be determined so that the star points are inside these physical limits.

Table 3. Coded CCD design for three factors (only valid when $\alpha = 1.682$).

	Run	U_1	U_2	U_3
Matrix trials	1	–1	–1	–1
	2	1	–1	–1
	3	–1	1	–1
	4	1	1	–1
	5	–1	–1	1
	6	1	–1	1
	7	–1	1	1
	8	1	1	1
Star trials	9	–1.628	0	0
	10	1.628	0	0
	11	0	–1.628	0
	12	0	1.628	0
	13	0	0	–1.628
	14	0	0	1.628
Center trials	15	0	0	0
	16	0	0	0
	17	0	0	0
	18	0	0	0
	19	0	0	0
	20	0	0	0

The execution order of these experiments should be randomized for statistical integrity. After the experiments are conducted, the interactions and results can be computed according to Table 4. Terms in each column are multiplied by the corresponding result, and the total interactions are calculated by summing each term in the column.

Table 4. Computation of interaction terms and results of CCD, where y is the measured process output (only valid when $\alpha = 1.682$).

U_1U_2	U_1U_3	U_2U_3	U_1^2	U_2^2	U_3^2	y
1	1	1	1	1	1	y_1
–1	–1	1	1	1	1	y_2
–1	1	–1	1	1	1	y_3
1	–1	–1	1	1	1	y_4
1	–1	–1	1	1	1	y_5
1	–1	–1	1	1	1	y_6
–1	–1	1	1	1	1	y_7
1	1	1	1	1	1	y_8
0	0	0	2.650	0	0	y_9
0	0	0	2.650	0	0	y_{10}
0	0	0	0	2.650	0	y_{11}
0	0	0	0	2.650	0	y_{12}
0	0	0	0	0	2.650	y_{13}
0	0	0	0	0	2.650	y_{14}
0	0	0	0	0	0	y_{15}
0	0	0	0	0	0	y_{16}
0	0	0	0	0	0	y_{17}
0	0	0	0	0	0	y_{18}
0	0	0	0	0	0	y_{19}
0	0	0	0	0	0	y_{20}

The column totals can be used to calculate the β coefficients of quadratic linear regression equation according to (Diamond, 2001). A regression program, such as corresponding MATLAB® functions, can be used in fitting the parameters of the following quadratic model:

$$Y = \beta_0 + \beta_1 U_1 + \beta_2 U_2 + \beta_3 U_3 + \beta_{12} U_1 U_2 + \beta_{13} U_1 U_3 + \beta_{23} U_2 U_3 + \beta_{11} {U_1}^2 + \beta_{22} {U_2}^2 + \beta_{33} {U_3}^2, \quad (15)$$

where Y is the modelled response, and

β is a coefficient of a term in the quadratic regression model.

The significance of the independent coefficients can be evaluated by looking at the T and P factors. High T and small P (≤ 0.1) indicate that the coefficient is significant. It is also possible to use both analysis of variance (ANOVA) and F-test in the same connection The results of the regression analysis can be utilized in determining the significance of linear, nonlinear, and correlative interactions of the design factors on the response. (Diamond, 2001).

4.2.2 Choosing input signals

Around the operating conditions of each experiments determined by CCD, the system is excited by smaller amplitude signal sequences for gathering informative data for system identification. In context of practical industrial process identification, the target of these sequences is to gain further dynamical data without disturbing normal operation.

The form of the input is often determined by the identification method. The input must be sufficiently rich to excite all process modes of interest during the experiments. Another requirement is that the input signal should be constructed to minimize certain model errors with respect to noise, input, and output signals (Payne, 1973; Isermann, 1980). Sampling time needs to be selected properly before the experiments, since it cannot be decreased afterwards (Isermann, 1980). The higher the number of samples, the more cost of analysis with large amounts of data and computing power. In practice, this choice has not been found to be critical and the sampling period is usually chosen to be of the same order of magnitude as the smallest time constant of interest (Payne, 1873).

Since many of the choices in designing a system-identification experiment require knowledge of the unknown system, the experiments are typically done in two steps. Preliminary experiments such as impulse and step responses are performed to gain primary knowledge about important system characteristics such as stationary gain, time delay and dominating time constants, and it should be possible to draw conclusions from these experiments on whether the system is linear and time invariant and if there are disturbances acting on the system. The obtained information allows the determination of the conditions for the main experiments. This procedure already shows the iterative nature of system identification. (Andersson et al., 2006; Verhaegen et al., 2007, p. 346)

For main identification experiments, it is typically useful to sequences with differing pulse lengths: Constant over such long periods that the step response settles, as well as shorter pulses that cover the rise time but will not result in the settlement of the process. The pulses should be made in both directions for unveiling the possible nonlinearity of the process. Pseudo-random binary sequence (PRBS) is a common choice of input signal, since it has a large energy content in a large frequency range. However, transient methods like step functions are easily generated and applied to the system, making them convenient for approximating the system from its step response. For manually inserted inputs, step sequences are more feasible to apply compared to computational sequences such as PRBS. (Ljung et al., 1994; Andresson et al., 2006)

4.2.3 State-space modeling

The model structure is generally derived using prior knowledge of the process. The input-output signals and internal components of the model are determined in this step of the identification procedure. For dynamic systems, the choice of model order should be chosen as a compromise to reducing the unmodelled dynamics and increasing the complexity of the model. Most of the suggested criteria can be seen as a minimization of a loss function (for example prediction error prediction error, or Akaike Information Criterion.) In many practical cases, a second order (or even a first order) model is adequate (Ikonen et al., 2002, p. 10).

Much of system identification theory has been developed by the adaptive estimation and control community, resulting in the natural emphasis being in input-output models such as transfer functions. However, modern control is built up on state-space models, which can provide insights into the control problem that may be more difficult to see from the input-output perspective. In the state-space form, the relationship between input and output is written as a first-order differential equation system using a state vector (x). This description of a linear dynamic system became a primary approach after Kalman's work on modern prediction and linear quadratic control (Goodwin and Payne, 1977; Liu, 2017; Ljung et al., 1994).

A linear time-invariant and time-discrete system can be described by the following state-space representation (Liu, 2017):

$$x(k+1) = Ax(k) + Bu(k); \tag{16}$$

$$y(k) = Cx(k) + Du(k); \tag{17}$$

where x is the state vector,
y is the output vector,
u is the input vector,
A is the state (or system) matrix,
B is the input matrix,
C is the output matrix, and
D is the feedthrough matrix.

With classical identification algorithms, priori knowledge of the order and of the observability indices is required for parameter estimation (Ljung, 1999). Using N4SID (numerical algorithm for subspace system identification) algorithms, most of this a priori parametrization can be avoided. The order of the system can be determined through inspection of the dominant singular values of a matrix that is calculated during the identification. The state-space matrices are calculated as full state-space matrices in a uniquely determined optimally conditioned basis. N4SID algorithms are non-iterative, and therefore they do not suffer from the typical disadvantages of iterative algorithms (no guaranteed convergence, local minima of the objective criterion, sensitivity to initial estimates etc.) (Van Overschee et al., 1994). The conceptual straightforwardness of subspace identification algorithms translates into user-friendly software implementations since the user is not confronted with highly technical and theoretical challenges such as canonical parametrizations. The routes of N4SID and classical parameter estimation methods are illustrated in Figure 9.

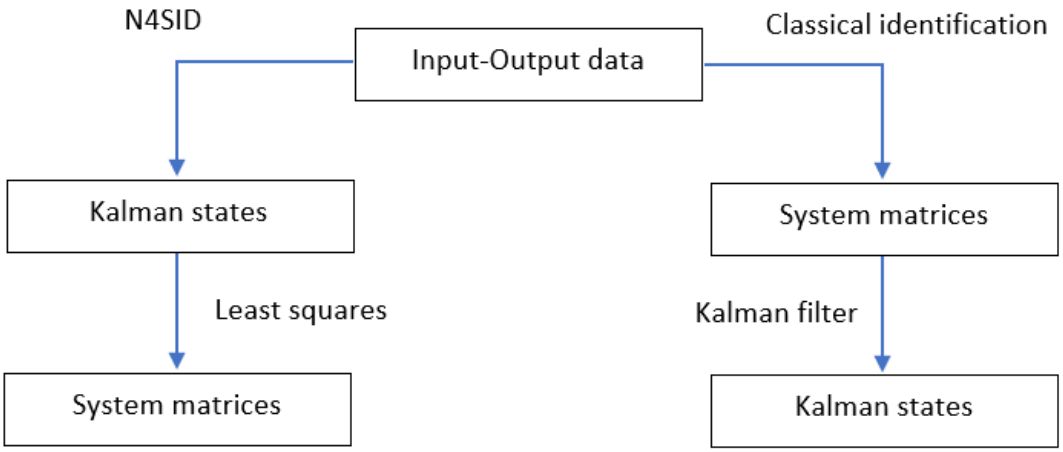

Figure 9. The routes of parameter estimation for the N4SID and classical identification methods (modified from Van Overschee et al, 1994).

In model validation, the "goodness" of the model is assessed. Utilized methods depend on the desired properties from the model. Typically, interpolating/extrapolating are the abilities desired from the model. Accuracy and generalization can be tested by cross-validation techniques (Ikonen et al., 2002, p. 11). Most model validation tests are based on simply the difference between the simulated and measured output: A suitable model should agree with the experimental data, it should describe the process accurately, and it should meet the purpose it was obtained for. It is also possible to reduce the model and compare it with the original model to see a simpler model suffices (Mikleš et al., 2007, pp 221–222). Often prior knowledge concerning the process to be modeled and statistical tests involving confidence limits are used to validate a model.

4.3 Model predictive control

MPC is a commonly used abbreviation for model predictive control. On some occasions, the same abbreviation is used for model-based process control, which denotes all control approaches making use of a process model (including model predictive control). In industry, MPC has become a synonym for multivariable control and advanced process control (Ikonen, 2017). MPC does not describe a specific control strategy, but rather a range of control methods which make explicit use of a model of the process to obtain the control signal by minimizing an objective cost function.

The introduction of MPC affects particularly the layer of advanced control, where MPC has the potential to replace the various cascade, feedforward, and other similar control structures by a model-based optimization approach. A series of advantages are presented by MPC over other methods, which include easier tuning, multivariable applicability, intrinsic compensation for dead times, disturbance compensation and possibility of systematic inclusion in process design. However, major challenges in industrial MPC still exist, including time-consuming model development, lack of robustness, and computational complexity (Ikonen, 2017). Despite this, (linear) MPC has proven to be a reasonable strategy for industrial process control, and many applications are currently used in process industries (Camacho et al., 2007, p. 2).

The ideas appearing in an MPC scheme (Figure 10) include: (1) explicit use of a model to predict the process output at future time instants, i.e. prediction horizon (p); (2) calculation of a control sequence over a control horizon (c) minimizing an objective function (J) within the limits of constraints, so that the predicted process output ($\hat{y}$) is as close to the reference (r) as possible; and (3) receding strategy, so that at each instant the horizon is displaced towards the future, which involves the application of the first control signal of the sequence calculated at the first step. (Camacho et al., 2007, p. 1).

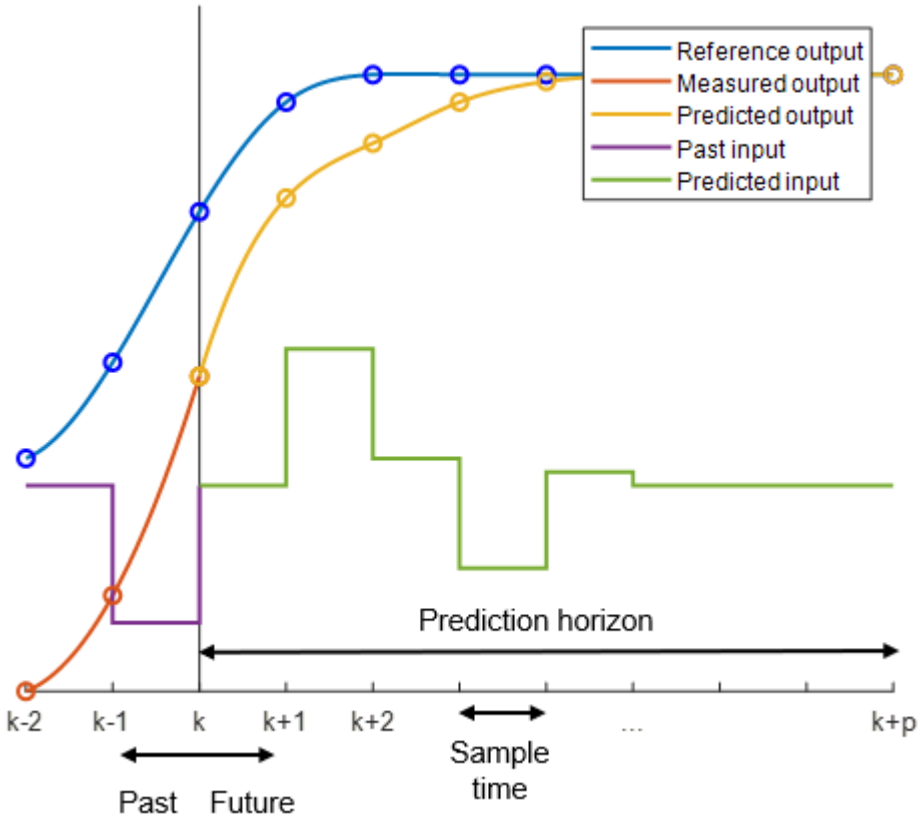

Figure 10. Example of a discrete MPC scheme, where k is the sampling instance, and p is the prediction horizon (modified from Behrendt, 2009).

The basic components of MPC are the dynamic process model, constraints, and optimization algorithm. The process model, which is the core of MPC, should be complete enough to capture the process dynamics and should also be capable of allowing the predictions to be calculated, and simultaneously to be intuitive. The constraints and targets are defined process dependently (Camacho et al., 2007, pp. 13–15; Posio, 2002). The placing of a model predictive controller in a process feedback loop is shown in Figure 11.

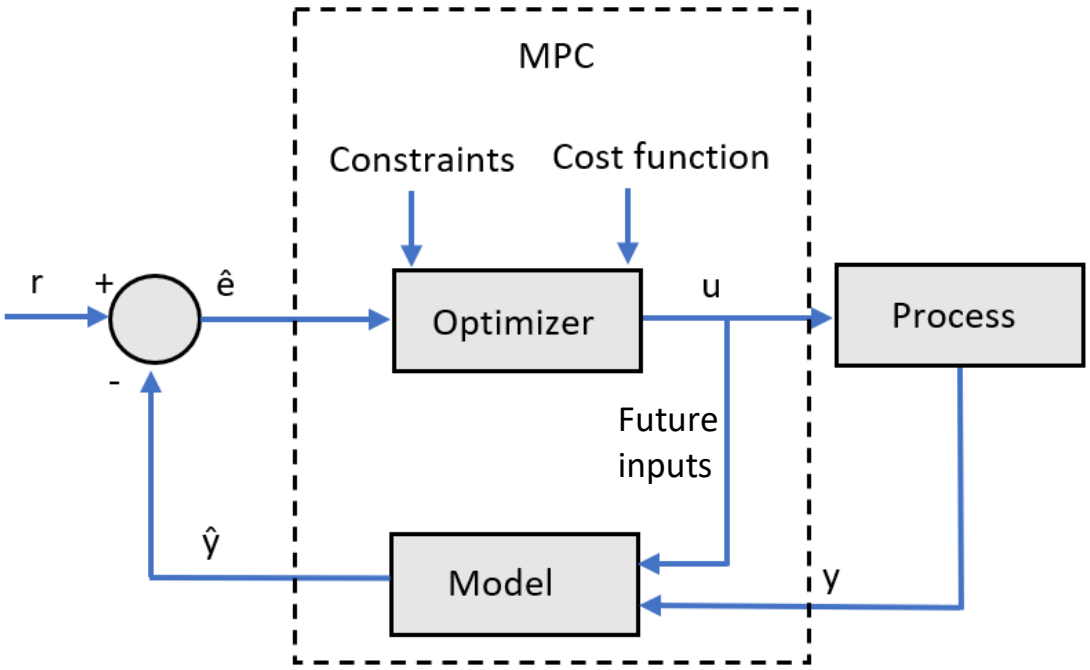

Figure 11. Placing of a model predictive controller in a process feedback loop, where r is the reference, u is the process input, y is the measured process output, ŷ is the predicted process output, and ê is the predicted error value (modified from Da Costa Mendes, 2016).

Given i = 1…p–1, the predicted initial process values ŷ(k+i) are described as a function of the current state x(k) of the process and the future control signals u(k+i), i = 1…c–1. If c is chosen to be smaller than p, the control signals can be manipulated only in a period of c, and the control signal stays constant post control horizon.

The future control sequence u(k+1) is calculated by optimizing a cost function (J). A classical cost function looks as follows (Ikonen, 2017):

$$J = a\sum_{i=1}^{p}\left(r(k+i) - \hat{y}(k+i)\right)^2 + b\sum_{i=1}^{c-1}\Delta u(k+i)^2, \quad (18)$$

where k is the sampling instant,
Δu is the manipulated variable rate (u(k) –u(k–1)),
a is the controlled variable weighing factor, and
b is the manipulated variable rate weighing factor.

The first term of the cost function covers the squared deviations of predictions from the reference, whereas the second term covers the effect of control move rates. The weighing factors a and b determine the effect of these terms in relation to each other and the

prediction step. The cost function can be varied in many ways, such as including a term for the absolute value of manipulated variable u. Minimization of the classical cost function is a classical optimization problem, subject to constraints in the controlled variable, manipulated variable and change of manipulated variable (Posio, 2002):

$$\min_{\Delta u} J$$

$$y_{min} < y < y_{max}; \tag{19}$$

$$u_{min} < u < u_{max}; \tag{20}$$

$$\Delta u_{min} < \Delta u < \Delta u_{max}; \tag{21}$$

where y_{min}, y_{max} are constraints for controlled variable,
u_{min}, u_{max} are constraints for manipulated variable, and
Δu_{min}, Δu_{max} are constraints for manipulated variable rates.

The optimization problem is solved at every sampling instant. Only the first value from the resulting control sequence is then applied to the process. At the next time instance, the predicted process value is available, and predicting and optimization is performed with the updated values according to the receding horizon.

5 IDENTIFICATION OF SFE PROCESS

The target supercritical fluid extraction system of this study and the conducted experiments are described in this chapter. The results of process behavior screening, PID controller tuning, and unit process identification are also presented.

5.1 Target process

The target process of the experiments is a pilot-scale supercritical fluid extraction unit Xtractor® 500/35 with a 2-liter batch extractor, manufactured by Chematur Ecoplanning Ltd (Figure 12). The system is promoted as being designed for research institutes, universities, and commercial production plant test laboratories. However, the system has not been used in active research since the late 1990's.

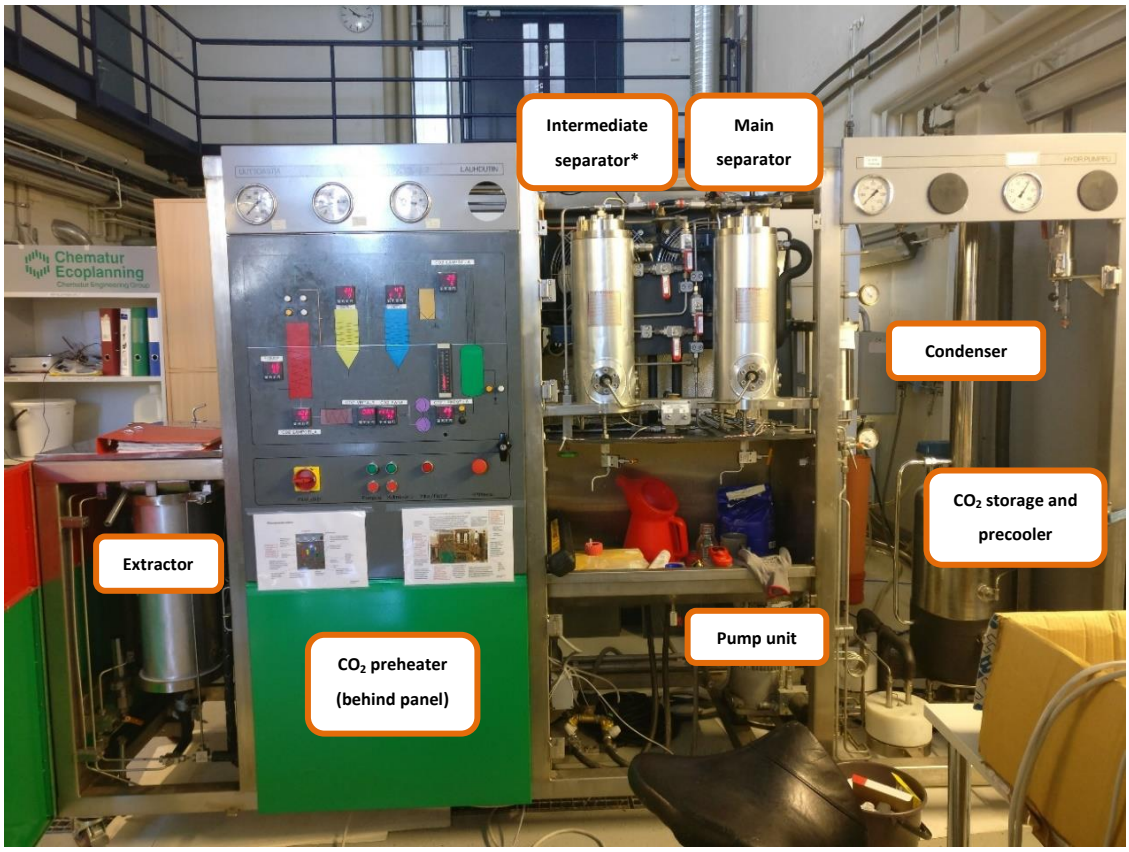

Figure 12. The target supercritical CO_2 extraction system with descriptions of main units (*not utilized in this study).

The specifications of the process system are presented in Table 5. The unit is built on a skid mounted frame, which can be directly connected to an electrical network, cooling water system and carbon dioxide storage.

Table 5. Target system specifications, as given by the manufacturer.

Specification (unit)	Value
Pilot unit size: length x width x height (mm)	3000 x 800 x 1800
Storage maximum pressure (bar)	75
Storage minimum temperature (°C)	–5
Storage maximum temperature (°C)	75
Storage capacity (m^3)	0.035
Pump motor maximum power (W)	750
Extractor maximum pressure (bar)	500
Extractor maximum temperature (°C)	280
Extractor capacity (m^3)	0.002
Extractor heater power (W)	3000
Separator 1 maximum pressure (bar)	200
Separator 1 maximum temperature (°C)	100
Separator 1 capacity (m^3)	0.003
Separator 2 maximum pressure (bar)	75
Separator 2 maximum temperature (°C)	100
Separator 2 capacity (m^3)	0.0035

5.1.1 Process description and equipment

The CO_2-loop consists of two high pressure membrane pumps, a hydraulic aggregate, heater, adjustable constant flow valve, two separator units and one condenser, precooler, and a storage tank. CO_2 is precooled using a cooling coil located inside the CO_2 storage. The subcooling prevents the CO_2 from boiling prior to pumping. The precooled CO_2 is then compressed and heated up to a desired level in a preheater and led to the extractor. After dissolving the organic impurities, the CO_2 passes through a pressure release valve which is specifically designed to allow a constant mass to flow through. In the pressure release valve, the pressure and temperature are decreased from the extraction conditions down to 80–200 bar and 60–120 °C. The CO_2-extractive mixture can be optionally directed into an intermediate separator before the main separator. The intermediate separator can be operated in pressures up to 200 bar and temperatures up to 100 °C, and the components that are less extractable in the conditions of the main separator can be extracted. The intermediate separator is bypassed in this study; therefore, it is not covered in detail. The CO_2/extractive mixture is led to the main separator at 50–80 bar and

15–30 °C where all residual components are separated. The separated, gaseous CO_2 is led to the condenser where gaseous CO_2 is condensed. An activated carbon filter is placed between the main separator and condenser to eliminate any compounds from circulating in the system. The liquid CO_2 is led to a storage tank, ready to be re-used. A cooling unit is connected to the evaporation and cooling process allowing maximum energy efficiency. Surplus energy can be used for preheating the compressed CO_2. The schematic diagram of the target process system is presented in Figure 13.

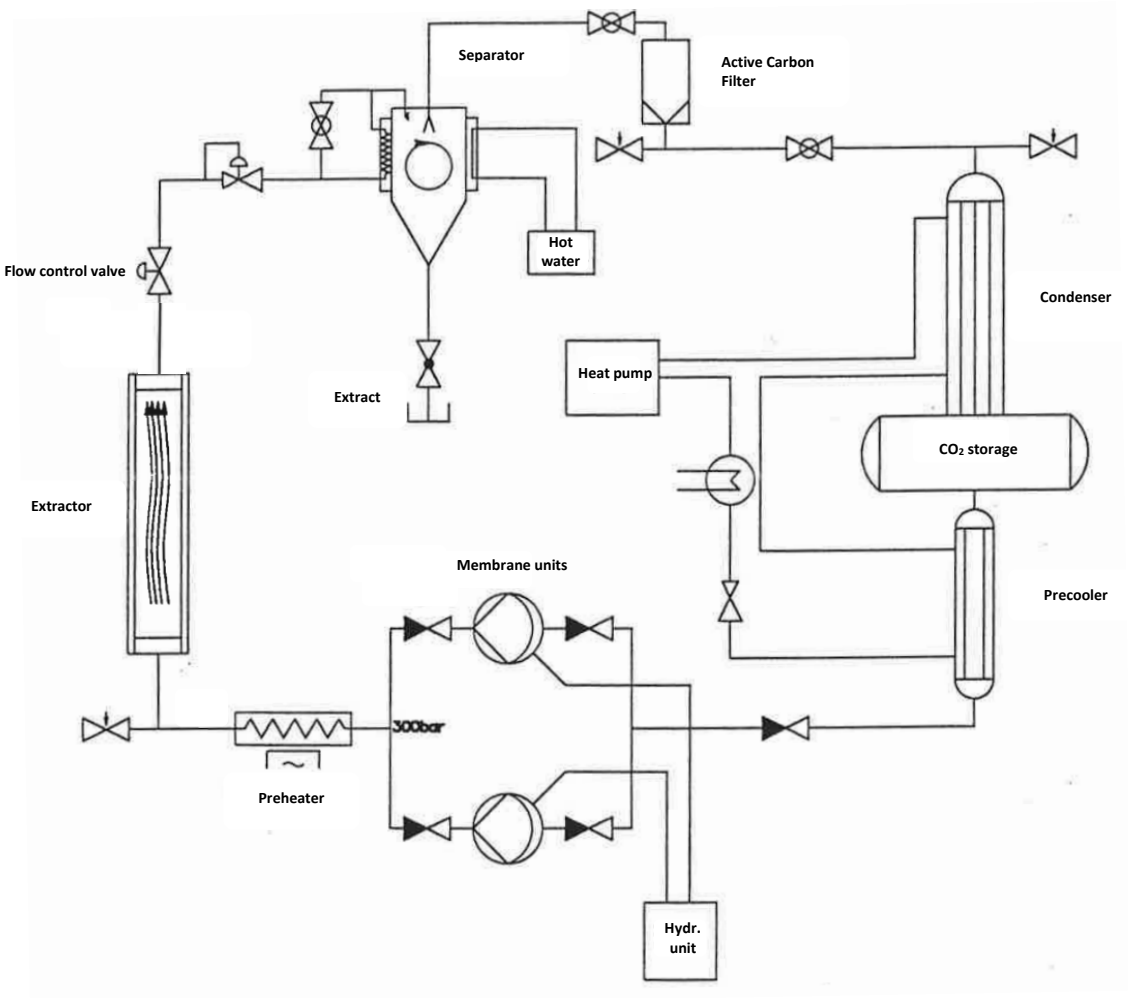

Figure 13. Schematic diagram of the target process system.

5.1.2 Control and measurement system

The SFE process unit has a fixed control panel display where the process parameters can be controlled independently (Figure 14). Approximately 5 automated feedback control loops exist in the system, each of them controlled by West N6100 PID controllers. For temperature control loops, the controller output type is relay, while other loops exert analog direct current as output.

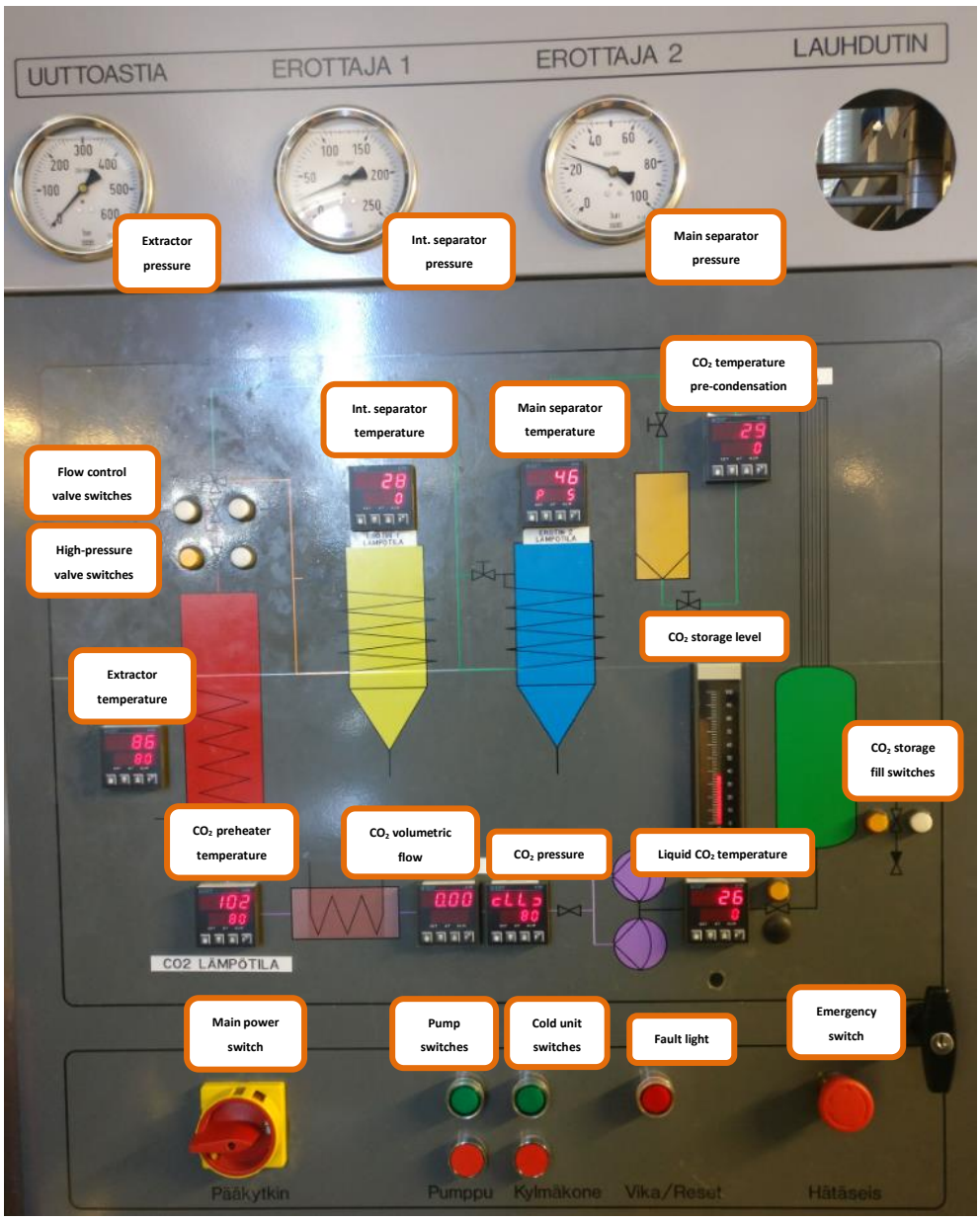

Figure 14. Control panel of the target process with descriptions of visible functions.

The cooling unit is started from a switch located on the control panel. As the cooling unit is running, the pressure in the condenser decreases to the vicinity of 50 bar. The unit may shut off because of pressure control but will initiate after pressure rises again. The unit can be shut off via a switch on the display.

CO_2 is added to the storage by opening a pressurized air-operated filling valve via a switch on the control panel. The CO_2 level in the storage should be at least 30 liters before extraction is started. The liquid level can be monitored from a digital display on the control panel. The level is measured using a capacitive level sensor.

The extractor is filled with CO_2 prior to extraction by opening the high-pressure valve via the control panel. This is done for preventing the volumetric flow rate measurement sensor from suddenly rushing and causing an emergency shutdown. The filling is continued until the extractor pressure is close to condenser pressure, around 50 bar.

The CO_2 pump unit, including the two turn-taking hydraulic pumps, is started via a switch on the panel. The condition for starting requires the cooling unit to be running or in standby mode. A unit PID controller adjusts the flow through the CO_2 pump and the hydraulic device through an inverter and does so until the pressure setpoint is reached. A strain gauge pressure transducer is used for measuring the CO_2 pressure.

A turbine flow meter is used to measure the CO_2 flow entering the extractor. CO_2 flow is controlled manually by using a constant flow control valve, located at the output of the extractor. The valve aims to keep the exit flow constant regardless of extractor pressure. The control valve is operated with two switches for opening and closing, located on the control panel. The normative controllable range for the flow stated by the manufacturer is 0.3–0.8 l/m.

The highly pressurized CO_2 is heated to a desired temperature using an electric heater. The heater is controlled by a unit controller. The maximum setpoint for the temperature is 150 °C. The heater includes an automatically operating overheating shield. The control is initiated when the CO_2 pump is operating. Pt100-type RTDs are used for temperature measurements in the process. The extractor is heated utilizing a capsule heater. The control is initiated when the main power of the system is switched on.

Heating of the separators is done with water heating, using hot tap water. Both separators have their own unit controllers. The controllers adjust the solenoid on/off valves for controlling the temperature in the separators. The controllers start controlling when power is initiated on the system, and the hand-operated backup valves are open.

The main parameters, CO_2 pressure, temperature and flow can be operated from the control panel. Extraction time cannot be set prior to operation; the extraction must be stopped manually by turning off the CO_2 pump. After this is done, the extractor empties itself of CO_2, and continues until the extractor pressure is the same as condenser pressure. Some CO_2 gets left in the extractor (leaving a pressure of 50 bar in the extractor), which

can be emptied after the cooling unit is shut off. After extraction, the CO_2/extractive mixture is directed into the main separator. The main separator can be set to temperatures of 30–50 °C, and a pressure of 50–200 bar.

The pressure of CO_2 decreases to about 50 bar as it passes through valves: Due to this, part of the CO_2 gasifies, and the rest of the liquid CO_2 is boiled in the main separator. This results in the extractives staying in the separator. The liquid-form extractives can be removed by opening a hand valve located at the bottom.

The CO_2 gas is condensed into liquid in a heat exchanger. The cooling is done by using the cooling liquid from the cooling unit. The cooling unit cannot be independently controlled, but it is determined by the pressure of the CO_2 storage.

CO_2 is pumped into a highly pressurized liquid by two hydraulic membrane pumps. Highly pressurized hydraulic oil is pumped in turn to both pumps. The switch from one pump to another happens automatically via an electric detector. The CO_2 flow and pressure are always about the same as for the hydraulic oil.

The panel has 4 mechanical Bourdon pressure gauges included, which display the pressure of the extractor, the two separators and the condenser. Emergency stop and main power switches are also included in the display. The measurement and control loops of the target system are listed in Table 6.

Table 6. Integrated measurement and control loops of the target SFE system.

Controlled/measured variable	Measurement instrument	Control method	Actuator	Manipulated variable
Liquid CO_2 temperature	RTD (Pt100)	None	-	-
Pressurized CO_2 pressure	Strain gauge trancuder	PID	Hydraulic pump	Pump power
CO_2 preheater temperature	RTD (Pt100)	PID	Electric heater	Heating power
Extractor temperature	RTD (Pt100)	PID	Electric heater	Heating power
Separator temperature (x2)	RTD (Pt100)	PID	Water heater	Hot water flow
CO_2 temperature pre-condensation	RTD (Pt100)	None	-	-
CO_2 volumetric flow rate	Turbine flow meter	Manual	Control valve	CO_2/solvent mixture flow
CO_2 storage level	Capacitive sensor	Manual	On/off valve	CO_2 flow to storage
Extractor pressure	Bourdon gauge	None	-	-
Separator pressure (x2)	Bourdon gauge	Manual	Pressure valve	Entering solvent flow
Condenser pressure	Bourdon gauge	None	-	-

5.1.3 Energy consumption

Since energy is the ultimate target of optimization, all factors concerning energy consumption are monitored and measured. The energy consumptions of the electric heaters and pumps could be accurately evaluated offline for each actuator. However, this would require capturing the controller output behavior, which is not done in this case because closed-loop identification is utilized, and the input signals are not coupled to the data gathering system. Due to this, a kWh energy meter (ABB C13) was installed on the power intake of the extraction system. This enabled the possibility of monitoring the total energy consumption during test runs, providing valuable practical information in terms

of the energy consumption of the system. For monitoring the energy consumed by separator heating control, an RTD (Pt1000) measurement and a mechanical turbine flow meter were installed on the exit flow.

5.1.4 Data acquisition system

For identification data gathering, a PC-based data acquisition system was developed (Figure 15). The system included a National Instruments Compact Fieldpoint™ programmable automation controller (cFP-2020) with RTD and analog input modules. All the temperature measurements were connected to the RTD module. Solvent pressure and volumetric flow measurements, both of which produce a current output, were connected to the analog input module. Industry standard device interface specification OPC (Object Linking and Embedding for Process Control) Data Access was used to import input/output items to MATLAB® software's OPC client. A program was developed for reading measured values of the input modules from the OPC client, displaying the data in conventional form for monitoring during operation in real-time, and for regularly saving data to the host PC.

Galvanic disconnector switches for current measurements were implemented in the system for coupling the measurements producing current output. The RTD measurements, which produce a voltage output, were coupled by manually crafting two sensors into a single metal sensor head. The PID controllers provide a software-implemented option for switching between automatic and manual operation modes. Manual operation was utilized for control-loop process behavior screening and PID tuning data gathering, while automatic operation was used for the process identification runs.

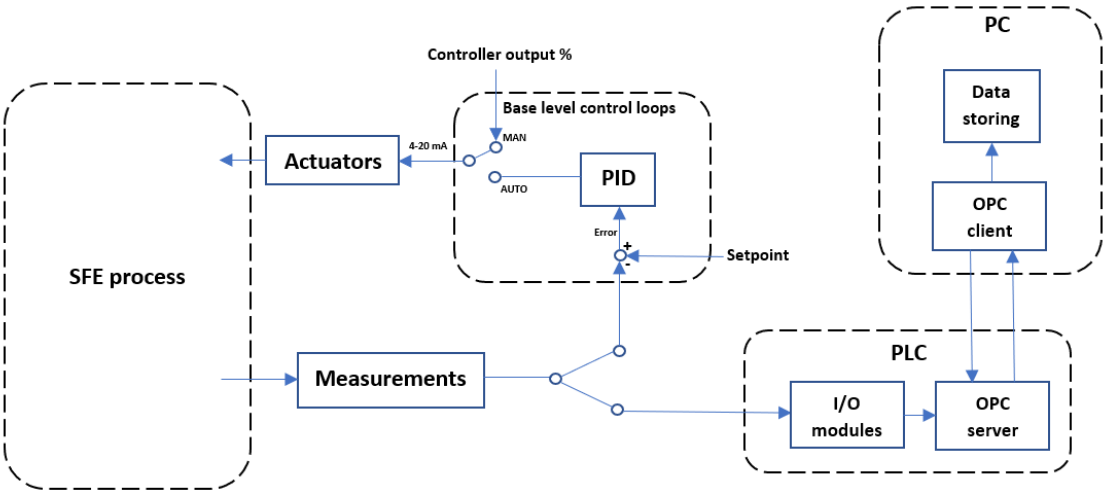

Figure 15. Schematic of the developed system for data acquisition.

5.2 Materials and chemicals

Oatmeal flakes manufactured by Raisio Ltd. (incl. 1550 kJ, 8 grams of fats and 11 grams of fiber per 100 grams) were used as raw material in the identification experiments. The flakes are placed inside the extractor in a porous textile bag made of flax. For preliminary experiments, the batch was not weighed. For identification runs, 698 g of oatmeal flakes was used in the batch. Carbon dioxide (99.9% purity) was provided by a local supplier.

The extractives produced in the extraction were not qualified or quantified in between runs. However, during the experiments it could be generally observed that the product had an oat oil-like texture. According to the mass loss of raw material, 30% of the extracted material was salvaged after the experiments.

5.3 Operating limits of feedback-controlled variables

The operative limits of process variables have a significant impact on selecting experimental conditions for each run of the design of experiments. The controlled variables have constraints determined by the physical limitations of the target system equipment. Some normative operative constraints given by the manufacturer of the target process system were presented in Table 5 on page 56. However, some process variables have stricter limits due to the emergency functions of the automation system: The temperatures of the preheater and extractor are limited by capillary temperature switch, which consists of a pipe filled with mercury; rising temperature causes the mercury to

expand, and as the temperature reaches a certain value the pipe fills with mercury, which causes a cut-off switch to activate. This action prevents the controller output current from reaching the heater-controlling relays. The maximum value for both electric heaters is set at 150 °C as the process is not typically run under higher temperatures during normal operation. Separator temperature is naturally constrained by the hot water temperature, which was measured at 60 °C. The lower limits for each temperature measurement are set at 25 °C, which is the average temperature in the process hall.

The upper limit for pressure, 500 bar, is given by the manufacturer. The lower limit needs to be set above the critical pressure of CO_2 (73.8 bar). In this case, 80 bar is chosen.

5.4 Preliminary experimental runs

Before trying to identify the unknown target SFE system, preliminary experiments are crucial to perform to gain primary knowledge about important system behavior such as time delays and dominating time constants, as well as interactions between process variables. Process behaviors were screened for each controlled variable by making step changes in open-loop control.

5.4.1 Data acquisition tests

Some preliminary runs were made for testing the developed data acquisition system. The main target of these experiments was to confirm the data transfer between the process and PC. This included validating the viability of sensor signals, input/output cards, wiring and the data acquisition script. Duplicate temperature measurements were installed to the system, so that the voltage signal could be directed to the unit controllers and data acquisition system simultaneously. The data acquisition script was updated to accommodate these modifications.

5.4.2 Screening

Before tuning any unit PID controller in the system, it is essential to gather information of process open-loop behavior in order to verify the performance of the instrumentation and final control element. This was done by manually changing the controller output current (4–20 mA) percentage and inspecting the process response. 4 mA corresponds to a minimum value, and 20 mA corresponds to a maximum value: These values can be

outside the constraints of the process variables. Therefore, step changes to the controller output must be moderate for carefully inspecting their significance on the process variable.

The two most common categories of process behaviors in response to input step changes in industrial manufacturing processes are self-regulating and integrating: The self-regulating response is characterized by a process variable change that stabilizes to a new value. An integrating response is characterized by a change in the slope of the process variable (Beall, 2016b). However, it is useful to treat self-regulating processes with a time constant much larger than the total loop dead time as “near-integrating” if the process value does not stabilize in a reasonable time.

From initial screening runs, it was observed that the temperature values in electrical heating loops do not settle at applied constant controller output values within a sufficient time. For example, the initial screening of extractor temperature showed that after making a step change from 0 to 5% on the controller output, the process values did not settle after 14000 seconds (about 4 hours), as shown Figure 16. Instead, the temperature steadily climbed from 28 °C to 72 °C during this time period. From this observation it can concluded that the extractor heating process is integrating (or near-integrating) within the operative limits of the process.

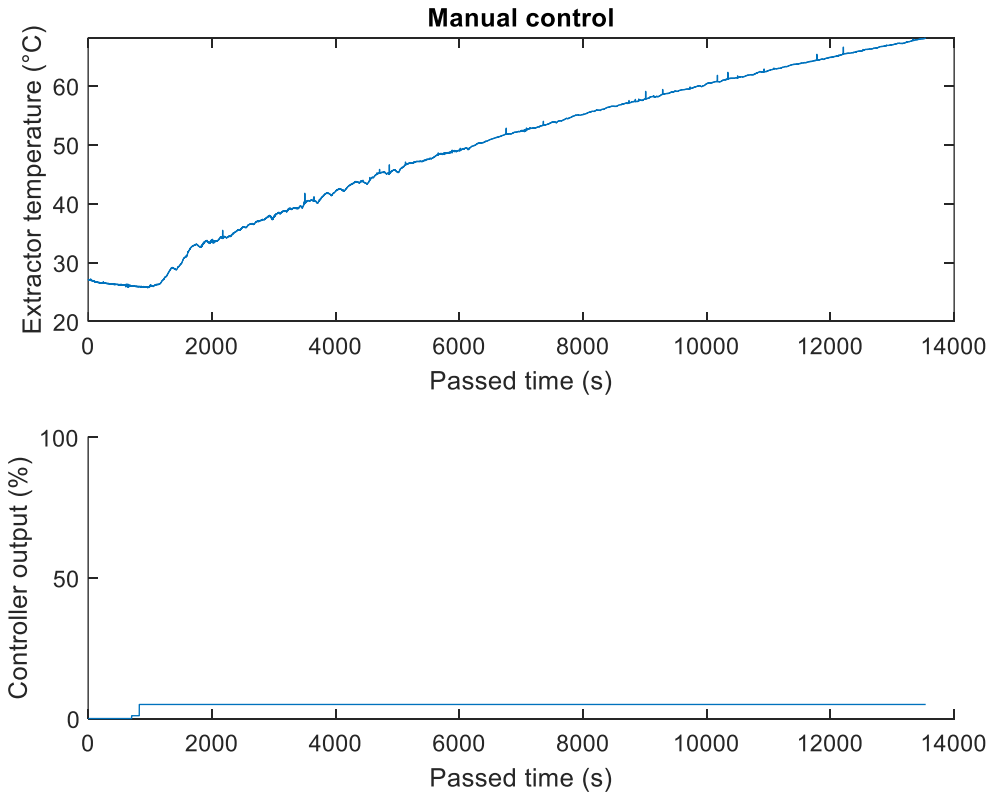

Figure 16. Open-loop response of extractor temperature to a single step input.

Another run inspecting the extractor temperature behavior was made by applying 3 step inputs. This experiment confirmed the initial observation, as the process value showed no signs of stability after a step input was initiated. Even after a wait of 1,5 hours after bumping the input from 5 to 15%, extractor temperature kept approaching the higher end of the operating region. The temperature at the end of the experiment was close to 110 °C, indicating that the upper operative limits are eventually reached after a long enough wait.

Similar behavior to extractor heating was observed in the initial screening run for CO_2 preheater temperature. Two step changes were made to the controller output. After bumping the input to 15%, the process value rose from 28 °C to 80 °C and kept climbing in a time of about 45 minutes. The open-loop responses also showed that both electrical heating loops suffer from significantly large dead times, up to over 3 minutes.

In contrary to electrical heating, the response of water-heated separator temperature showed signs of self-regulation. Multiple step changes were made for inspecting the response, gradually bumping the input from 0% up to 20%. The temperature values settled

between 50 °C and 60 °C, depending on controller output percentage. The dead times of separator heating were notably shorter compared to extractor and preheater heating loops, although the rise time was still relatively long. For all the heating control loops, no integrated cooling exists, making cooling dynamics much slower than the heating.

The initial remark in CO_2 pressure open-loop behavior was that the process value vibrated and oscillated periodically. The smaller vibrations (with a frequency of about 0.05 Hz) seemed to occur because the two hydraulic pumps of the pump unit take turns in producing pressure in the system. The high-amplitude oscillations (0.001 Hz) are most likely caused by the differential characteristics of the two hydraulic pumps, enforced by the pump cycles. However, the process values seem to naturally oscillate around an equilibrium. Therefore, the process is interpreted as self-regulating. Three input step changes were made in the screening runs, bumping the controller output between 15% and 30%, as seen in Figure 17.

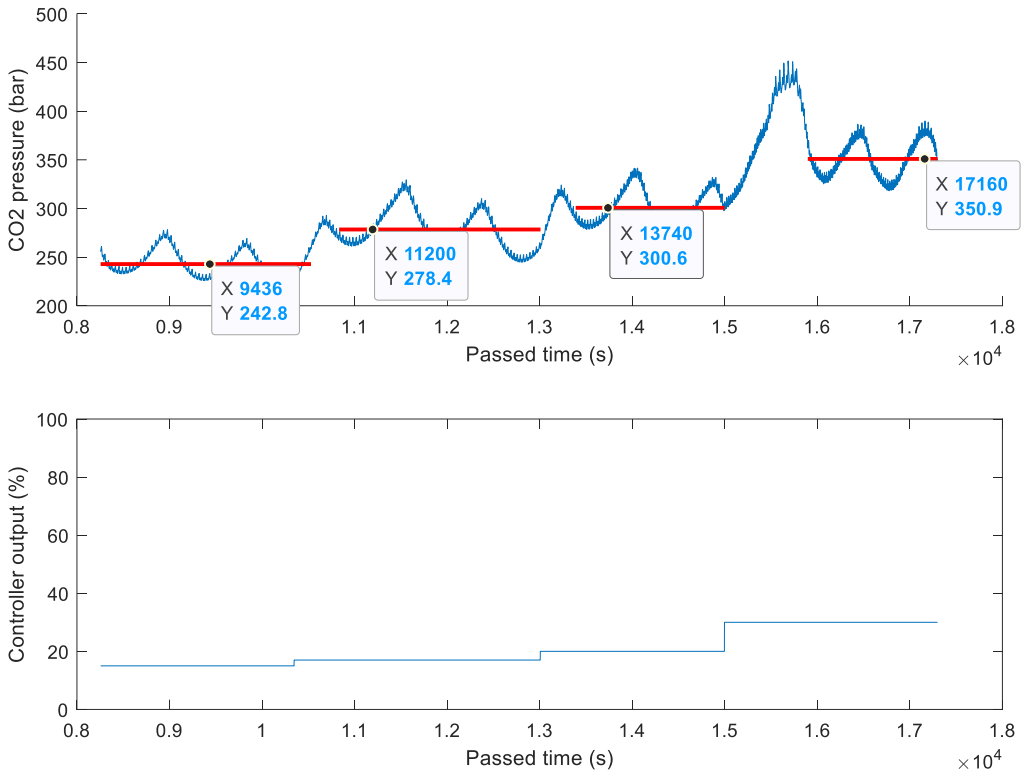

Figure 17. Open-loop response of pressure control to multiple step inputs with calculated steady-state values.

Unlike the other process variables, CO_2 volumetric flow rate in the target system is not controlled by automated closed-loop control. The screening procedure was done manually by adjusting the control valve located on the output of the extractor. The pressure controller output was kept constant at 30%, achieving an equilibrium pressure of around 350 bar. The base level for valve position was set to ¼ rounds, the normative valve position in prior extraction runs. In the screening runs (Figure 18), the valve was opened gradually ¼ to ½ rounds at a time and the flow value was let to settle before returning to the base position. The maximum valve opening was found to be approximately 1 ¾ rounds. Due to the pump cycles, the flow values varied between a peak value and zero. However, the peak values were largely consistent at constant pressure and valve position, showing the self-regulative nature of CO_2 volumetric flow open-loop behavior.

From the flow behavior screening runs, the interaction between pressure and control valve position was also observed. While on open-loop control, the pressure could not be maintained at a constant value when the flow valve was adjusted, as pressure gradually dropped when the valve position is increased.

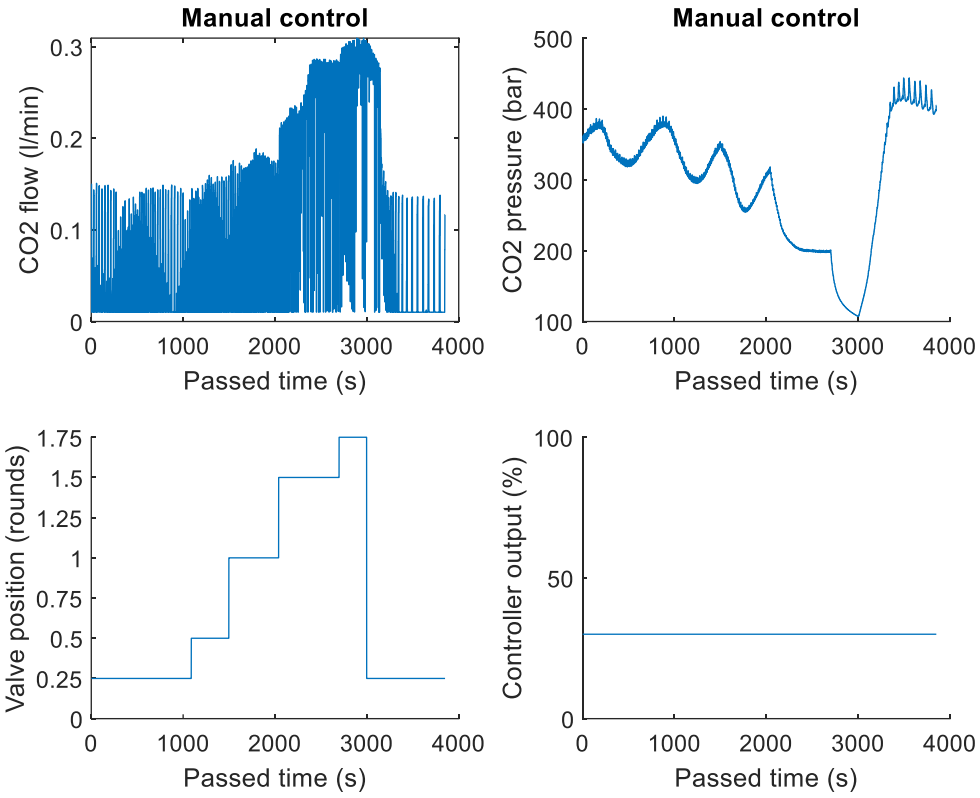

Figure 18. Open-loop response of CO_2 volumetric flow control to multiple step inputs, and interactions of these inputs to CO_2 pressure.

In conclusion, the open-loop process runs showed that heating processes of the target system exhibit undesirably slow dynamics caused by long time constants, whereas CO_2 pressure and CO_2 volumetric flow processes had much quicker responses to input changes. The operative limits and observed open-loop behaviors of the unit processes are listed in Table 7.

Table 7. Operative limits and dynamic behavior classifications of the process variables.

Controlled variable	Operative limits	Control method	Process behavior in open-loop control
CO_2 pressure	80–500 bar	PID	Self-regulating
CO_2 volumetric flow	0–0.8 l/min*	Manual	Self-regulating
Preheater temperature	25–150 °C	PID	(Near-)integrating
Extractor temperature	25–150 °C	PID	(Near-)integrating
Separator temperature	25–60 °C	PID	Self-regulating

* Normative

5.4.3 Tuning of PID controllers

Since the electric heating control loops were found to be (near-)integrating, the system identification task was unfeasible to be performed in open-loop mode of the controllers. This leads to the surrogate solution of conducting the process identification runs on automatic controller modes for the closed-loop processes. Although this is objectively the more inefficient way to approach system identification (Harju et al., 2000), tuning the PID controllers before identification runs ensure that identification can be made as efficient as possible.

Before any tuning adjustments were made, the processes were run in closed-loop control with the default parameters set by previous operators of the extraction system. If control performance was not sufficient with the parameters, new parameters were trialed: For extractor and CO_2 preheater heating control loops, due to their integrative nature, Lambda tuning-based controller design was utilized for determining the initial values of the tuning parameters. The parameters calculated according to Lambda tuning gave the base for further manual adjustments. For separator heating and CO_2 pressure control loops, only necessary manual tuning adjustments were utilized, as the self-regulating dynamics make following simple rules for tuning more feasible. The utilized manual tuning rules in this study were presented in Table 2. For the heating control loops, the main criteria for control performance were initial overshoot and settling time due to slow cooling dynamics. The heating control loops were tuned without CO_2 flowing through them (pumps off), ensuring as much of a disturbance free environment as possible. The CO_2 pressure control loop tuning runs were conducted with the electrical heaters set to above the critical temperature of CO_2, and the separator heater set to a high enough value for extractives to separate from the fluid to avoid clogging in the process equipment.

Three step changes in the extractor heating controller output were made, and the differential slopes and dead times of each step were calculated. This procedure is illustrated in Figure 19.

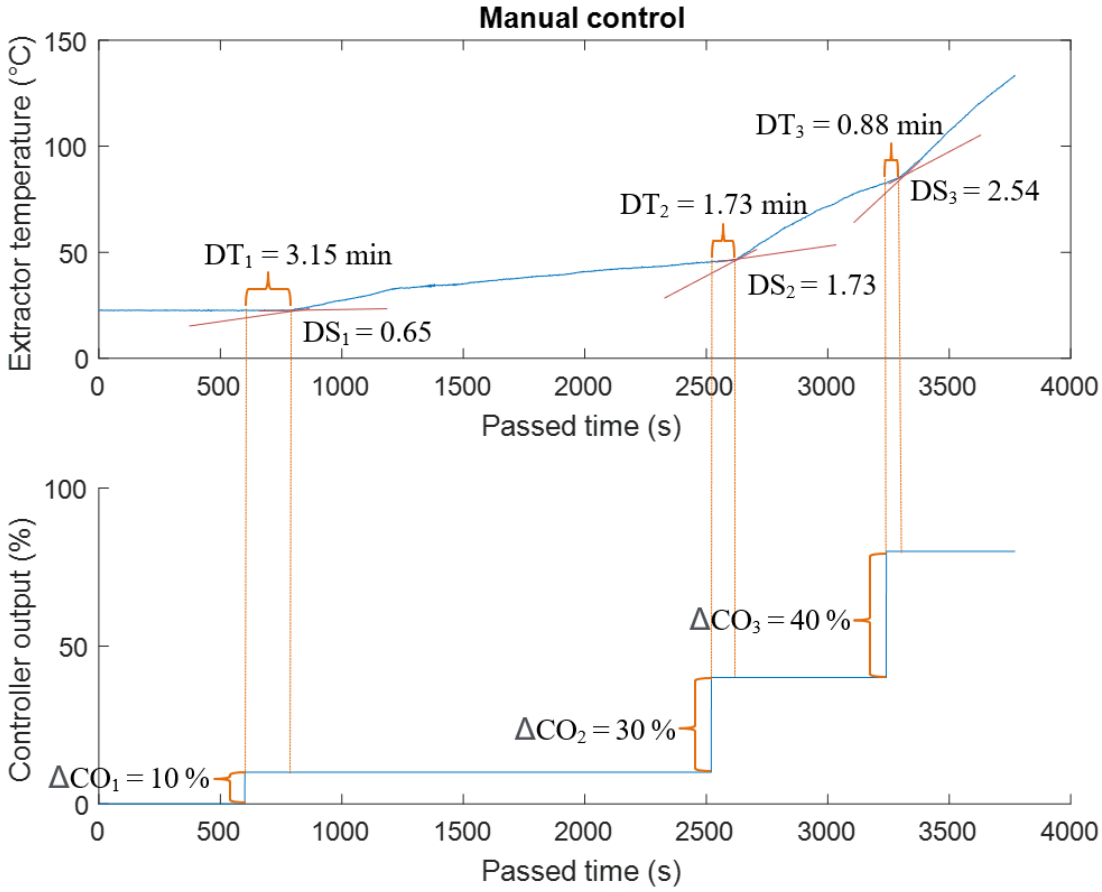

Figure 19. Response of extractor temperature after three step changes in controller output, where DT is dead time, DS is the difference between initial and final slopes of the process variables, and ΔCO is the difference between initial and final controller outputs.

For each step response, the process gains were determined according to Equation 6 on page 40. The average of the three calculated gains and dead times were calculated. Using these averages, the PID tuning parameters were calculated according to Equations 11, 12 and 13 on page 41. The value for λ was chosen to be the minimal theoretically feasible value, which is the (average) process dead time. The proportional gain was converted to proportional band values using equation 4 on page 37. After an experimental run using the Lambda tuning parameters, manual tuning was utilized until improvements were seen in some control performance criteria. Experimental runs, where a setpoint step from 0 °C to 80 °C was made, were conducted for each set of parameters, and the controller performance of each run was evaluated. The summaries and results of these runs and used parameters are collected in Table 8.

Table 8. Summary of PID controller parameter tuning runs for extractor temperature, where PB is proportional band, T_I is integral time, T_D is derivative time, RT is rise time, OS is overshoot, ST is settling time, and SSE is steady-state error.

Tuning run/adjustment	PB (%)	T_I (min:sec)	T_D	RT (min)	OS (%)	ST (min)	SSE (°C)
1/Default	9.00	5:00	1:30	5.65	9.0	36.0	0.2
2, 3, 4/Lambda, manual, manual	23.00	2:30	2:30	5.5	9.4	33.3	0.3
			Difference	–3%	+4%	–8%	+50%

The tuning experiments for extractor temperature only net a slightly quicker control response in the extractor temperature process. The comparison of process responses using default and tuned parameters after a step change is illustrated in Figure 20.

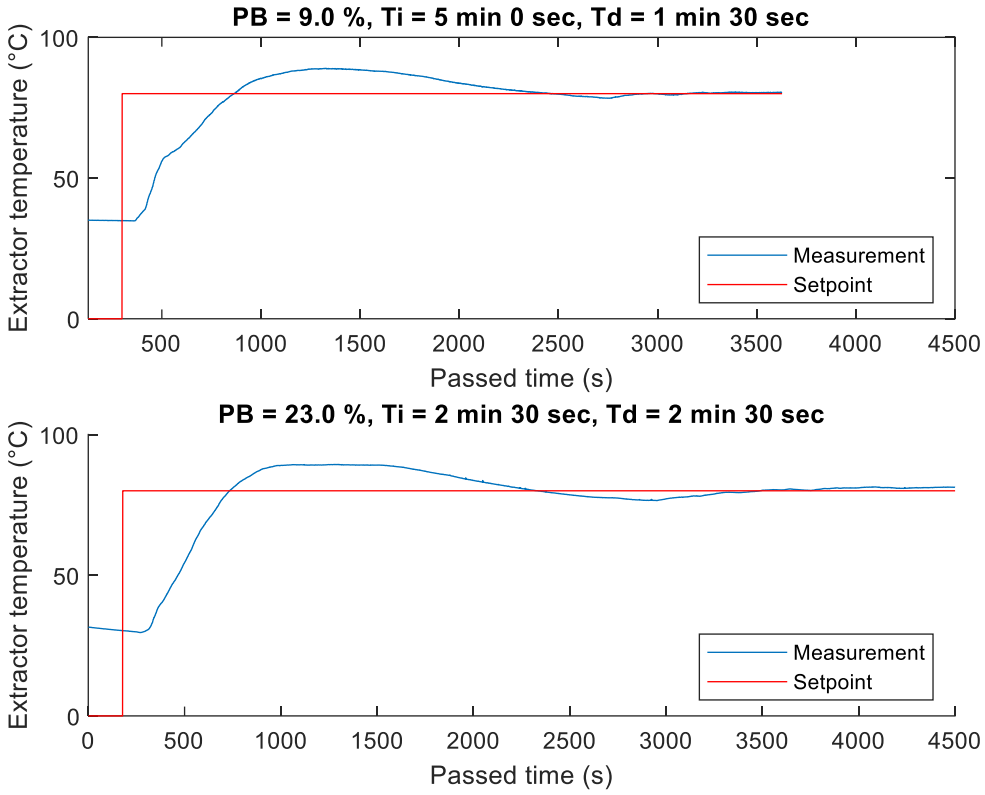

Figure 20. Comparative closed-loop extractor temperature responses using default (upper figure) and tuned (lower figure) PID controller parameters.

For CO_2 preheater temperature control, the tuning procedure was similar to extractor temperature control. First, three step changes were made for identifying essential parameters of process dynamics. The determination of dynamic characteristics is visualized in Figure 21.

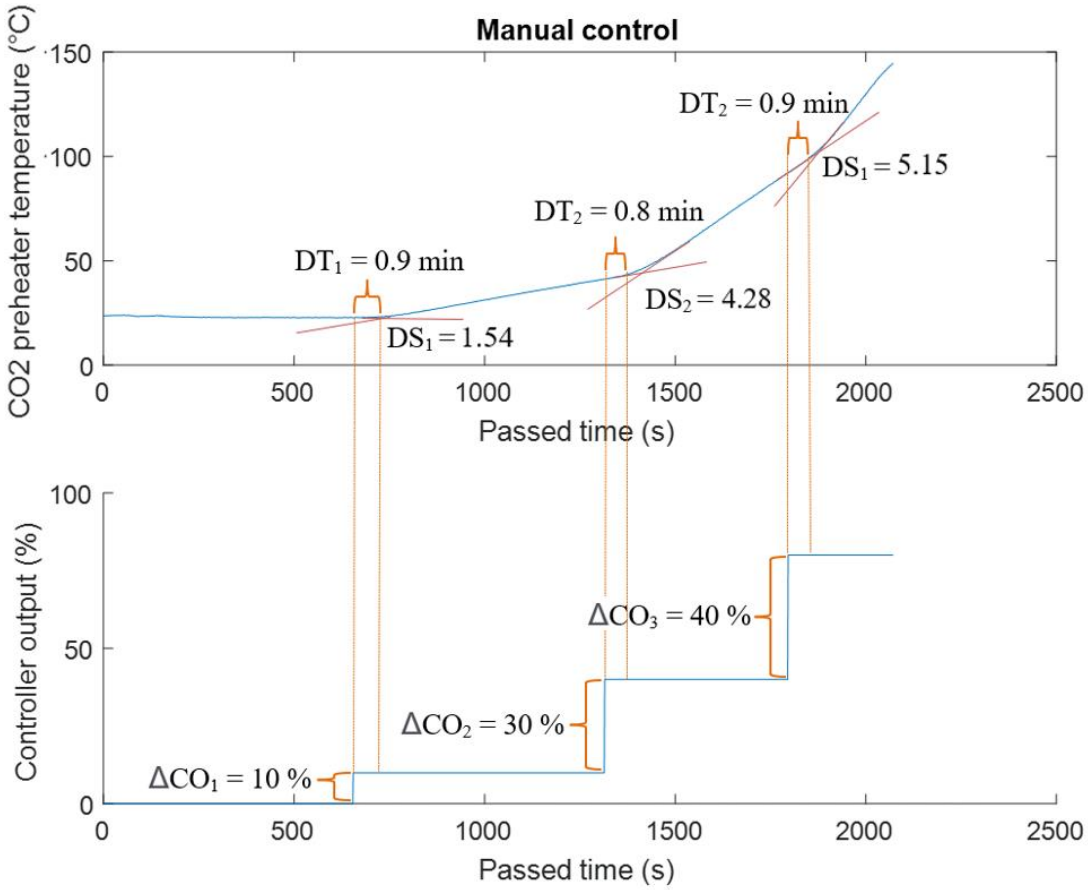

Figure 21. Response of CO_2 preheater temperature after three step changes in controller output, where DT is dead time, DS is the difference between initial and final slopes of the process variables, and ΔCO is the difference between initial and final controller outputs.

Similar to extractor temperature, the initial PID tuning parameters for CO_2 temperature control were calculated according to the Lambda tuning procedures, and further adjustments were conducted by manual tuning. In the experimental tuning runs, the process was bumped from 0 to 80 °C. The comparative results of the experimental tuning runs for CO_2 preheater temperature control are presented in Table 9.

Table 9. Summary of PID controller parameter tuning runs for CO_2 preheater temperature, where PB is proportional band, T_I is integral time, T_D is derivative time, RT is rise time, OS is overshoot, ST is settling time, and SSE is steady-state error.

Tuning run/adjustment	PB (%)	T_I (min:sec)	T_D	RT (min)	OS (%)	ST (min)	SSE (°C)
1/Default	9.00	5:00	1:30	3.3	34.6	125.2	0.6
2, 3/Lambda, manual	16.80	2:42	3:00	9.2	8.5	36.7	0.7
			Difference	+179%	–75%	–71%	+17%

The experimental tuning runs for preheater temperature control yielded major improvements in overshoot and settling time. The comparative process response for default and tuned parameters is illustrated in Figure 22.

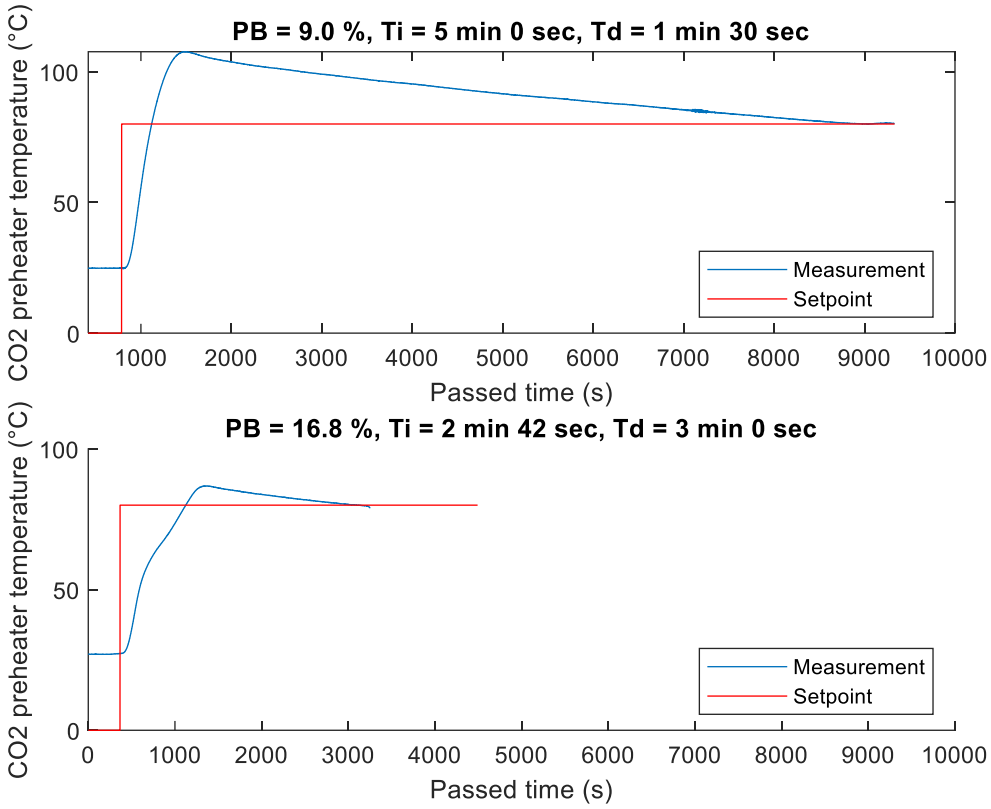

Figure 22. Comparative closed-loop CO_2 preheater temperature responses using default (upper figure) and tuned (lower figure) PID controller parameters.

Separator heating control loop was tuned solely using manual tuning. Experimental tuning runs were made by making a single step change from 0 to 52 °C. The comparative results of the experimental tuning runs for separator temperature control are presented in Table 10.

Table 10. Summary of PID controller parameter tuning runs for separator temperature, where PB is proportional band, T_I is integral time, T_D is derivative time, RT is rise time, OS is overshoot, ST is settling time, and SSE is steady-state error.

Tuning run/adjustment	PB (%)	T_I (min:sec)	T_D	RT (min)	OS (%)	ST (min)	SSE (°C)
1/Default	10.00	5:00	1:15	3.7	8.1	47.9	0.1
2, 3, 4/Manual, manual, manual	25.00	2:00	4:00	9.9	4.4	40.3	0.5
			Difference	+168%	–45%	–16%	+60%

The experimental tuning runs for separator control resulted in major improvements in overshoot and settling time. The comparative process response for default and tuned parameters is illustrated in Figure 23.

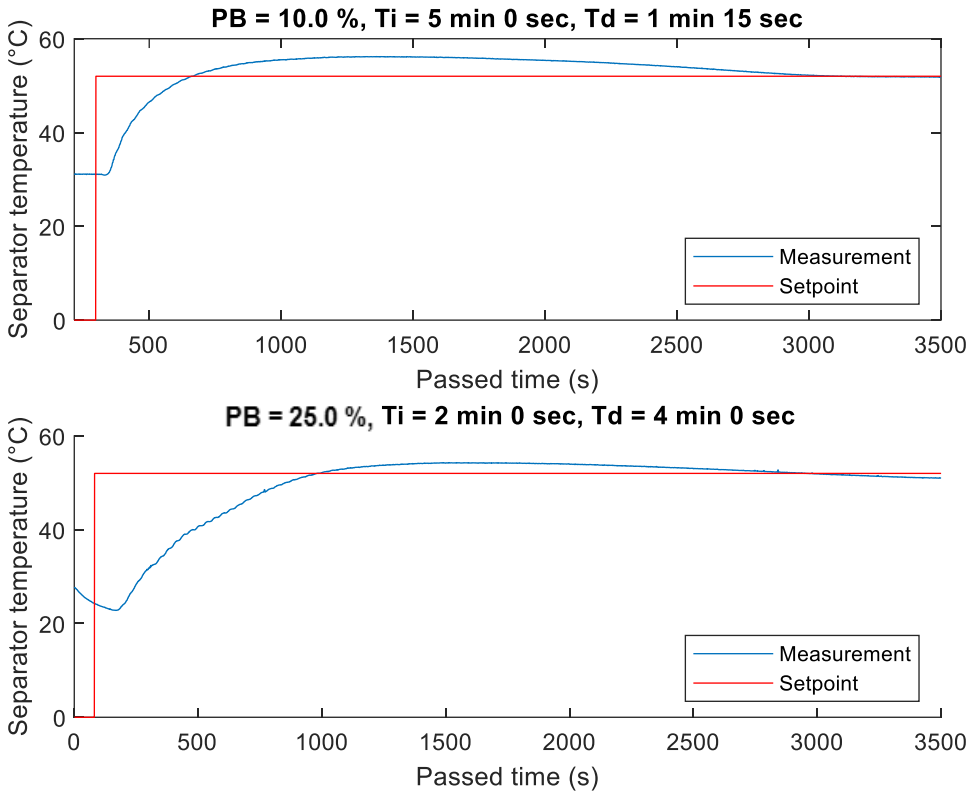

Figure 23. Comparative closed-loop separator temperature responses using default (upper figure) and tuned (lower figure) PID controller parameters.

For pressure control, experimental tuning runs were conducted by making three step changes (0 to 300 bar, 300 to 450 bar, 450 to 250 bar, as shown in Figure 24). From the initial tuning run for CO_2 pressure control, it was observed that the default parameters produced a sufficient control performance: The process values seemed to reach their setpoints efficiently when bumping the process value up or down. Only small vibrations, which increased in amplitude at higher pressures, occurred in the response as a result of the pump cycles. Therefore, the default parameters were concluded sufficient, and no further experimental runs were made for pressure control loop tuning.

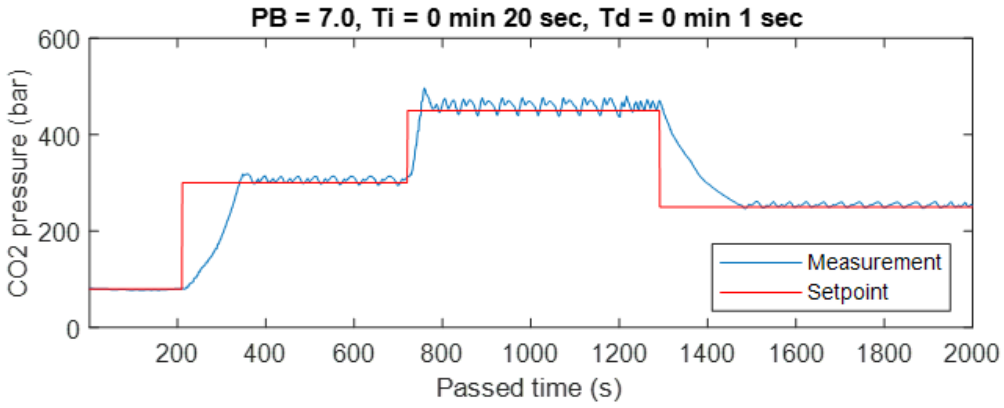

Figure 24. Closed-loop pressure response using default PID controller parameters.

5.5 Experiments

Data-driven system identification requires careful planning for ensuring effective modeling of processes, as experimental design is the starting step of the system identification procedure (shown in Figure 7 on page 43). The measured factors, input signal choices and results of the runs are described in detail.

5.5.1 Measured factors

The output measurement data produced by all four closed-loop controlled variables of the SFE system, including CO_2 pressure (P), CO_2 preheater temperature (T_{CO2}), extractor temperature (T_E), separator temperature (T_S), and the manually controlled CO_2 volumetric flow (F) was gathered via the developed data acquisition system. Energy consumption was monitored by manually monitoring electricity consumption (E) and heating water consumption (H_2O) via installed monitoring instruments.

5.5.2 Design factors and operating conditions

The outcome of SFE is dependent on the operative parameter values. Therefore, the identification experiments were run in differing operating conditions. The experimental conditions were designed using a central composite design in the form of a 2^3 full factorial design, using P, T_E and F as the independent design factors, due to their significance in extraction outcomes (as discussed in Chapter 2.3 on pages 16–18). This resulted in a total of 20 experimental runs.

The selection of variable levels for P and T_E was based on the operative limits of the variables (Table 7 on page 69), with the star points located well within these constraints. As the volumetric flow of CO_2 is controlled manually, the flow values were screened for each pressure level in separate test runs by manipulating the control valve position. Also, the effect of valve position on pressure control was inspected. The base value for the valve was set at ¼ rounds. After the pressure was settled to a desired value, the valve opening was increased ¼ rounds at a time at sufficient time intervals (2–4 minutes after the flow settled). The normative controllable range given by the manufacturer (0.3–0.9 l/min) was also verified in these runs. The flow screening experiments were made in two separate sets: The first of these sets consisted of screening procedures in the lower pressure values of the CCD design (139 bar, 200 bar, and 290 bar). This set is illustrated in Figure 25.

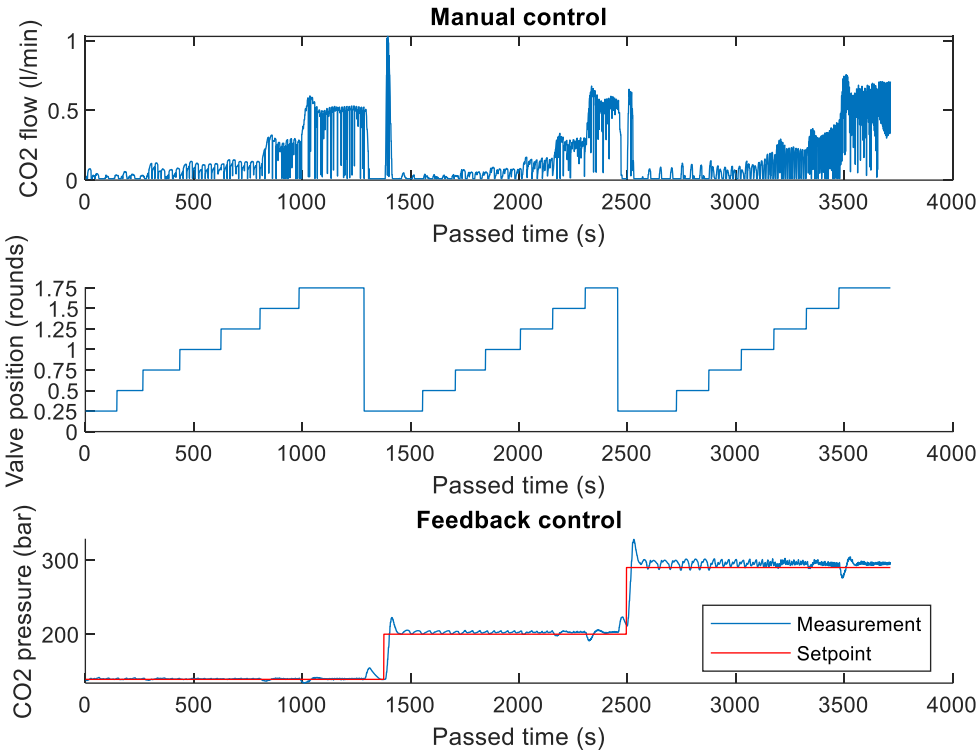

Figure 25. Flow screening procedure at pressures of 139 bar, 200 bar and 290 bar.

The second screening set included the flow screening procedures in the higher CCD pressure conditions (380 bar and 441 bar). This set is illustrated in Figure 26.

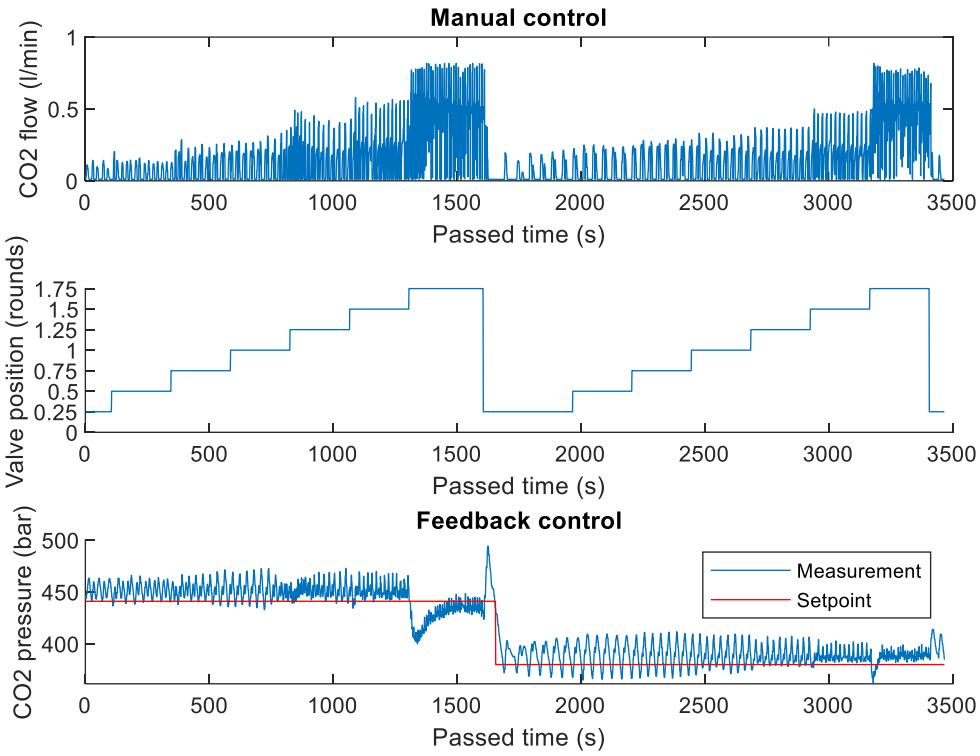

Figure 26. Flow screening procedure at pressures of 380 bar and 441 bar.

The flow screening runs showed that the values settled quite consistently at an equilibrium after each step change. However, higher pressures caused higher peaks in volumetric flow during pump cycles. Also, the flow values made a relatively bigger jump when the valve was opened to 1 ½ rounds. This is an indicator of the control valve shape: The valve enabled a bigger area for the gas to pass through after a certain point was passed in the opening. At a pressure of 441 bar, the pumps could not maintain the set pressure when the valve was fully open, settling at about 425 bar. Similar drop in pressure happened at 380 bar, but the pressure steadily climbed back to desired value.

The mean flow and peak values were determined from 30 seconds after each valve position change to the next step change time, excluding non-settled process values. Averages of each mean and peak value for each condition were calculated, and standard deviation of the averages was determined. These calculations are compiled in Table 11. The mean values were in the range of 0.02–0.53 l/min, while peak values laid between 0.04–0.82 l/min: both differing from the normative limits (0.3–0.8 l/min).

Table 11. Averages of mean and peak flow values at constant pressures and valve openings (peak values in brackets), and standard deviations of the mean values.

Pressure (Bar)	F at ¼ rounds (l/min)	F at ½ rounds (l/min)	F at ¾ rounds (l/min)	F at 1 round (l/min)	F at 1 ¼ rounds (l/min)	F at 1 ½ rounds (l/min)	F at 1 ¾ rounds (l/min)
139	0.02 (0.05)	0.03 (0.06)	0.06 (0.12)	0.07 (0.13)	0.11 (0.15)	0.20 (0.32)	0.49 (0.60)
200	0.02 (0.05)	0.02 (0.04)	0.04 (0.08)	0.06 (0.13)	0.11 (0.16)	0.24 (0.33)	0.53 (0.67)
290	0.02 (0.10)	0.03 (0.11)	0.05 (0.10)	0.08 (0.20)	0.14 (0.29)	0.28 (0.49)	0.50 (0.76)
380	0.04 (0.15)	0.05 (0.16)	0.09 (0.29)	0.11 (0.35)	0.14 (0.48)	0.23 (0.57)	0.45 (0.82)*
441	0.05 (0.25)	0.08 (0.25)	0.11 (0.29)	0.12 (0.33)	0.14 (0.49)	0.21 (0.49)	0.47 (0.80)**
Avg.	0.03 (0.12)	0.04 (0.12)	0.07 (0.18)	0.09 (0.22)	0.13 (0.31)	0.23 (0.44)	0.49 (0.73)
SD	0.014	0.024	0.029	0.026	0.017	0.031	0.030

* Pressure dropped, but returned to desired level

** Pressure conditions could not be maintained

Since pressure could not be maintained at 441 bar when the valve was fully opened, flow values at 1 ¾ rounds were excluded from the experimental design. The second highest flow value, 0.23 l/min (at 1 ½ rounds), was picked as the positive star point. The negative star point is picked according to the lowest standard deviation of the flow means, which is 0.04 l/min (at ½ rounds). According to these limits, rest of the CCD volumetric flow values were determined. In addition, the valve positions were calculated proportionally to the CCD points. The variable levels for the independent variables are combined in Table 12.

Table 12. Variable levels of chosen independent factors for CCD.

Factor	–α	–1	0	1	α
P (bar)	139	200	290	380	441
T_E (°C)	69	80	98	115	127
F (l/min)	0.04 (0.5 rounds)	0.09 (0.7 rounds)	0.14 (1 rounds)	0.19 (1.3 rounds)	0.23 (1.5 rounds)

The CO_2 preheater temperature and separator temperatures were set to a fixed value in every identification run. The value for preheater temperature was chosen to be 60 °C, higher than the critical temperature of CO_2. Separator temperature was chosen to be 52 °C, a value advised by a process expert for ensuring separation of extractives.

Due to the large time constants of the heaters, the wait for the temperatures to cool down to desired valued would extend the experiment time significantly. Because of this, the run executions were divided into two sets (including 11 and 9 runs each), and each set was arranged from lowest extractor temperature to highest. This ensured avoiding the delays in between experiments due to long cooling dynamics. The sets were then randomized according to pressure and flow values. The CCD arrangement, including fixed parameters and run orders is shown in Table 13.

Table 13. CCD arrangement for the experiments.

	Run	P (bar)	T_E (°C)	F (l/min)	T_{CO2} (°C)	T_S (°C)	Run order
Matrix	1	200	80	0.09 (0.7 rounds)	60	52	1
trials	2	380	80	0.09 (0.7 rounds)	60	52	13
	3	200	115	0.09 (0.7 rounds)	60	52	8
	4	380	115	0.09 (0.7 rounds)	60	52	20
	5	200	80	0.19 (1.3 rounds)	60	52	14
	6	380	80	0.19 (1.3 rounds)	60	52	2
	7	200	115	0.19 (1.3 rounds)	60	52	9
	8	380	115	0.19 (1.3 rounds)	60	52	10
Star	9	139	98	0.14 (1 rounds)	60	52	5
trials	10	441	98	0.14 (1 rounds)	60	52	16
	11	290	69	0.14 (1 rounds)	60	52	12
	12	290	127	0.14 (1 rounds)	60	52	11
	13	290	98	0.04 (0.5 rounds)	60	52	6
	14	290	98	0.23 (1.5 rounds)	60	52	17
Center	15	290	98	0.14 (1 rounds)	60	52	3
trials	16	290	98	0.14 (1 rounds)	60	52	4
	17	290	98	0.14 (1 rounds)	60	52	7
	18	290	98	0.14 (1 rounds)	60	52	18
	19	290	98	0.14 (1 rounds)	60	52	15
	20	290	98	0.14 (1 rounds)	60	52	19

5.5.3 Input signals

In addition to the start-up step changes determined by the CCD conditions, manually applied step sequences with small amplitudes were conducted around these conditions for capturing the process dynamics. For pressure and flow control loops, these sequences included bumping the process above/below the steady-state value with varying input times, resembling a PRBS signal. For extractor and separator temperature control loops, the sequences only included 1–2 step changes due to the slow dynamics of the processes.

Overall, the identification runs followed the following procedure:

1) Bump the electrical heater setpoints from 0 to their CCD values (capture the process dynamics)
2) Start up the CO_2 pump unit by bumping the pressure setpoint from 0 to the CCD value (let settle).
3) Open the control valve to its CCD value (let settle).
4) Manually apply the following step sequence to pressure setpoint:
   Increase of 20 bar (let settle) → Decrease of 40 bar (let settle) → Increase of 20 bar (let settle) → Increase of 20 bar (no settling) → Decrease of 40 bar (no settling) → Increase of 20 bar (let settle)
5) Manually apply the following step sequence to valve position:
   Increase of 0.1 rounds (let settle) → Decrease of 0.2 rounds (let settle) → Increase of 0.1 rounds (let settle) → Increase of 0.1 rounds (no settling) → Decrease of 0.2 rounds (no settling) → Increase of 0.1 rounds (let settle)
6) Apply an increase of 2 °C in extractor temperature setpoint (capture dynamics)
7) Apply the following step sequence to separator temperature setpoint:
   Increase of 3 °C (capture dynamics) → Decrease of 1 °C (capture dynamics)
8) Follow shut-down operations of the process and stop data acquisition.

5.5.4 Energy consumptions

The 20 experimental runs were conducted in two separate sets over a course of two days. Electricity consumption was logged after each input procedure, resulting in 8 measured values per run. Heating water consumption was logged before and after each run. In addition to total consumption, the average electricity consumption per minute in steady-

state operation (E_{ss}avg) was determined for each run. E_{ss}avg was calculated from the period after startup and shutdown. These results are combined in Table 14.

Table 14. Energy consumption during the experiments, where E_{ss}avg is steady-state electricity consumption.

Run order (runtime)	Electricity (Wh)	E_{ss}avg (Wh/min)	Heating water (l)
1 (1 hr 18 min 40 sec)	1215.7	13.7475	121
13 (1 hr 8 min 17 sec)	1124.1	19.3743	75
8 (1 hr 5 min 45 sec)	943.0	16.8647	60
20 (1 hr 13 min 15 sec)	1342.7	20.7822	71
14 (0 hr 57 min 52 sec)	966.4	19.5483	72
2 (0 hr 59 min 20 sec)	1308.8	24.1630	90
9 (1 hr 2 min 55 sec)	1118.0	20.1250	67
10 (0 hr 53 min 16 sec)	1209.2	27.2867	60
5 (1 hr 10 min 21 sec)	976.7	15.7872	66
16 (1 hr 2 min 9 sec)	1447.7	29.0282	67
12 (1 hr 22 min 16 sec)	1118.0	16.5094	111
11 (1 hr 14 min 8 sec)	2430.3	35.3455	74
6 (1 hr 4 min 9 sec)	922.1	17.2046	66
17 (1 hr 4 min 1 sec)	1612.6	32.2913	91
*3** (1 hr 8 min 40 sec)	1162.0	18.4688	71
4* (1 hr 4 min 5 sec)	1122.6	20.4070	71
7* (1 hr 4 min 34 sec)	1183.5	21.9128	77
18* (1 hr 2 min 15 sec)	981.0	17.3793	66
*15** (1 hr 0 min 43 sec)	999.7	17.7998	63
19* (1 hr 3 min 22 sec)	1060	18.7698	72

Bold indicates cold start; *Italic* indicates T_E condition step-up from previous run; *indicates center trial

5.6 Unit process identification

The data gathered from the identification experiments was utilized in identifying process models for the unit processes and the linear significance of the factors on steady-state electricity consumption in the target SFE system. The identified models form a full batch-extraction process simulator, simulating each unit process control loop as well as consumed energy. The main desired attribute of the models is sufficient covering of

process dynamics, as it primarily determines the efficiency and reliability of further model utilization.

5.6.1 Regression model for steady-state electricity consumption

The arrangement of the central composite design (as described in Chapter 4.2.1 on pages 44–46) allows the development of appropriate second order polynomial multiple regression model (Equation 15 on page 46) for determining the significance of operative conditions on electricity consumption. The measured steady-state electricity consumption (E_{ss}avg) was therefore correlated to the set of regression coefficients, including intercept (β_0), linear (β_1, β_2, $\beta3$), interaction (β_{12}, β_{13}, β_{23}) and quadratic (β_{11}, β_{22}, β_{33}) term coefficients. The results obtained were then analyzed to assess the "goodness" of fit. Functions provided by MATLAB® Statistics and Machine Learning Toolbox™ were used for regression and graphical analyses of the obtained data. Student's t-distribution was used to determine the significance of coefficients in the regression equation. Calculated values for the regression coefficients and their corresponding calculated t-values are collected in Table 15. The value of t-distribution, given 10 degrees of freedom and a confidence interval of 80%, is 0.889 (Ifran et al., 2011).

Table 15. Values of the regression coefficients (β) of the steady-state electricity consumption equation and their t-values, where $t_{0.2,10}$ is t-distribution value at 10 degrees of freedom, and confidence interval is 80%.

	Factors	Coefficient	Value	t-value
Constant	-	β0	35.3052	0.6839
Linear terms	P	β1	0.0261	0.1917
	T_E	β2	–0.7153	–0.8874
	F	β3	–9.4831	–0.4599
Interaction terms	PT_E	β12	–0.0001	–0.0678
	PF	β13	0.0038	0.0738
	T_EF	β23	–0.0493	–0.1871
Quadratic terms	P^2	β11	0.0000	0.1772
	T_E^2	β22	0.0049	1.3827
	F^2	β33	12.3685	1.3488

$t_{0.2,10} = 0.889$

From Table 15, it can be observed that the quadratic effects of T and F are significant, but other terms are insignificant at the given confidence interval. Modeled steady-state energy

consumption values were moderately well matched against the experimental data with a correlation coefficient value of 0.7357. The adequacy of the model was also evaluated by the residuals (difference between the observed and the predicted response value). Residuals are thought as elements of variation unexplained by the fitted model and then it is expected that they occur according to a normal distribution. Normal probability plots are a suitable graphical method for judging the normality of residuals (Khataee et al., 2010). The observed residuals are plotted against the expected values, given by a normal distribution. The residual analysis is shown in Figure 27.

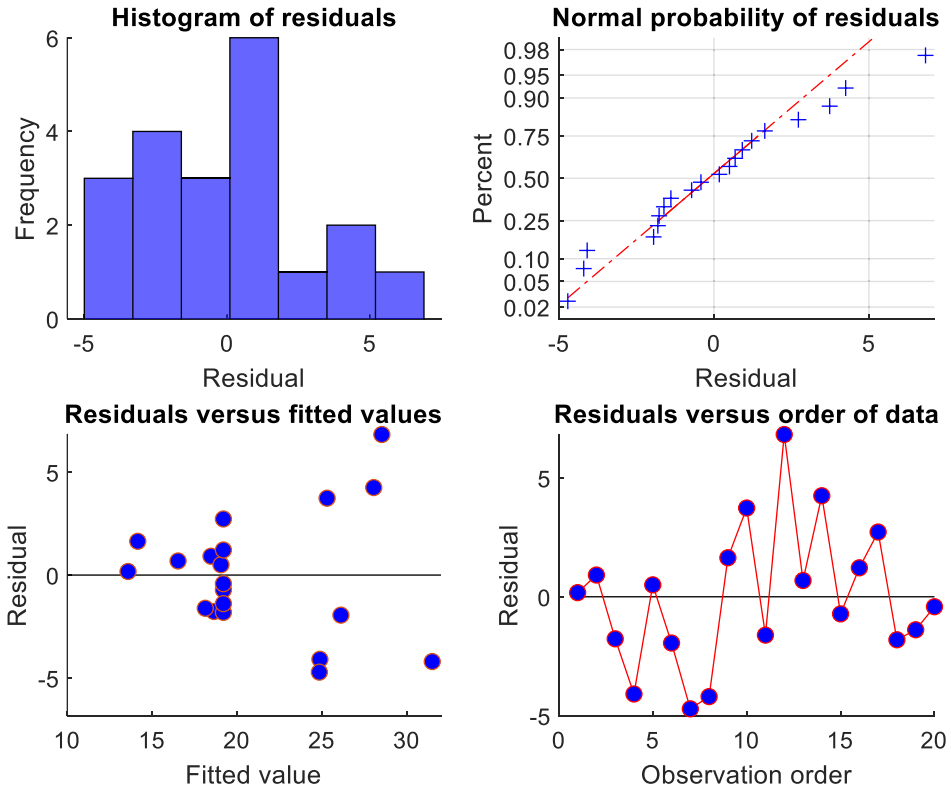

Figure 27. Residual analysis for steady-state electricity consumption.

The trend observed in the normal probability plot reveals reasonably normally distributed residuals. The residuals appear to be randomly scattered according to residual plots.

5.6.2 Identification of process models

Using the data gathered from the system identification experiments, models of each process were identified by utilizing the functions provided by MATLAB® System Identification Toolbox™. This included modeling of seven unit processes in total: CO_2 pressure, CO_2 volumetric flow, CO_2 preheater temperature, extractor temperature,

separator temperature, heating water consumption and electricity consumption. The mean values of pressure and flow during two pump cycles (80 seconds) were used for modeling pressure and flow responses, eliminating (most of) the oscillation in the responses caused by the pump unit.

It was assumed that the dynamics and input-output relations of the process could be modelled by applying linear models. However, visual inspection of experimental data showed that the heating process responses showed notable nonlinearity and varying dynamics, specifically in heating and cooling stages. Also, some behavior of the processes seemed to vary when the pump was turned on. For these reasons, some unit processes were modeled using more than one submodel if a single model could not produce a satisfactory outcome. Interactions between unit process responses were taken into account by adding measured disturbances in the models.

Generally, state-space model structures (described in Chapter 4.2.3 on pages 48–50) provided the best fit in initial modeling tests and are deemed as suitable for control purposes; therefore, state-space models were chosen as the primary model structure. Identification of the model parameters was performed utilizing the N4SID prediction error method. The identified model was then validated over independent validation data sets by cross-validation. Experimental data was divided into identification and validation data sets, using at least 50% of the available process data for identification, and at least 25% for validation. Band-limited white Gaussian noise was introduced to the unit process model outputs to simulate unmeasured noise (sensor noise, process noise etc.). The identified state-space models and their specifications are shown in Table 16.

Table 16. Specifications of the identified target SFE unit process models, where Py is pressure process output (average from two full pump cycles), Fy is CO_2 volumetric flow process output (average from two full pump cycles), T_Ey is extractor temperature process output, T_Sy is separator temperature process output, T_{CO2}y is CO_2 preheater temperature output, H_2Oy is heating water consumption process output, Ey is electricity consumption process output, Pu is CO_2 pressure process input, Fu is CO_2 volumetric flow process input, T_Eu is extractor temperature process input, T_Su is separator temperature process input, T_{CO2}u is CO_2 preheater temperature process input and Pe is pressure error (difference between measured pressure value and setpoint).

Controlled variable	Submodel	Manipulated variable	Measured disturbance	Model order	Fit to validation data (median)
Py	Pre pump start	Pu	T_Ey	14	92.6%
	Post pump start	Pu	T_Ey	3	70.1%
Fy	-	Fu	Pe	2	44.4%
T_Ey	Heating	T_Eu		2	81.6%
	Cooling	T_Eu		10	91.2%
T_Sy	Heating	TSu	Fu	13	62.8%
	Cooling	TSu	Fu	2	63.3%
T_{CO2}y	Heating	T_{CO2}u		14	96.6%
	Cooling (pre pump start)	T_{CO2}u		4	76.8%
	Cooling (post pump start)	T_{CO2}u	Pe	1	59.4%
H_2Oy	-	TSu	Py, T_Ey, Fu	1	77.2%
Ey	-	Pu, Fu, T_Eu, T_Su		1	91.6%

According to the cross-correlation percentages, the fit of the temperature unit process models was quite high, with all models having higher fits than 59.4%. Demonstration of a simulated response of extractor temperature against a validation data set is shown in Figure 28.

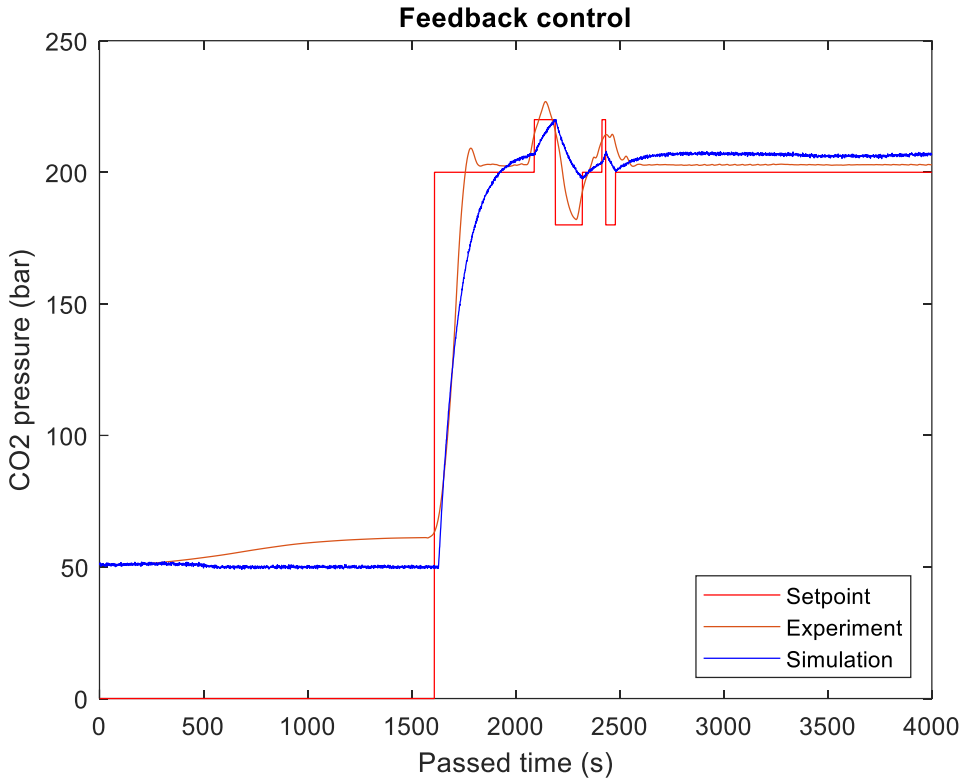

Figure 28. Simulated response of CO_2 pressure plotted against a validation data set.

The fit percentages for CO_2 pressure models were higher or equal to approximately 70.1%, Demonstration of a simulated response of pressure against a validation data set is shown Figure 29.

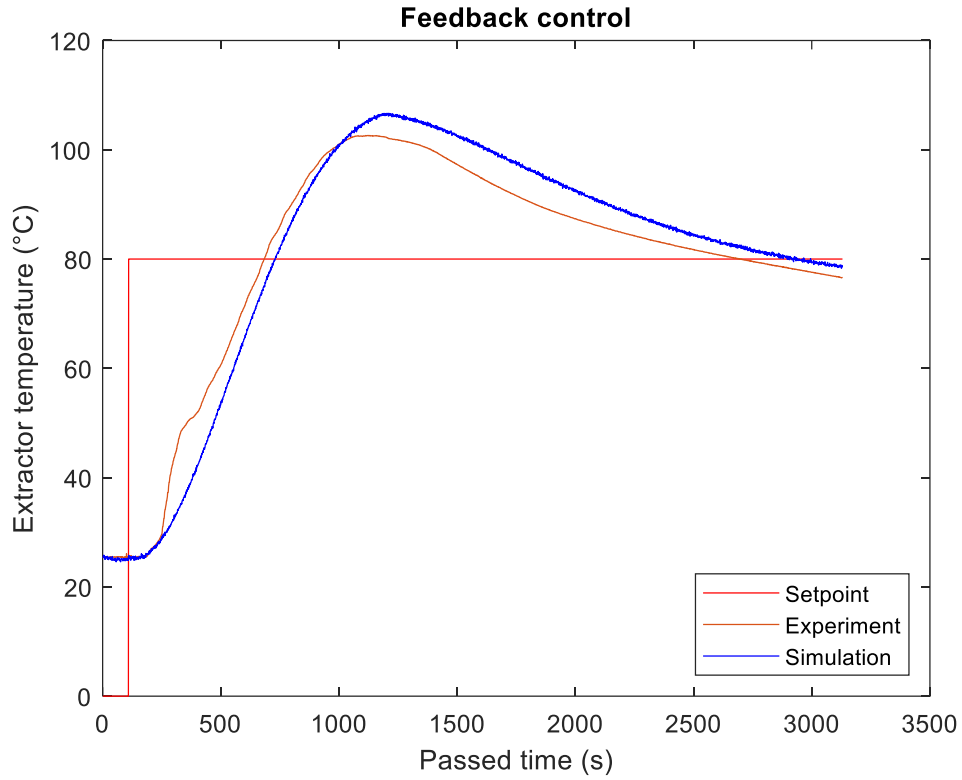

Figure 29. Simulated response of extractor temperature plotted against a validation data set.

The fit for the state-space model of CO_2 volumetric flow was noticeably low (44.4%). The steady-state values and peaks caused by pressure error varied between experiences run with same parameters. However, the identified model covered the general dynamics of the process sufficiently, as shown in Figure 30.

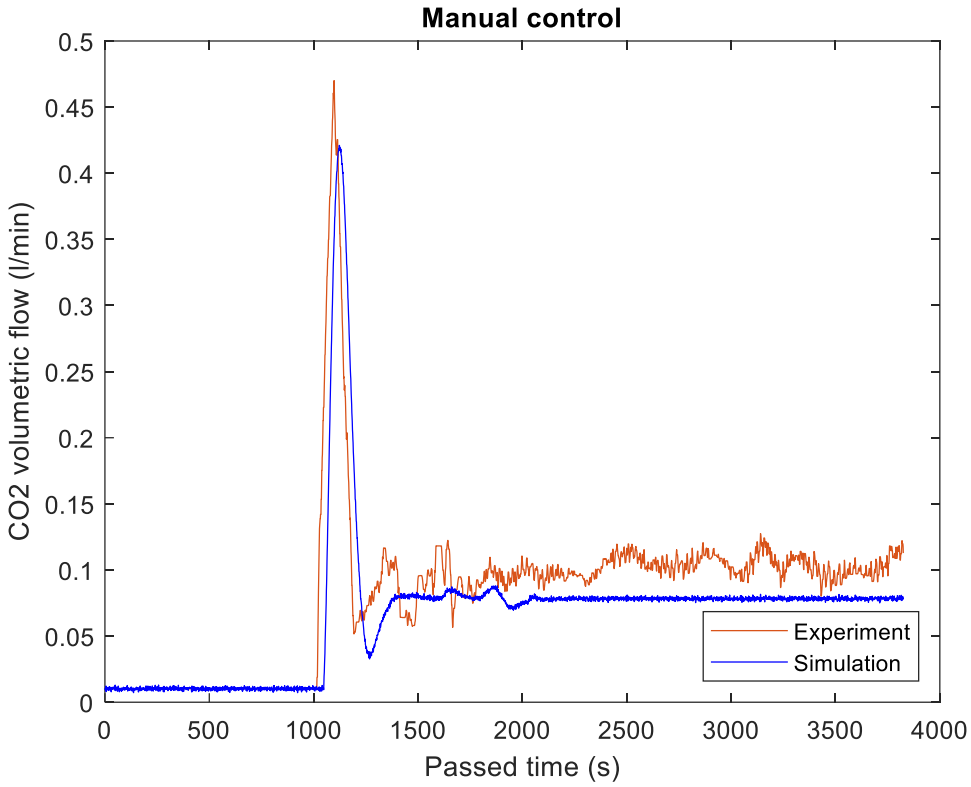

Figure 30. Simulated response of CO_2 volumetric flow plotted against a validation data set.

Electricity consumption was assumed to be directly related to the operational unit process inputs; thus, inputs for T_E, P and F were set as the manipulated variables for electricity consumption models. Heating water consumption was assumed to be directly proportional to the inputs applied to the water heating based T_s, and the operational unit process responses were included in the model as measured disturbances.

5.6.3 Process simulator

The identified models were utilized for developing a SFE batch process simulator in MATLAB® environment, simulating the responses of the process according to user-defined batch operation conditions and total runtime. In the simulator, the total runtime determines the simulation time. The setpoints and step times for operative closed-loop processes (T_E and P) are given as inputs; the setpoints for T_S and T_{CO2} are fixed at 52 °C and 60 °C respectively, and they are applied simultaneously with T_E. For the open-loop process F, the input is given as the desired control valve position instead of setpoint. Based on these inputs, step input sequence arrays, including input values for each time step of the total runtime, are computed, and fed into their appropriate process models.

The responses of the models are displayed to the user. In addition, the open-loop identified steady-state value for CO_2 volumetric flow after settling at given valve position (F_{ref}) is determined and displayed. The structure of the simulator is shown in Figure 31.

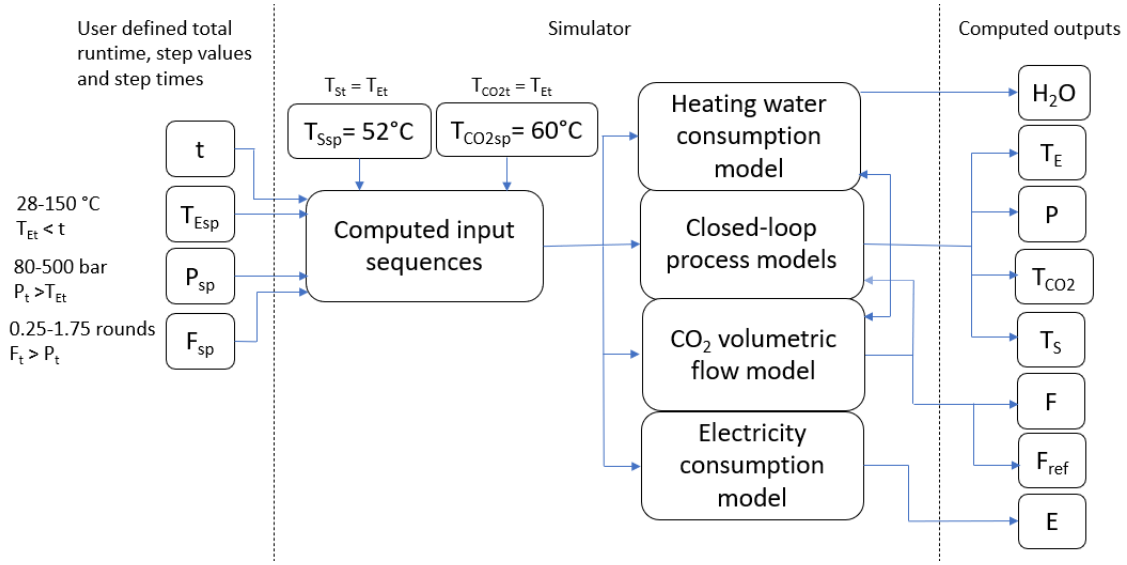

Figure 31. Structural description of the developed batch SFE process simulator, where t is the total simulation runtime, T_{Esp} is extractor temperature setpoint value, P_{sp} is CO_2 pressure setpoint value, F_{sp} is step time for CO_2 volumetric flow control valve step value, T_{Ssp} is separator temperature setpoint value, T_{CO2sp} is CO_2 preheater temperature setpoint value, T_{Et} is step time for extractor temperature setpoint, P_t is step time for CO_2 pressure setpoint, F_t, is step time for CO_2 volumetric flow control valve step value, T_{St} is step time for separator temperature setpoint, T_{CO2t} is step time for CO_2 preheater temperature setpoint, H_2O is heating water consumption model output, T_E is extractor temperature model output, P is CO_2 pressure model output, T_{CO2} is CO_2 preheater temperature model output, T_S is separator temperature model output, F is CO_2 volumetric flow model output, F_{ref} is open-loop identified steady-state value for CO_2 volumetric flow, and E is electricity consumption model output.

6 MODEL PREDICTIVE CONTROLLERS

Linear MPC strategies were designed for the processes that played a part in the energy consumption models, them being the operational variables (extractor temperature T_E, CO_2 pressure P, CO_2 volumetric flow F) and the water heating-based separator temperature T_S. The goal of the MPC strategies was to improve control performance, and through it optimize energy consumption of the batch SFE operation. The functions provided by MATLAB® MPC Designer Toolbox™ were used in identifying the MPCs. In the simulator, the implementation of MPC's affects the generation of inputs for the processes in question: The reference values (setpoints) of these processes are fed into the MPC, which produces its own input sequence according to the set optimization problem. The input sequence, differing from the single step change of the base control system, is fed to the process models. The role of MPC in the simulator framework is shown in Figure 32.

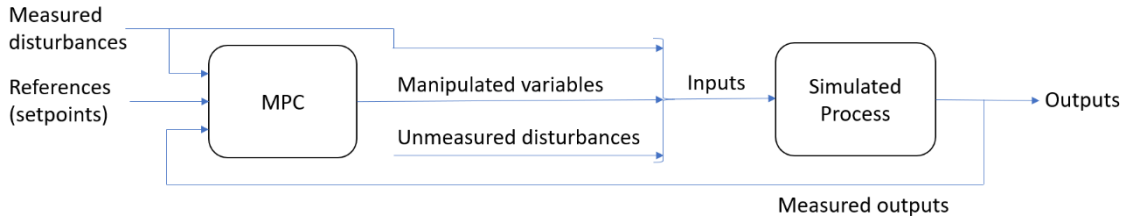

Figure 32. Role of MPC in the identified process simulator.

6.1 Controller formulations

The identified process models were utilized in MPC identification. Some of the unit processes had more than one submodel, as shown in Table 16 on page 86. Therefore, MPC schemes were designed for the models that initiate after a step input is applied (heating models for heaters, and post-pump start model for pressure). The realization of the MPC strategies was put forward by investigating different MPC parameter combinations. The significance of these parameters is described in detail in Chapter 4.3 on pages 51–54. Constraints, sampling time (t_s) and horizons were chosen according to MPC response, and weighing factors were used in tuning the controller.

Manipulated variables of the closed-loop controlled unit processes are constrained between 0 and the upper operative limit (shown in Table 7 on page 69). The input (control

valve position) of open-loop identified CO_2 flow process is constrained between 0 and 1.75 rounds, namely the physical limits of the control valve. These constraints are hard constraints in the system, since they represent the physical capability of the actuators; therefore, they cannot be violated in the optimization procedure (minimization of the cost function J, as described in Chapter 4.3 on pages 53–54). For the closed-loop processes, the setpoint can be manipulated in the integrated PID controllers in the form of step inputs with high resolution. Therefore, manipulated variable change rates are not constrained for these processes. Output variables are not constrained in any MPC to avoid confusion and unnecessary overlap with the hard-coded physical limits of the simulator. Hard constraining of output variables could also complicate optimization procedures.

The selection of sampling time depended on model order. It was found that higher order process models required smaller sampling times for reaching control performance improvements. This increased the controller ability to reject disturbances, with the cost of higher computational effort. The only low order start-up model was the extractor heating model, for which a t_s of 10 seconds was used. A t_s value of 1 second was used for other processes.

Using large prediction horizons with a significantly smaller control horizons eliminated the overshoot caused by the dynamics of the heating processes. On the contrary, relatively small prediction and control horizons resulted in control performance improvements in CO_2 pressure and flow control responses. as their time constants are much smaller compared to temperature control loops. The chosen sampling times, horizons and constraints for each unit process are compiled in Table 17.

Table 17. Sampling times, horizons and constraints for the developed model predictive controllers, where t_s is sampling time, p is prediction horizon, c is control horizon, u_{min} is the lower limit for manipulated variable, and u_{max} is the upper limit for manipulated variable.

Unit process	t_s (s)	p (s)	c (s)	u_{min}–u_{max}
P	1	20	3	0–500 bar
T_E	10	200	30	0–150 °C
F	1	40	2	0–1.75 rounds
T_S	1	180	60	0–60 °C

The parameters used for tuning MPC performance were the weighing factors for manipulated variable rate and output variables (b and a respectively, as seen in Equation 18 on page 53). A weighing value of 1 indicated average priority value, lower values allowed larger tracking errors and higher values desired smaller tracking errors. Output variable weighing values were set on the average priority due to the number of manipulated variables being the same as degrees of freedom in the processes, making it possible to minimize tracking errors without prioritizing output variable tracking too much. Changing the manipulated variable rate weighing value was used as the primary tuning method.

6.2 MPC tuning

Each MPC was tuned by running simulations in set conditions and varying the values of b. The values used for demonstrating the significance of tuning were 0.1, 1, 5 and 20. The operative conditions for MPC tuning simulations were T_{Esp} = 80 °C, P_{sp} = 200 bar, and F_{sp} = 0.7 rounds. The selected runtime for the simulations (t) was 4000 seconds.

In extractor temperature control, MPC strategy provided significant improvements to control performance, as seen in Figure 33. Smaller overshoots reduced the process cooling period, and therefore settling times decreased. Rise time was found to be adjustable through the values of b: Smaller values led to shorter rise times, while larger values prolonged rise times.

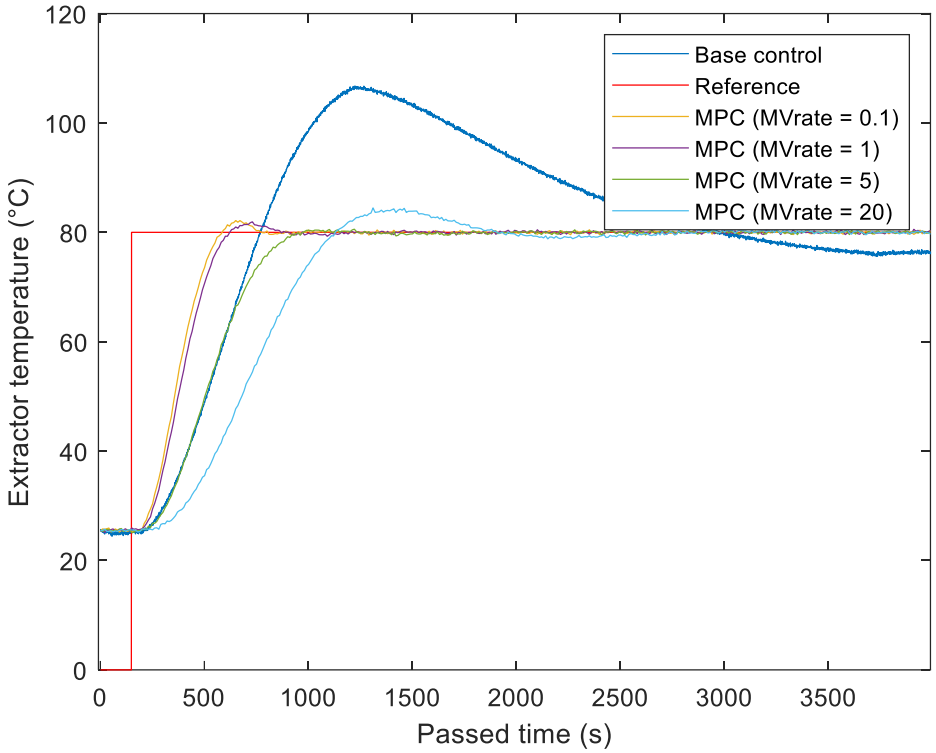

Figure 33. Responses of extractor temperature to a reference step input using simulated base control and MPC with differing MPC weighing values, where MVrate is the manipulated variable weighing factor (b).

Differing the values of b affected the separator temperature control differently compared to extractor temperature, as shown in Figure 34. Using large values resulted in response instability. The smaller values of b, which provided stable responses, did enhance control performance. However, the response was very similar between tuning sets that produced a stable response with no visible fine-tuning possibility.

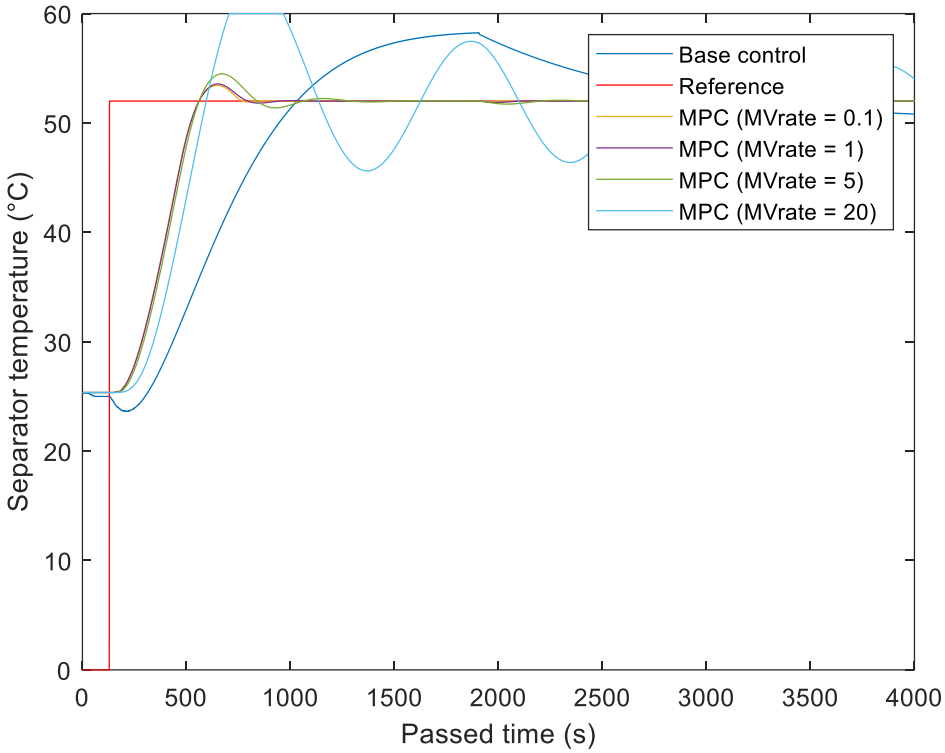

Figure 34. Responses of separator temperature to a reference step input using simulated base control and MPC with differing MPC weighing values, where MVrate is the manipulated variable weighing factor (b).

Changing the values of b had varying effects on pressure control, as seen in Figure 35. Mostly, the MPC strategy improved control performance: Smaller values of b eliminated overshoot and steady-state error, as well as shortened response times. A value of 20 increased rise time significantly, hinting a possibility of fine-tuning. However, using a value of five for factor b caused significant initial oscillations in the response, showing that the effects of tuning need to be carefully examined for reaching safe operation and desired action in control performance.

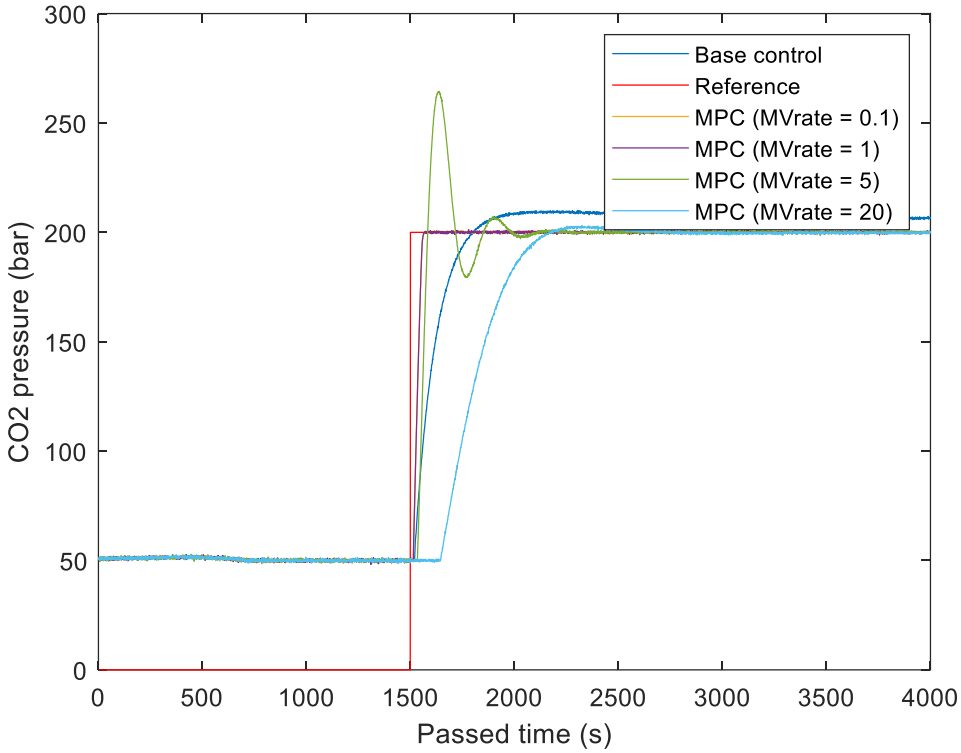

Figure 35. Responses of CO_2 pressure to a reference step input using simulated base control and MPC with differing MPC weighing values, where MVrate is the manipulated variable weighing factor (b).

The CO_2 volumetric flow process was open-loop identified, and the manipulated variable was the control valve position. The reference for MPC was determined according to the simulated open-loop steady-state value of F at given valve position (F_{ref}). The manual control of volumetric flow had desirable attributes, such as stability and short response times. In the simulations (Figure 36), MPC produced a good control response, with negligible overshoot at most. Manipulating the values of b indicated that fine-tuning could be possible, with smaller values producing quicker responses compared to larger values. However, the performance between 0.1 and 1 was barely any different, so control response could only be made faster to an extent.

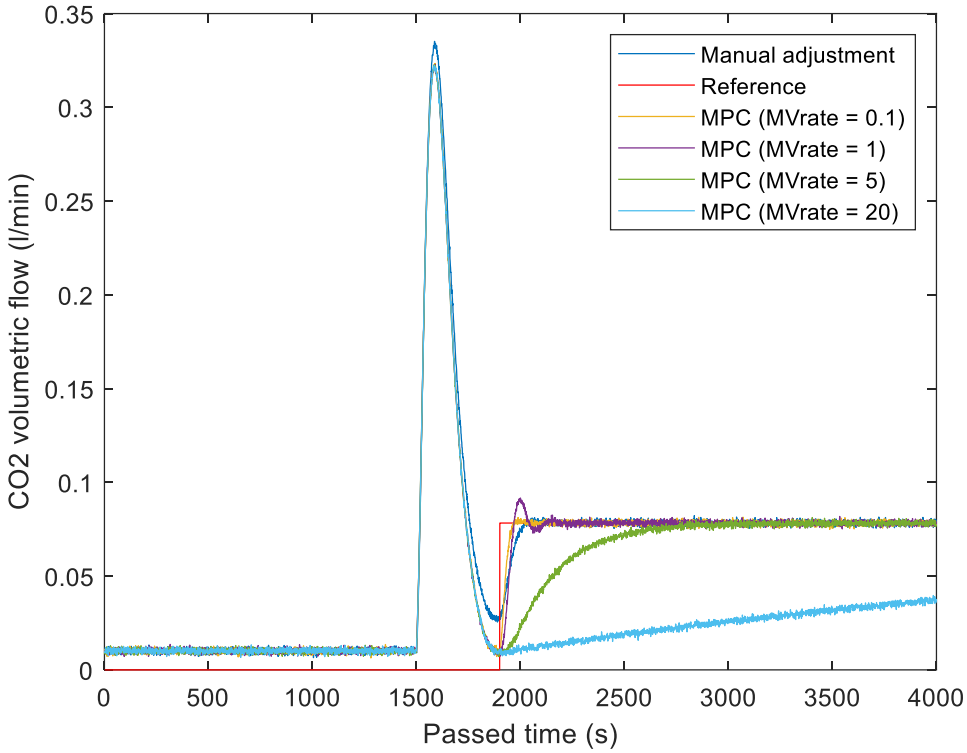

Figure 36. Responses of CO_2 volumetric flow to a reference step input using simulated base control and MPC with differing MPC weighing values, where MVrate is the manipulated variable weighing factor (b).

6.3 Results of MPC implementations

The developed MPC strategies for unit processes were implemented in differing simulation conditions. Using a value of 1 for b produced significant improvements in every control loop; thus, it was used in demonstrating the results of MPC implementations. The simulations were run using the base control and MPC schemes, and their responses were compared. The results were evaluated in terms of unit process control performance (rise time, overshoot, settling time) and effect on energy consumption during a simulation run (electricity consumption, heating water consumption). Three values for conditions were chosen for each operative variable: Two limit values and a center value. The limits were picked within the physical operating limits of the output variables. The chosen values are 70 °C, 90 °C and 100 °C for T_E; 200 bar, 300 bar and 400 bar for P; and 0.6 rounds, 0.9 rounds and 1.2 rounds for F. Separate simulations were run for each parameter value. When a single unit process was under scrutiny, the other processes were kept constant in their center values. The effect of MPC strategy for T_S was investigated at a fixed simulation condition of 52 °C. Each simulation

had a total runtime of 4000 seconds. The results of the MPC evaluations are compiled in Table 18.

Table 18. Control performance and energy consumption comparison between simulated processes using base control and MPC, where RT is rise time, OS is overshoot, ST is settling time, E is the total electricity consumption of a simulation run, and H_2O is the total heating water consumption of a simulation run.

Process	Control	Condition	RT	OS	ST	E	H_2O
T_E	Base	70 °C	395 s	22.8 °C	2379 s	824.4 Wh	65.2 l
	MPC	70 °C	–33.7%	–93.4%	–75.1%	–24.8%	–1.5%
	Base	90 °C	397 s	31.8 °C	2439 s	957.2 Wh	70.3 l
	MPC	90 °C	–28.7%	–93.4%	–75.7%	–23.3%	–2.0%
	Base	110 °C	409 s	38.8 °C	2452 s	1090.1 Wh	75.3 l
	MPC	110 °C	–24.9%	–93.2%	–75.0%	–22.4%	–2.5%
P	Base	200 bar	173 s	12.3 bar	849 s	910.1 Wh	65.4 l
	MPC	200 bar	–79.8%	–67.3%	–90.7%	+0.6%	–0.4%
	Base	300 bar	197 s	9.8 bar	670 s	957.2 Wh	70.3 l
	MPC	300 bar	–65.5%	–68.8%	–81.9%	+0.8%	–0.1%
	Base	400 bar	210 s	6.7 bar	730 s	1004.4 Wh	75.2 l
	MPC	400 bar	–42.4%	–75.4%	–72.6%	+0.8%	0%
F	Base	0.6 rounds	82 s	0.029 l/min	662 s	902.0 Wh	70.8 l
	MPC	0.6 rounds	–52.4%	+257.4%	–81.0%	+3.3%	+0.1%
	Base	0.9 rounds	85 s	0.029 l/min	186 s	957.2 Wh	70.3 l
	MPC	0.9 rounds	–50.6%	+406.7%	–29.0%	+3.2%	+0.1%
	Base	1.2 rounds	85 s	0.049 l/min	179 s	1012.5 Wh	69.7 l
	MPC	1.2 rounds	–36.5%	+222.3%	–36.5%	+3.0%	+0.1%
T_S	Base	52 °C	548 s	0.1202	2174 s	957.2 Wh	70.3 l
	MPC	52 °C	–53.1%	–75.0%	–76.8%	0.0%	–21.1%

7 DISCUSSION

The target SFE system identification and developed MPC strategies provided a variety of results. The results and the utilized experimental methods, including their uncertainties, are discussed, emphasizing on the performance of the base control system and developed MPC strategies, as well as the system identification procedure

7.1 PID control performance

Commercial supercritical fluid extraction systems have traditionally been controlled using basic control schemes, mainly PID control. Challenges in PID control performance, such as poor setpoint tracking and disturbance rejection, have been commonly addressed in previous studies on supercritical fluid extraction control (Cygnarowicz et al., 1990; Ramchandran et al., 1992; Roodpeyma et al., 2018). These challenges were largely present in the integrated control system of the target SFE process of this study, consisting of four PID controlled closed-loop processes. The three heating control loops initially exhibited long time constants and slow dynamics, resulting in large overshoots and long settling times. The poor response to setpoint changes generated waste energy in the form of consumed electricity and heating water. The only closed-loop controlled unit process in the system that had a sufficient control response was CO_2 pressure control, with much shorter time constants compared to the heating control loops. Even though pressure setpoint tracking was efficient, some issues with disturbances caused by the CO_2 volumetric valve position were noted, as pressure dropped when the control valve was close to completely open. The observed control performances of the unit process control loops reinforce the importance of designing PID controller parameters for specific operating conditions, as has been also shown by previous studies. Practically, this would require special PID tuning means such as gain scheduling, leading into extensive amounts of experiments. In a multi-control loop system, this approach for improving control performance would be very laborious and time consuming.

7.2 Identification of SFE

For any model-based control, a model, namely a mathematical presentation of the controlled process is essential. The goal of modeling has a significant effect on the model

structure: Many studies on SFE have focused on maximizing the yield or quantity of certain compounds (as seen in Sharif et al., 2014) by finding the optimal values for parameters and operating conditions. Only few have touched upon the subject of energy modeling and optimization of SFE: Smith et al. analyzed the energy efficiency of SFE by investigating energy losses through pump and compressor cycles (Smith et al., 1998). Sievers optimized SFE by investigating the effects of CO_2 pressure, extractor temperature and separator pressure on energy costs and produced soybean oil (Sievers, 1998). Rój et al. discussed the effect of differing solvent flow rates on extraction costs while maintaining a desired cumulative yield of the product (Rój et al., 2012). However, elementary research on data-driven system identification for SFE control is largely missing. The few modeling studies for control purposes (described in Chapter 3.2 on pages 32–34) have primarily been based on various first principles of SFE processes. However, due the complex interaction of affecting factors and lack of knowledge on the in-depth fluid dynamics of supercritical fluid in extraction, these modeling approaches tend to make harsh assumptions of the processes, affecting the modeling outcome.

The operating conditions for identification data acquisition experiments were based on a central composite design, providing the possibility of sufficient statistical analysis from a range of conditions with a relatively small number of trials. This approach is common in supercritical fluid extraction studies, where a large number of factors need to be properly adjusted before every run (Sharif et al., 2014). The selection of the CCD design variables (CO_2 pressure, CO_2 volumetric flow, and extractor temperature) was based on their operational significance on extraction outcomes. The experiments could not be fully randomized due to the slow cooling dynamics of extractor temperature. Therefore, as the experiments were divided in two sets (ordered from lowest to highest temperature) and performed on separate days, reliable data on heater start-up could only be collected from two experiments, potentially affecting the reproducibility and precision of the modeling outcome. Having more identification and validation data could have resulted in more reliable heating models. Also, input sequences of the heaters only included a few step inputs because of time delays caused by cooling. For compensating the time delays caused by cooling, and therefore ensuring the credibility of the results, an experimental design with less experiments and slightly longer run times could have been used. This could have also increased the statistical independency of the center trials. The most practical way of evaluating the uncertainty of the experiments in this study is to repeat the experiments in a similar set of experimental practices and conditions. However, as can be seen from

Table 14 on page 82, the variance between the center trial results was quite small. Due to this, the systematic error of the experiments can be interpreted as quite insignificant. Therefore, it can be concluded that the experimental runs can be held quite reliable in terms of cumulative energy and steady-state electricity consumptions.

Input signal sequences were applied manually during the experiments. Even though they were interpreted as sharply edged signals, the step inputs had to be applied with a delay of a few seconds, as the unit controllers and control valve only allowed gradual changes in their operation. However, the step inputs were treated similarly across this whole study, minimizing the uncertainty regarding applied inputs.

The yield of the extractive was measured to be up to 30%. This quantitative result cannot be held reliable since it was only measured once after 20 experimental runs, and the system was not cleaned prior to the runs or between independent experiments. As the quality parameters of the extractives do not play a significant role in the system identification of this study, they were not under scrutiny. However, they should be considered in future research.

The results of linear regression analysis showed good correlation between modeled and measured steady-state energy consumption as a function of the design factors. However, further analysis showed that the spread of residuals was heteroskedastic. The reasons for this may include that the explanatory variables do not explain enough of the variation in the response, or there may be unmodelled nonlinear associations.

The data-driven unit process and energy consumption state-space models showed quite high fits to validation data sets (medians between 59.4%–92.6%). The only notable exception was the model for CO_2 volumetric flow, with a median fit of 44.4%. This was most likely related to the unmeasured CO_2 liquid level in the storage tank (the tank was sometimes filled in between runs); a higher level generally resulted in higher flow values. For ensuring more precise modeling, the liquid level should have been quantified during the experiments. Interactions between unit processes were modeled by including the interacting responses in the models as measured disturbances. As this was done largely based on visual inspection, accurate interpretation caused by control loop coupling cannot be expected. However, the SFE modeling task can be deemed successful overall in the context of this study, as the main goal was to capture the dynamics of the unit processes

instead of maximum simulated response precision. In addition to the control-related targets of this study, the identified models could be utilized in digital twin developments for similar process types.

7.3 MPC strategies

Past research has suggested that model-based control strategies, including model predictive control, led to improved control performance in SFE processes over basic control schemes (such as Cygnarowicz et al., 1990; Ramchandran et al., 1992; Samyudia et al., 1995; Venkat et al., 2007, Riverol et al., 2005). These studies mostly focused on single unit processes, such as pressure or solvent flow or extractive outcomes. In this study, MPC strategies were developed for four simulated unit processes, and the impact on their control performances and total energy consumption of simulation runs were evaluated.

The developed process models give possibilities for developing advanced, model-based control strategies to the target SFE system. As discussed in Chapter 4.3 on pages 50–51, MPC is a commonly utilized advanced control scheme in industries, providing many hypothetical advantages to process control. Linear MPC was picked to demonstrate the benefits of model-based control schemes due to the simple application on the developed submodels consisting of linear state-space representations. However, the data-driven models could also be utilized in developing other model-based control strategies, such as nonlinear MPC algorithms, Smith predictor, neural networks, or fuzzy control. These possibilities should be addressed in future studies.

A classical cost function structure (Equation 18 on page 53), including terms for manipulated variable rate and output variable, was utilized in the MPC algorithm. The hypothetical idea behind this was that increasing control performance (such as decreasing temperature overshoots) leads to less energy being introduced in the system, resulting in a major decrease in total energy consumption. The effect of simulated MPC on control performance was examined individually for each unit process. The impact of MPC responses on total electricity and heating water consumptions of simulation runs was then examined, which included their effect on interacting control loops.

The comparative outcomes of the base control system and MPC were compiled in Table 18 on page 98. The developed simulated MPC strategies for extractor and separator heaters seemed to provide significant improvements in control performance (including rise time, overshoot and settling time), even with a single set of MPC tuning parameters for differing conditions. For extractor temperature control, not only did MPC decrease the suboptimality in control drastically, but also provided the ability to fine-tune rise time with simple tuning adjustments. The simulation results also showed that the MPC strategy for extractor temperature control was the only implementation that reduced electricity consumption significantly, with improvements up to 25%. Accordingly, the MPC implementation for the heating water-based separator temperature control improved H_2O consumption most efficiently, with improvements up to 21%.

According to the simulations, the MPC brought large percentual improvements in CO_2 pressure control performance. However, these were smaller compared to heating control loops due to the inherently smaller time constants of pressure control. Also, MPC in pressure control did not show the same flexibility as in extractor temperature control and had an insignificant effect on energy consumption overall. Here, the pressure prediction data generated by MPC could make the developed scheme more useful over the robust base pressure control if future developments are desired.

Control of CO_2 volumetric flow was the only inherently open-loop controlled unit in the process system. Initial experiments showed that the manual response of flow control provided good performance to step inputs. The results showed significant percentual improvements in control performance, except for overshoot. However, visual inspection of the response values show that the differences were barely noticeable, as they were massively exaggerated by the inherently short time constants of flow control. Therefore, even small changes in performance showed up as significant percentual changes. From a performance point of view, the developed MPC strategy does not bring significant advantages to the flow process. Also, MPC for flow control did not result in significant improvements in energy consumption. However, like in extractor temperature control, fine-tuning of the rise time of volumetric flow control response was possible by simple tuning adjustments, providing flexibility and fine-tuning of the process response by MPC.

8 CONCLUSIONS AND RECOMMENDATIONS

The ever-growing focus on energy efficiency and environmental awareness continues to contribute to the emergence of green chemistry in industries. In the past decades, commercial applications for supercritical fluid extraction (SFE) have been established as an efficient and reliable alternative in a variety of industries for other separation techniques, such as distillation and extraction using organic solvents. However, demonstrated process control is a significant factor in scaling-up processes to an industrial scale. Studies regarding process control and elementary research on system identification for SFE has been scarce; therefore, most applications are controlled only by basic control schemes.

The base control system of the target pilot-scale batch supercritical carbon dioxide extraction process consisted of PID controllers. The controllers produced largely suboptimal control performance in the unit processes, specifically in the heating control loops. This was evident mostly in the form of large time constants, leading into large overshoots and settling times, as well as wasted energy. For reaching optimal control using only PID control, laborious tuning procedures such as gain scheduling would be required, resulting in an extensive number of experimental runs. The nonlinear dynamics of the processes suggested that a model-based control scheme could be beneficial to implement for overcoming these challenges.

The goal of this study was to improve control performance and ultimately to optimize energy consumption of the target SFE system. Model predictive control was chosen as an advanced control method for improving the performance produced by the base control system. 5 target system unit process control loops (CO_2 pressure P, CO_2 volumetric flow F_{CO2}, CO_2 preheater temperature T_{CO2}, extractor temperature T_E and separator temperature T_S), as well as energy intakes (electricity consumption E and heating water consumption H_2O) were modeled through data-driven system identification. The nonlinear dynamics of the processes were taken into account by designing more than one submodel for some processes. The identified models mostly showed decent fits to validation data, but slight modification in the experimental design could have made the models more reliable and persistent. However, the models covered the process dynamics sufficiently.

As central composite design was used as the experimental design for identification data acquisition experiments, linear regression analysis could be utilized for modeling steady-state electricity consumption of the process as a function of the operative variables (P, $F_{CO2,}$ T_E). Despite decent correlation, residual analysis showed that the operative variables could not explain enough of the variation in the response, indicating possible nonlinearities in the electricity consumption.

MPC strategies were designed in a simulator environment for the unit processes that played a part in electricity and heating water consumption models (P, $F_{CO2,}$ T_E, T_s). As a result of MPC, heating processes gained the largest percentual improvements in control performance. The reduced overshoots and settling times of temperature responses also resulted in large energy consumption reductions (up to 25% in electricity consumption and 21% in heating water consumption). Simulated MPC also provided improvements in pressure and flow control, but they did not lead into significant energy reductions. For some processes, MPC provided the possibility of manipulating rise time by only slight changes in tuning parameters. Overall, the improvements caused by MPC could increase efficient extraction time, ultimately resulting in better and more energy-efficient extractions over the base control system.

The identified process and controller models have further potential in model-driven engineering research and development for supercritical fluid extraction. Efficient and optimal process control is a crucial part of industrial process feasibility; Therefore, more research should be made regarding data-driven SFE control as it enables further advances in simulation, optimization, and automation. The developed MPC strategies provide the base for more dependable research on the analytes, such as component yields and concentrations, with optimized energy and efficient production. The implementation of the MPC strategies to the real-life system could the next logical step in future research. This includes expanding the developed data acquisition system into a fully functional real-time control system. The vast amount of prediction data generated by the MPC and simulations could also be utilized in further control and modelling research, such as soft sensor developments.

9 SUMMARY

Reducing energy consumption and replacing environmentally harmful solvents in extraction and other processes has gained an increasing amount of significance in the processing industry. Supercritical fluid extraction offers many important improvements to these challenges over traditional extraction methods, with carbon dioxide (CO_2) being the most commonly utilized solvent. In past research, little emphasis has been given to process control, and especially advanced process control of supercritical extraction. This is a significant challenge to emphasize since the lack of demonstrated control for maintaining product quality and energy efficiency is crucial for developing future scaled-up supercritical fluid extraction applications.

The goal of this study was to improve control performance, and ultimately to optimize energy consumption of a pilot-scale batch supercritical carbon dioxide extraction process system by utilizing model predictive control strategies. The control performance of the unit processes of the target system was suboptimal, especially in the heating control loops which exhibited long time constants, slow dynamics, and integrating open-loop responses. The base control system consisting of PID controllers did not produce a satisfactory process response in most cases, and controller tuning for varying process conditions would have been laborious. The application of an advanced control scheme could overcome these challenges, as well as improve the production economics of the system.

A mathematical representation of a system, a model, is the prerequisite for any model-based control scheme. A total of five unit processes (CO_2 pressure, CO_2 volumetric flow, CO_2 preheater temperature, extractor temperature and separator temperature) and 2 energy intakes (electricity and heating water consumption) were modeled by data-driven system identification. Additional sensor and instrument installation work were conducted on the developed PC-based data acquisition system, ensuring that necessary data could be gathered. Both closed-loop and open-loop identification were utilized in experimental design, depending on process characteristics and behavior. For closed-loop controlled processes, the PID controllers were tuned as well as possible in advance to identification experiments. Central composite design was used for determining operative conditions for each experiment, and step input sequences were designed and applied for each unit

process in each identification experimental run. Linear regression analysis indicated possible nonlinearities between steady-state electricity consumption response and operative supercritical fluid extraction parameters.

MATLAB® software and the functions provided by its various toolboxes were utilized in identification and development of a supercritical extraction process simulator and model predictive control strategies. State-space models were chosen as the model structure for the unit processes and energy consumption. The notable nonlinear dynamics of some unit processes were considered by developing more than one model if a single model could not produce a satisfactory outcome. Interactions between control loops were taken into account by adding measured disturbances in the process models. Overall, the models showed satisfactory fits against validation data and covered the process dynamics sufficiently.

Simulated model predictive control strategies were developed for four unit processes (CO_2 pressure control, CO_2 volumetric flow control, extractor temperature and separator temperature) due to their involvement in the electricity and heating water consumption models. The main model predictive control tuning parameter was the weighing value for manipulated variable rate, for which 4 different values were used for demonstrating model predictive control response to parameter adjustments. After controller tuning, the effect of unit process model predictive control schemes was evaluated in a range of conditions, demonstrating the effect of control strategy on different control performance parameters (rise time, overshoot, settling time) and total energy consumption.

The simulated model predictive controller implementations seemed to significantly improve the control performance of every unit process control loop. The model predictive control strategies of heating control loops provided the biggest reductions in energy consumption: Model predictive control of extractor temperature improved electricity consumption most significantly (up to 25%), whereas the model predictive control scheme for separator temperature showed largest improvements in heating water consumption (up to 21%). Some MPC strategies also provided flexibility in process control, since rise time could be tuned with simple parameter modifications.

In addition to optimized energy consumption, the identified process simulator has further potential in model-driven engineering research and development for supercritical fluid

extraction processes. The practical implementation of the strategies to the target system bring up more interesting research possibilities, such as production optimization, increased automation, and other process developments.

REFERENCES

Ahmad T., Masoodi F.A., Rather S.A., Wani S.M., Gull A., 2019. Supercritical Fluid Extraction: A review. J. Biol. Chem. Chron. 2019, 5(1), 114–122.

Amador-Herández J., Fernández J.M., de Castro M.D.L., 1999. Near Infrared Thermal Lens Spectrometry for the Real-time Monitoring of Supercritical Fluid Extraction. Talanta 49 (1999) 813-823.

Amador-Herández J., Fernández-Romero J.M., Ramis-Ramos G., de Castro M.D.L., 1999. Monitoring Supercritical Fluid Extraction by Thermal Lens Spectrometry with Pulsed Laser Excitation. Analytica Chimica Acta 390 (1999) 163–173.

Andersson L., Jönsson U., Johansson K.H., Bengtsson J., 2006. A Manual for System Identification [online document]. Mathworks [referenced on 19.4.2020].

Ang K.H., Chong G., Li Y., 2005. PID Control System Analysis, Design and Technology. IEEE Transactions on Control Systems Technology, 13(4), pp. 559-576.

Åström K.J., 2002. Control System Design. Department of Mechanical and Environmental Engineering, University of California, GooSanta Barbara, p. 217.

Bansal H., Sharma R., Ponpathirkoottam S., 2012. PID Controller Tuning Techniques: A Review. Journal of Control Engineering and Technology Vol 2., Issue 4, pp. 168–176.

Beall J., 2016. Loop Tuning Basics: Integrating Processes. InTech Magazine, Mar-Apr 2016.

Beall J., 2016. Loop tuning basics: Self-regulating processes. InTech Magazine, May-June 2016.

Behrendt M., 2009. A basic principle of Model Predictive Control [online document]. Wikipedia Commons [referenced on 29.7.2020].

Bertucco A., Vetter G., 2001. High Pressure Process Technology: Fundamentals and Applications, Volume 9. Darmstadt: Elsevier Science, 684 pp., ISBN 9780444504982.

Breet E., Nortjé Y., Greuning C., 2011. Supercritical carbon dioxide extracted oil from Jatropha curcas: Directive for the biodiesel industry? J. Supercrit. Fluids, 60: 38–44.

Camacho E.F., Bordons C., 2007. Model Predictive Control. Second Edition. London: Springer-Verlag, 404 pp. ISBN 978–1–85233–694–3.

Catchpole O.J., Tallon S.J., Grey J.B., Fletcher K., Fletcher A.J., 2008. Extraction of Lipids from a Specialist Dairy Stream. The Journal of Supercritical Fluids, Vol. 45, Issue 3, July 2008, pp. 314–321.

Cavalcanti R.N., Meireles M.A.A., 2012. Fundamentals of Supercritical Fluid Extraction. Comperhensive Sampling and Sample Preparation, Elsevier Inc., 2012, 2, 117–133.

Chematur Ecoplanning Ltd, 1998. Operating manual of Xtractor® SFE system.

Corostiaga L., Gutiérrez F., Baeyens E., Antolín G., Perán J.R., 2002. Integrated Design of the Process and Control of Supercritical Extraction Plants with Re-circulation. University of Valladolid, Valladolid, Spain.

Coughran M.T., 2013. Lambda Tuning – the Universal Method for PID Controllers in Process Control [online document]. Control Global Digital Edition [referenced on 29.7.2020].

Cui Y., Ang C.Y.W., 2002. Supercritical Fluid Extraction and High-Performance Liquid Chromatographic Determination of Phloroglucinols in St. John's Wort (Hypericum Perforatum L.). J Agric Food Chem 2002 May 8, 50(10):2755–9

Cygnarowicz M.L., Seider W.D., 1990. Design and Control of a Process to Extract β-carotene with Supercritical Carbon Dioxide. Biotechnol. Prog., 1990, 6, 82–91.

Da Costa Mendes P.R., 2016. Predictive Control for Energy Management of Renewable Energy Based Microgrids. Doctorate thesis, Fraunhofer Institute for Industrial Mathematics ITWM, 9/2016.

Da Porto C., Decorti D., Natolino A., 2014. Water and Ethanol as Co-solvent in a Supercritical Fluid Extraction of Proanthocyanidins from Grape Marc: A Comparison and a Proposal. The Journal of Supercritical Fluids, Vol. 87, March 2014, pp. 1–8.

De Azevedo A.B.A., Kieckbusch T.G., Tashima A.K., Mohamed R.S., 2008. Extraction of Green Coffee Oil Using Supercritical Carbon Dioxide. The Journal of Supercritical Fluids, Vol. 44, Issue 2, March 2008, pp. 186–192.

De Prada C., 2014. Overview: Control Hierarchy of Large Processing Plants. University of Valladolid, Valladolid, Spain.

Del Castillo E., 2007. Process Optimization: A Statistical Approach. Pennsylvania, USA: Springer Science + Business, ISBN 978–0–387–71434–9.

Diamond W.J., 2001. Practical Experiment Designs for Engineers and Scientists. Wiley, third edition, ISBN 978–0–471–39054–1, pp. 281–291.

Eisenmenger M., Dunford N.T., 2008. Bioactive Components of Commercial and Supercritical Carbon Dioxide Processed Wheat Germ Oil. Journal of the American Oil Chemists' Society 85, 55–61(2008)

Filliben J.J., Gutherie W.F., Heckert N.A., Splett J.D., Zhang N-F., 2003. E-Handbook of Statistical Methods [online document]. NIST/SEMATECH, referenced on 09/2020.

Fornari T., Hernández E.J., Ruiz-Rodríguez A., Señorans F.J., Reglero G., 2009. Phase Equilibria for the Removal of Ethanol from Alcoholic Beverages using Supercritical Carbon Dioxide. The Journal of Supercritical Fluids, Vol. 50, Issue 2, September 2009, pp. 91–96.

Gani R., Hytoft G., Jaksland C., 1997. Design and Analysis of Supercritical Extraction processes- Applied Thermal Engineering, Vol 17, Nos 8–10, pp. 889–899.

Goodwin G.C, Graebe S.F., Salgado M.E., 2000. Control System Design. Pearson (October 6, 2000), Ch. 2, ISBN–13: 978–0139586538.

Gracia I., Rodríguez J.F., Garciá M.T., Alvarez A., García A., 2007. Isolation of Aroma Compounds from Sugar Cane Spirits by Supercritical CO_2. The Journal of Supercritical Fluids, Vol. 43, Issue 1, November 2007, pp. 37–42.

Guerra R.M., Marín M.L., Sánchez A., Jiménez A., 2002. Effect of Pressure, Temperature and Time on Supercritical Fluid Extraction of Citrate and Benzoate Plasticizers from Poly (Vinyl Chloride). Journal of Supercritical Fluids 22 (2002) 111–118.

Gustavsson I., 1975. Survey of Applications of Identification in Chemical and Physical Processes. Automatica, Vol. 11, pp. 3–24.

Harju T., Marttinen A., 2000. Educational material for Control Engineering (in Finnish). Control CAD, Espoo, 3/2020, pp. 97–156.

Hedrick J.L., Mulcahey L.J., Taylor L.T., 1992. Fundamental Review: Supercritical Fluid Extraction. Mikrochimica Acta 108, 115–132 (1992).

Herrero M., Mendiola J.A., Cifuentes A., Ibáñez E., 2010. Supercritical Fluid Extraction: Recent Advances and Applications. Journal of Chromatography A, 1217 (2010) 2495–2511.

Horvat G., Aladić K., Jokić S., 2017. Supercritical CO_2 Extraction Pilot Plant Design – Towards IoT Integration. Technical Gazette 24, 3(2017), 925–934.

Ifran M., Raza M.A., 2011. A Simple Method for Generation of Statistical Tables by the Help of Excel Software. Journal of Social and Development Sciences, 2(1): 38–50.

Ikonen E., Najim K., 2002. Advanced Process Identification and Control. New York: Marcel Dekker, Inc, ISBN 0–8247–0648–X.

Ikonen E., 2017. Model Predictive Control and State Estimation. University of Oulu, Systems Engineering Laboratory, Oulu, Finland.

Isermann R., 1980. Practical Aspects of Process Identification. Automatica, Vol. 16 pp. 575–587.

Ivanovic J., Ristic M., Skala D, 2012. Supercritical CO_2 extraction of helichrysum italicum: Influence of CO_2 density and moisture content of plant material. Journal of Supercritical Fluids 2011, 57, 129–136.

Johnson M.A., Horadi M.H., 2005. PID control: New identification and Design Methods. Springer-Verlag London, ISBN 1–85233–702–8.

Jokić S., Nagy B., Zeković Z., Vidović S., Bilić M., Velić D., Simándi B., 2012. Effects of Supercritical CO_2 Extraction Parameters on Soybean Oil Yield. Food and Bioproducts Processing 90 (2012) 693–699.

Kazarian S.G., 1997. Applications of FTIR Spectroscopy to Supercritical Fluid Drying, Extraction and Impregnation. Applied Spectroscopy Reviews, 32(4), 301–348 (1997).

Khataee A.R., Farhinia M., Aber S., Zarei M., 2010. Optimization of Photocatalytic Treatment of Dye Solution on Supported TiO2 Nanoparticles by Central Composite Design: Intermediates Identification. Journal of Hazardous Materials, 181(1–3), 886–897.

Khaw K-Y., Parat M-O., Shaw P.N., Falconer R.J., 2017. Solvent Supercritical Fluid Technologies to Extract Bioactive Compounds from Natural Sources: A Review. University of Queensland, Brisbane.

King J.W., 2002. Supercritical Fluid Extraction: Present Status and Prospects. Grasas y Aceitesv Vol. 53, Fasc. 1 (2002), 8–21.

King J.W., List G.R., 1996. Supercritical Fluid Technology in Oil and Lipid Chemistry. Peoria, Illinois: AOCS Press, 435 pp. ISBN 0–935315–71–3.

Kumoro A.C., Hasan M., 2007. Supercritical Carbon Dioxide Extraction of Andrographolide from Andrographis paniculate: Effect of the Solvent Flow Rate, Pressure, and Temperature. Chinese Journal of Chemical Engineering. December 2007.

Laitinen A., 2000. Supercritical Fluid Extraction of Organic Compounds from Solids and Aqueous Solutions. Technical Research Centre of Finland, Espoo 1999.

Lang Q., Wai C.M., 2000. Supercritical Fluid Extraction in Herbal and Natural Product Studies – A Practical Review. Talanta 52 (2001) 771–782.

Li H, Yang S.X., Shi J., 2001. Modeling of Supercritical Fluid Extraction by Artificial Neural Networks. University of Guelph, Canada.

Ling Y.C., Teng H.C., Catwright C., 1999. Supercritical Fluid Extraction and Clean-up of Organochlorine Pesticides in Chinese Herbal Medicine. Journal of Chromatography A, 1999 Mar 12, 835(1–2), 145–57.

Liu W., 2017. Hybrid Electric Vehicle System Modeling and Control, Second Edition, Appendix A: System Identification, State and Parameter Estimation Techniques. John Wiley and Sons Ltd., ISBN 9781119279327.

Ljung L., 1999. System Identification: Theory for the User (Second Edition). Prentice-Hal PTR, 1999, pp. 197–245. ISBN 0–13–656695–2.

Ljung L., Glad T., 1994. Modeling of Dynamic Systems. Prentice Hall Inc.,Englewood Hills, New Jersey, ISBN 0–13–597097–0, pp. 36–40.

Lozowski D., 2010. Supercritical CO_2: A Green Solvent [online document]. Chemical Engineering [referenced on 18.4.2020].

Machado B.A.S, Pereira C.G., Nunes S.B., Padilha F.F., Umsza-Guez M.A., 2013. Supercritical Fluid Extraction Using CO_2: Main Applications and Future Perspectives. Separation Science and Technology, 48(18), 2741–2760.

Machmudah S., Kawahito Y., Sasaki M., Goto M., 2007. Supercritical CO_2 extraction of rosehip seed oil: Fatty acids composition and process optimization. Journal of Supercritical Fluids 41(3), pp. 421–428.

Martinez J.L., 2008. Supercritical Fluid Extraction of Nutraceuticals and Bioactive Compounds. United States of America: Taylor & Francis Group, 402 pp., ISBN 978–0–8493–7089–2.

McNally M.E.P., Wheeler J.R., 1988. Increasing Extraction Efficiency in Supercritical Fluid Extraction from Complex Matrices: Predicting Extraction Efficiency of Diuron and Linuron in Supercritical Fluid Extraction Using Supercritical Fluid Chromatographic Retention. Journal of Chromatography A, Vol. 447, 1988, pp. 53–63.

Melo S.S., Rodrigues F.S., Kamimura E.S., Lacerda R.S., Gomide C.A., Oliveira A.L., 2011. Availability of cellulose pulp from cane sugar by treatment with sub and supercritical CO_2. 9° Latin American Symposium on Food Science, Unicamp, Campinas.

Metso Oy, 1987. Comparison of PID Control Algorithms. Control Engineering Magazine, March 1987.

Mikleš J., Fikar M., 2007. Process Modeling, Identification, and Control. Springer Berlin Heidelberg New York, ISBN 978–3–540–71969–4.

Molino A., Mehariya S., Di Sanzo G., Larocca V., Martino M., Leone P.G., Marino T., Chianese S., Balducchi R., Musamarra D., 2020. Recent Developments in Supercritical Fluid Extraction of Bioactive Compounds from Microalgae: Role of Key Parameters, Technological Achievements and Challenges. Journal of CO_2 Utilization 36 (2020) 196–209.

Morin P., Beccard B., Caude M., Rosset R., 1988. Influence of Temperature on FTlR Spectra of Various Organic Compounds Analyzed by On-Line Carbon Dioxide SFC/FTIR. J. High Res. Chromatogr. Chromatogr. Corn. 11 (1988) 697.

Norhuda I., Jusoff K., 2008. Supercritical Carbon Dioxide (SC-CO_2) as a Clean Technology for Palm Kernel Oil Extraction. J. Biochem Tech (2009) 1(3): 75–78.

Payne R.L., 1974. Optimal Experiment Design for Dynamic System Identification. Department of Computing and Control, University of London.

Perretti G., 2006. Supercritical Carbon Dioxide Extraction of Agricultural and Food Processing Wastes and Byproducts. ACS Symposium Series 926.

Posio J., 2002. Model Predictive Control (in Finnish). University of Oulu, Laboratory of Control Engineering, Report B No. 39, 11/2002, ISBN 941–42–6887–3.

Pourmortazavi M.S., Hajimirsadeghi S.S., 2007. Supercritical Fluid Extraction in Plant Essential and Volatile Oil Analysis. Journal of Chromatography A, 1163 (2007) 2–24.

Pourmortazavi MS., Saghafi Z., Ehasani A., Yousefi M., 2018. Application of Supercritical Fluids in Cholesterol Extraction from Foodstuffs: A Review. Association of Food Scientists & Technologists (India).

Rai A., Mohanty B., Bhargava R., 2018. Optimization of Parameters for Supercritical Extraction of Watermelon Seed Oil. Separation Science and Technology 2018, Vol. 53, NO. 4, 671–682.

Ramchandran B., Riggs. J.B., Heichelheim G.R., 1992. Nonlinear Plant-Wide Control: Application to a Supercritical Fluid Extraction Process. Ind. Eng. Chem. Res. 1992, 31, 290–300.

Reverchon E., 1996. Supercritical Fluid Extraction and Fractionation of Essential Oils and Related Products. Journal of Supercritical Fluids 10 (1997) 1–37.

Riverol C., Cooney J., 2005. Assessing Control Strategies for the Supercritical Extraction from Coffee Beans: Process-Based Control Versus Proportional Integral Derivative. Journal of Food Process Engineering 28 (2005) 494–505.

Rój E., Gagós M., Dobrzyńska-Inger A., 2012. Cost Optimization of Extract Production in Supercritical Extraction Process with the Use of CO_2 – a Novel Approach. Procedcia Engineering 42 (2012), 323–328.

Roodpeyma M., Guigard S.E., Stiver W.H., 2018. Pressure Control of a Continuous Pilot Scale Supercritical Fluid Extraction (SFE) Process. The Journal of Supercritical Fluids 135 (2018) 120–129.

Ruel M., 2010. Closed Loop Tuning vs Open Loop Tuning: Tuning All Your Loops While the Process Is Running Is Now Possible. Top Control Inc., 49, Bel-Air, #103.

Samyudia Y., Lee L.P., Cameron I.T., 1995. Control Strategies for a Supercritical Fluid Extraction Process. Chemical Engineering Science, Vol. 51, No 5., pp. 769–787.

Sapkale G.N., Patil S.M., Surwase U.S., Bhatbhage P.K., 2010. Supercritical Fluid Extraction – A Review. Int. J. Chem Sci: 8(2), 2010, 729–743.

Shahrokhi M., Zomorrodi A., 2012. Comparison of PID Controller Tuning Methods. Department of Chemical and Petroleum Engineering, Sharif University of Technology.

Shamsuzzoha M., 2018. PID Control for Industrial Processes. London, United Kingdom, IntechOpen, ISBN 978–1–78923–700–9.

Sharif K.M., Rahman M.M., Azmir J., Mohamed A., Jahurul M.H.A., Sahena F., Zaidul I.S.M., 2014. Experimental Design of Supercritical Fluid Extraction – A Review. Journal of Food Engineering 124 (2014), pp. 105–116.

Sievers U., 1998. Energy Optimization of Supercritical Fluid Extraction Processes with Separation at Supercritical Pressures. Chemical Engineering and Processing 47 (1998) pp. 451–469.

Smith R.L., Inomata H., Kanno M., Arai K., 1998. Energy Analysis of Supercritical Carbon Dioxide Extraction Processes. Journal of Supercritical Fluids 15 (1999) pp. 135–156.

Stahl E., Quirin K.W., Gerard D., 1988. Dense Gases for Extraction and Refining, Springer, Berlin, Heidelberg.

Sunarso J., Ismandi S., 2009. Decontamination of Hazardous Substances form Solid Matrices and Liquids Using Supercritical Fluids Extraction: A Review. J Hazard Mater, 2009, Jan 15, 161(1), 1–20.

Temelli F., 2009. Perspectives on Supercritical Fluid Processing of Fats and Oils. The Journal of Supercritical Fluids, Vol. 47, Issue 3, January 2009, pp. 583–590.

Tena M.T., de Castro M.D.L., Valcárcel M., 1996. Screening of Polycyclic Aromatic Hydrocarbons in Soil by On-Line Fiber-Optic-Interfaced Supercritical Fluid Extraction Spectrofluorometry. Analytical Chemistry, 1996, 68, 2386–2391.

Tilotta D. C., Heglund D. L., Hawthorne S. B., 1996. On-line SFE-FTIR spectroscopy with a fiber optic transmission cell. American Laboratory 26 (6) (1996) 36R.

Van Overschee P., De Moor B., 1994. N4SID: Subspace Algorithms for the Identification of Combined Deterministic Stochastic Systems. Automatica, Vol. 30, No.1, pp. 75–93.

Venkat A.N., Rawlings J.B., Wright S.J., 2007. Distributed Model Predictive Control of Large-Scale Systems. Assessment and Future Directions, Springer-Verlag Berlin Heidelberg, pp. 591–605.

Verhaegen M., Verdult V., 2007. Filtering and System Identification: A Least Squares Approach. Cambridge University Press, ISBN–10 0–521–87512–9.

Wagner J., Mount E.M., Giles H.F., 2014. Design of Experiments. Extrusion, pp. 291–308.

Wang Q-G., Cai W-J., Ye Z., Hang C-C., 2008. PID Control for Multivariable Processes. Springer-Verlag-Berlin Heidelberg, p. 6 (preface), ISBN 978–3–540–78481–4.,

Yépez B., Espinosa M., López S., Bolaños G., 2002. Producing antioxidant fractions from herbaceaus matrices by supercritical fluid extraction. Fluid Phase Equilibr., 194–197: 879–884.

Zehnder B., Trepp C., 1993. Mass-Transfer Coefficients and Equilibrium Solubilities for Fluid-Supercritical-Solvent Systems by Online Near-IR Spectroscopy, J. Supercrit. Fluids 6 (1993) 131.

Zhou H., Zhao Q., Zhenhua Z., Tong M., Wang Z., 2011. Multi-ANN Predictive Control of Citrus Peel Supercritical Extraction Temperature. Advanced Materials Research Vols. 2236–238 (2011) pp. 1472–1479.

Zhu Y., 2001. Multivariable System Identification for Process Control. Elsevier Science and Technology books, ISBN 0080439853.